

PHOSPHO-REGULATION AND METASTATIC POTENTIAL OF
MURINE DOUBLE MINUTE 2

Christopher N. Batuello

Submitted to the faculty of the University Graduate School
in partial fulfillment of the requirements
for the degree
Doctor of Philosophy
in the Department of Biochemistry and Molecular Biology,
Indiana University

August 2012

Accepted by the Faculty of Indiana University, in partial fulfillment of the requirements for the degree of Doctor of Philosophy.

Lindsey D. Mayo, Ph.D., Chair

Joseph R. Dynlacht, Ph.D.

Doctoral Committee

Mark G. Goebel, Ph.D.

June 7, 2012

Karen E. Pollok, Ph.D.

ACKNOWLEDGEMENTS

I would like to thank my entire family for all of their love and support. I especially thank my wife, Emily, for supporting me in everything I do. I want to thank my advisor, Dr. Lindsey Mayo, for mentoring and guiding me throughout my graduate career. I would also like to thank my committee members, Dr. Joseph Dynlacht, Dr. Mark Goebel, Dr. Karen Pollok, Dr. Hua Lu, and Dr. Ann Roman for all their assistance, knowledge, and direction. Finally I need to thank all the members of the Mayo lab, Dr. Jason Lehman, Dr. David Waning, and Jacob Eitel, for helping me throughout this process.

ABSTRACT

Christopher N. Batuello

Phospho-regulation and metastatic potential of Murine Double Minute 2

Murine double minute (Mdm2) is a highly modified and multi-faceted protein that is overexpressed in numerous human malignancies. It engages in many cellular activities and is essential for development since deletion of *mdm2* is lethal in early stages of embryonic development. The most studied function of Mdm2 is as a negative regulator of the tumor suppressor protein p53. Mdm2 achieves this regulation by binding to p53 and inhibiting p53 transcriptional activity. Mdm2 also functions as an E3 ubiquitin ligase that signals p53 for destruction by the proteasome. Interestingly recent evidence has shown that Mdm2 can also function as an E3 neddylation enzyme that can conjugate the ubiquitin-like molecule, nedd8, to p53. This modification results in inhibition of p53 activity, while maintaining p53 protein levels. While the signaling events that regulate Mdm2 E3 ubiquitin ligase activity have been extensively studied, what activates the neddylation activity of Mdm2 has remained elusive. My investigations have centered on understanding whether tyrosine kinase signaling could activate the neddylation activity of Mdm2. I have shown that c-Src, a non-receptor protein tyrosine kinase that is involved in a variety of cellular processes, phosphorylates Mdm2 on tyrosines 281 and 302. This phosphorylation event increases the half-life and neddylation activity of Mdm2 resulting in a neddylation dependent reduction of p53 transcriptional activity. Mdm2 also has many p53-independent cellular functions that are beginning to be linked to its role as an oncogene. There is an emerging role for Mdm2 in tumor metastasis. Metastasis is a

process involving tumor cells migrating from a primary site to a distal site and is a major cause of morbidity and mortality in cancer patients. To date, the involvement of Mdm2 in breast cancer metastasis has only been correlative, with no *in vivo* model to definitively define a role for Mdm2. Here I have shown *in vivo* that Mdm2 enhances breast to lung metastasis through the up regulation of multiple angiogenic factors, including HIF-1 α and VEGF. Taken together my data provide novel insights into important p53-dependent and independent functions of Mdm2 that represent potential new avenues for therapeutic intervention.

Lindsey D. Mayo, Ph.D., Chair

TABLE OF CONTENTS

List of Tables	viii
List of Figures	ix
List of Abbreviations	xii
1. Background and Significance	
1.1. Mdm2	1
1.2. c-Src	12
1.3. Cancer Metastasis	16
2. Materials & Methods	
2.1. Cell culture	25
2.2. Transfection	25
2.3. Generation of shGFP and shMdm2 TMD-231 cell lines	25
2.4. Luciferase assay	26
2.5. GST pulldown assay	26
2.6. Cloning of Mdm2 mutants	27
2.6.1. Wild-Type Mdm2	27
2.6.2. Mdm2 90-383	27
2.6.3. Mdm2 4-268	27
2.6.4 Mdm2 102-491	27
2.7. His-ubiquitin and His-nedd8 pulldowns	29
2.8. Purification of recombinant proteins	29
2.9. <i>In vitro</i> kinase reactions	30
2.10. <i>In vitro</i> ubiquitination assays	30
2.11. Protein analysis, immunoprecipitation, and Western blotting	30

2.12. Cell cycle analysis	31
2.13. Plating Efficiency	32
2.14. Cell Attachment	32
2.15. Matrigel Invasion Assay	32
2.16. Assessment of tumorigenicity <i>in vivo</i>	33
2.17. Tissue Preparation and Staining	33
2.18. Lung metastasis evaluation	33
3. c-Src phosphorylates and switches Mdm2 to a neddylation enzyme	
3.1. Introduction	34
3.2. Results	35
3.3. Discussion	69
4. Mdm2 enhances breast cancer metastasis	
4.1. Introduction	77
4.2. Results	79
4.3. Discussion	93
5. Summary and Perspectives	99
References	106
Curriculum Vitae	

LIST OF TABLES

Table 1: Mdm2 binding partners	13
Table 2: SH3 domain array	36

LIST OF FIGURES

Figure 1: Schematic of Mdm2 domains.....	2
Figure 2: The Mdm2/p53 auto-regulatory feedback-loop.....	5
Figure 3: Organization of the human <i>mdm2</i> gene	9
Figure 4: Known phosphorylation sites on Mdm2.....	10
Figure 5: Structure and activation of c-Src.....	15
Figure 6: The tumor metastatic process.....	17
Figure 7: HIF-1 α /VHL pathway	21
Figure 8: Restriction sites used for cloning of Mdm2 truncation mutants.....	28
Figure 9: c-Src binds Mdm2 between aa90-268.....	37
Figure 10: Mdm2 and c-Src interact <i>in vivo</i>	39
Figure 11: Schematic of tyrosines in Mdm2.....	40
Figure 12: c-Src phosphorylates Mdm2 <i>in vitro</i>	41
Figure 13: c-Src phosphorylates Mdm2 at Y281 and Y302.....	42
Figure 14: Mdm2 is phosphorylated by c-Src <i>in vivo</i>	44
Figure 15: Overexpression of CA-Src increases Mdm2 protein levels.....	46
Figure 16: Increases in Mdm2 protein levels by c-Src is dependent on c-Src phosphorylation sites Y281 and Y302 of Mdm2.....	47
Figure 17: Activation/inhibition of endogenous c-Src regulates endogenous Mdm2 protein levels.....	49
Figure 18: c-Src does not induce Mdm2 transcription from the P2-promoter.....	50
Figure 19: c-Src increases Mdm2 protein half-life.....	51

Figure 20: Y281 and Y302 of Mdm2 are required for c-Src mediated increase of Mdm2 half-life	53
Figure 21: Loss of Mdm2 ubiquitination by CA-Src	54
Figure 22: c-Src inhibits Mdm2 mediated ubiquitination of p53	55
Figure 23: Exogenous CA-Src elevates p53 protein levels	57
Figure 24: Activation/Inhibition of endogenous c-Src regulates endogenous p53 protein levels	58
Figure 25: c-Src inhibits p53 transcriptional activity dependent on Mdm2 ligase activity	59
Figure 26: c-Src activates Mdm2 neddylation activity, dependent on Y281 and Y302	61
Figure 27: MLN4924 decreases c-Src dependent modifications of p53	63
Figure 28: Inhibition of c-Src results in loss of endogenous neddylated p53	64
Figure 29: Specific <i>in vitro</i> E2 requirement to Mdm2 by c-Src phosphorylation	65
Figure 30: Inhibition of neddylation reverses c-Src downregulation of p53 transcriptional activity	66
Figure 31: Inhibition of <i>maspin</i> promoter by c-Src is dependent on neddylation and Mdm2 Y281/Y302	68
Figure 32: Inhibition of c-Src upregulates maspin transcription and protein levels	70
Figure 33: Model of c-Src phosphorylation of Mdm2 and its downstream effects	76

Figure 34: Analysis of Mdm2 and p53 protein levels in shGFP and shMdm2 TMD-231 cells.....	81
Figure 35: Growth and cell cycle analysis of TMD-231shGFP and shMdm2 cells.....	82
Figure 36: <i>In vitro</i> invasion potential of shGFP and shMdm2 TMD-231 cells.....	83
Figure 37: <i>In vivo</i> tumor growth and final tumor weights.....	84
Figure 38: shMdm2 cells have diminished ability to bind fibronectin.....	86
Figure 39: Lung metastatic potential of shGFP and shMdm2 tumors.....	87
Figure 40: Loss of CD-31 staining in shMdm2 tumors.....	88
Figure 41: Mdm2 increases HIF-1 α and VEGF protein levels <i>in vitro</i>	90
Figure 42: Mdm2 increases HIF-1 α protein levels in tumors.....	91
Figure 43: Mdm2 augments protein levels of lung metastasis genes.....	92
Figure 44: c-Src phosphorylation of Mdm2 increases Mdm2/HIF-1 α binding.....	101
Figure 45: Neddylaton of HIF-1 α by Mdm2.....	103
Figure 46: Inhibition of c-Src impairs Mdm2's ability to enhance HIF-1 α / transcriptional activity.....	104

ABBREVIATIONS

AKT/PKB	Protein Kinase B
ATM	Ataxia telangiectasia mutated
bFGF	Basic Fibroblast Growth Factor
CK2	Casein Kinase 2
DMEM	Dulbecco's Modified Eagle's Medium
E1	Ubiquitin-Activating Enzyme
E2	Ubiquitin-Conjugating Enzyme
ECM	Extra Cellular Matrix
EGF	Epidermal Growth Factor
EGFR	Epidermal Growth Factor Receptor
EMT	Epithelial-Mesenchymal Transition
FAK	Focal Adhesion Kinase
GM-CSF	Granulocyte-Macrophage Colony-Stimulating Factor
GST	Glutathione S-Transferase
H&E	Hematoxylin and Eosin
HECT	Homologous to E6-associated protein C-terminus
HER2	Human Epidermal Growth Factor Receptor 2
HER3	Human Epidermal Growth Factor Receptor 3
HIF-1 α	Hypoxia Inducible Factor 1-alpha
HR	Hormone Receptor
HRE	Hypoxic Response Element
IGF	Insulin Growth Factor

IHC	Immunohistochemistry
IL	Interleukin
ILK	Integrin Linked Kinase
LB	Lysogeny Broth
Mdm2	Murine Double Minute 2
MMP	Matrix Metalloproteinases
mTOR	Mammalian Target of Rapamycin
NAE	Nedd8 Activating Enzyme
Nedd8	Neural Precursor Cell Expressed, Developmentally Down-Regulated Eight
NUB1	Nedd8 Ultimate Buster 1
OD	Optical Density
PE	Plating Efficiency
PHD	Prolyl Hydroxylases
PR	Progesterone Receptor
PTHRP	Parathyroid Hormone-Related Protein
RANK-L	Receptor Activator of Nuclear Factor Kappa-B Ligand
Rb	Retinoblastoma
RING	Really Interesting New Gene
RLU	Relative Luciferase Units
RSL	Reactive Site Loop
SDS-PAGE	Sodium Dodecyl Sulfate Polyacrylamide Gel Electrophoresis
SH2	Src homology 2 domain
SH3	Src homology 3 domain

SPARC	Secreted Protein Acidic and Rich in Cysteine
STATs	Signal Transducer and Activator of Transcription
TGF	Tumor Growth Factor
TNF- α	Tumor Necrosis Factor
VEGF	Vascular Endothelial Growth Factor
VEGF-R	Vascular Endothelial Growth Factor Receptor
VHL	von Hippel Lindau

1. Background and Significance

1.1 Mdm2

The murine double minute genes 1-3 (*mdm*) were identified in a transformed murine BALB/C cell line, as genes that were amplified greater than 50 fold (1, 2). The second gene product (Mdm2) was the only copy that was able to cause cellular transformation, leading to its characterization as an oncogene (3). Its characterization as an oncogene is further validated as its expression is elevated in high grade-human cancers. This overexpression of Mdm2 correlates with poor prognosis for patients. MDM2 is amplified in one-third of human sarcomas and detected at high levels (40-90%) by immunohistochemistry (IHC) in tumors of the brain, breast, ovary, cervix, lung, colon, and prostate (4, 5).

Murine Mdm2 protein contains 489 amino acids, whereas the human form is 491 amino acids. Mdm2 has several conserved functional regions: the p53 binding domain in the amino terminus, a region containing a nuclear localization sequence and nuclear export signal; a central acidic domain that is essential for ubiquitination of p53 and itself; a zinc finger which functions in Mdm2 interactions with ribosomal proteins; and a C-terminal RING finger domain that is required for dimer formation and ligase activity (Figure 1).

The C-terminal end of Mdm2 contains a RING (Really Interesting New Gene) finger E3 ligase. The main purpose of this region is to mediate the attachment of ubiquitin to substrates. While ubiquitination is normally associated with protein degradation by the 26S proteasome (6), it is also involved in cellular trafficking, endosomal sorting, polarization of neurons, and in development (7). The process of

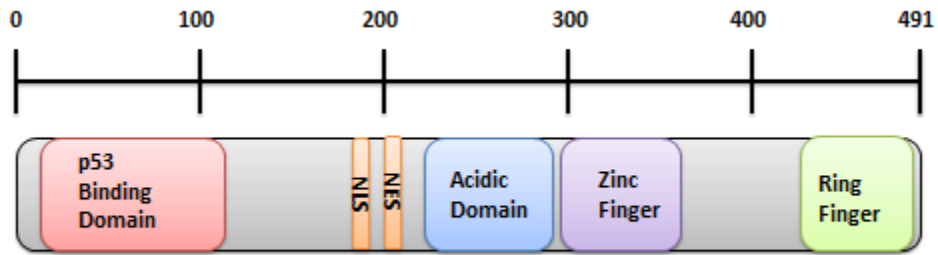


Figure 1: Schematic of Mdm2 domains

Mdm2 contains multiple protein domains that regulate its function. The N-terminus contains the p53 binding domain. The central region harbors the nuclear localization and export sequences (NLS and NES), the acidic domain, and the zinc finger. The RING finger E3 ligase is found on the C-terminus of Mdm2.

ubiquitination starts with the activation of ubiquitin by an ubiquitin-activating enzyme (E1) through an ATP-dependent reaction. The activated ubiquitin is then transferred to the catalytic cysteine of an ubiquitin-conjugating enzyme (E2). The E2 then interacts with an E3 ligase to transfer ubiquitin to the lysine of a substrate. There are three types of E3 ligases, HECT (homologous to E6-associated protein C-terminus), RING, and U-Box, a modified RING motif without the full complement of Zn^{2+} -binding ligands. HECT ligases have a direct role in transferring ubiquitin to substrates, whereas RING and U-Box ligases act as adapter proteins that facilitate protein ubiquitination. Humans have an estimated eight E1 enzymes (2 for ubiquitin) (8), around 40 E2s (28 for ubiquitin)(9), and over 600 E3s (10). Ubiquitin modification of proteins can be either mono- or poly-ubiquitination events and can take place through conjugation to any of the seven lysines or the amino terminal methionine of the ubiquitin molecule. Interestingly, specific linkage between ubiquitin may impart certain functions. Lysine 48 linkages are used as a modification for targeting proteins to the proteasome, while lysine 63 is thought to induce aggresome formation, lysosomal degradation, and protein-protein interactions (11).

The oncogenic activity of Mdm2 is attributed to its ability to bind and inhibit the tumor suppressor protein p53. Mdm2 is able to accomplish this regulation through functioning as an E3 ubiquitin ligase that signals p53 for destruction by the proteasome (12-14). p53 plays an important role in the maintenance and integrity of the genome. p53's role in cellular stress response is to function as a transcription factor, through both activation and repression, in a wide variety of cellular pathways including apoptosis, cell cycle arrest, senescence, DNA repair, and cell metabolism (15). Due to involvement of p53 in a multitude of cellular processes, it is highly regulated by many post-translational

modifications. p53 is modified on more than 36 amino acids as determined by various biochemical and cell culture studies (16).

Interestingly one target of p53 transcriptional activity is *mdm2*. Due to the negative regulation Mdm2 has on p53, an auto-regulatory feedback loop is formed, whereby p53 transcriptionally activates Mdm2, which in turn degrades p53 (Figure 2). The ubiquitination of p53 by Mdm2 has been determined to occur on 6 C-terminal lysine of p53 (K370, K372, K373, K381, K382, and K386) (16). Mutation of these 6 lysines largely prevents degradation of p53 and modulates p53 transcriptional regulation. Mdm2 can both mono- and poly- ubiquitinate p53 depending on Mdm2 levels. When Mdm2 levels rise, Mdm2 promotes p53 degradation through poly-ubiquitination. Conversely, when Mdm2 levels are low mono-ubiquitination of p53 occurs resulting in p53 nuclear export (17). Another role of Mdm2 mediated ubiquitination is to prevent p53 acetylation by p300/CBP. The lysines required for acetylation are the same lysine residues used for ubiquitination. Acetylation activates p53 allowing it to bind to p53 response elements in the genome (18).

The importance of Mdm2 in regulating p53 is shown by *in vivo* experiments in which mice lacking the *mdm2* gene are embryonic lethal, but a viable mouse can be generated if both *mdm2* and *p53* are deleted (19, 20). Interestingly, it is the function of the RING finger of Mdm2 that is vital for p53 regulation during development as knock-in mice bearing a RING mutant (C462A) of Mdm2 still die before day E7.5 but can be rescued by p53 deletion (21).

Mdm2 also functions as an E3 neddylation enzyme that conjugates the ubiquitin-like molecule neural precursor cell expressed, developmentally down-regulated eight

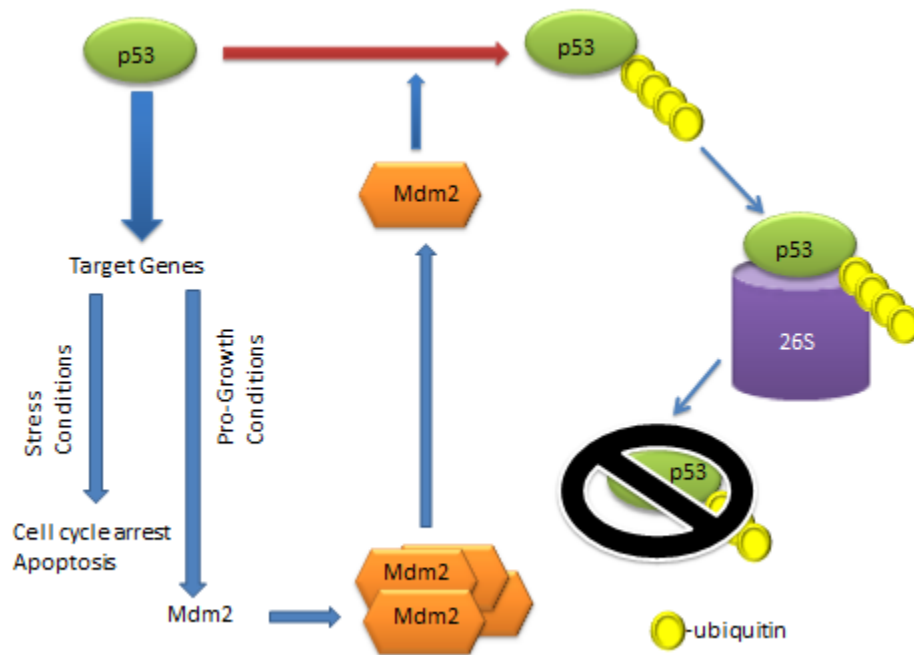


Figure 2: The Mdm2/p53 auto-regulatory feedback-loop

Under non-stressed conditions p53 transcriptionally activates Mdm2, which in turn targets p53 for degradation. This feedback loop is a primary mechanism for regulating p53 activity in normal cells.

(nedd8) to p53, which neutralizes p53 transcriptional activity (22). The nedd8 pathway has been demonstrated to be crucial for viability of mice, *C. elegans*, and *S. pombe* (23-25). In addition, the mammalian cell line TS-41, which has a temperature sensitive mutation in the SMC gene (APP-BP1 in human) participates in multiple rounds of DNA replication without entering a mitotic cycle (26). Interestingly, nedd8 conjugation has been shown to be upregulated in certain types of cancer and recently a general inhibitor of the nedd8 pathway, MLN4924, has been developed (27). Inhibition of neddylation in HCT 116 cells using MLN4924 leads to the same phenotype observed in the TS-41 cell line. This phenotype of re-replication is known to induce DNA damage and leads to apoptosis in human cancer cells and suppresses the growth of human tumors in mouse xenografts.

The most well studied and first discovered substrate of nedd8 was Cdc53 in yeast and Cul4a in humans. Both are member of the Cullin family and are neddylated at a conserved lysine in their C-terminal domain. All yeast and mammalian cullins are now known to be neddylated. The cullin family of proteins (Cul1, 2, 3, 4A, 4B, 5, 7) serves as scaffolding proteins for multi-subunit ubiquitin E3 ligases. The cullins interact in their C-terminal domain with a RING finger E3, either Rbx1 or Rbx2 and a substrate recognition subunit is attached to the N-terminal region (28). This entire complex is needed for an active ubiquitin ligase. The modification of cullins by nedd8 has been shown to increase the ubiquitin activity of cullin ring ligases. This increase in ubiquitination activity is due to a nedd8 dependent conformational change that increases Rbx binding of E2 and also decreases the distance between E2 and the substrate (29). The cullins are responsible for

the ubiquitination of numerous proteins involved in cell cycle progression and cell growth/survival (30).

While the cullins are the most studied, they are not the only proteins modified by nedd8. Many other proteins have been shown to be neddylated. Relevant to this thesis is the neddylation of p53 and Mdm2. There are two E3 ligases capable of conjugating a nedd8 to p53, Mdm2 and FBXO11 (22, 31). Conjugation of a nedd8 molecule to p53 inhibits its transcriptional activity. This was shown as the TS-41 cells, which have a temperature sensitive mutant of the Nedd8 Activating Enzyme (NAE), show higher levels of p53 activity when grown at the restrictive temperature (39° C). Also a fusion protein of p53 with a nedd8 attached to the C-terminal end resulted in lower activity as determined by luciferase activity from the p21 promoter (31). The sites neddylated by Mdm2 are lysines K370, K372, and K373 whereas FBXO11 neddylates K320 and K321 (22). The actual mechanism of p53 transcriptional inhibition by neddylation is still under investigation. Unlike mono-ubiquitination of p53, which results in the movement of p53 from the nucleus to the cytoplasm, neddylation by itself has no effect on p53 cellular compartmentalization (32). However expression of a nedd8 interacting protein, Nedd8 ultimate buster 1 (NUB1), has been shown to enhance cytoplasmic p53 through an Mdm2/nedd8 dependent pathway (33). This mechanism cannot be fully responsible for inhibition though, as neddylated p53 was still detectable in the nucleus, even with overexpression of NUB1. Mdm2 itself has also been shown to be neddylated (22). This neddylation modification results in an increase in Mdm2 protein half-life. This is reversed when NEDP1 (a human nedd8-specific protease) removes nedd8 from Mdm2.

Moreover, NEDP 1 which can be induced by chemotherapeutics, and thus help to activate p53 (34).

There are numerous splice variants of *mdm2* mRNA and multiple isoforms of the Mdm2 protein have been identified in tumors and normal tissues (35). Two of these isoforms, p75 and p90, predominate in cells and migrate at 75 and 90 kDa on sodium dodecyl sulfate polyacrylamide gels. The 90 kDa form of Mdm2 is transcribed from the p53 responsive P2 promoter of Mdm2. This transcript results in a full length Mdm2 protein capable of regulating p53. Along with p53, the P2 promoter has been shown to be responsive to AP-1, SP-1, and Smad3 transcription factors (11, 36, 37). The 75 kDa form is produced from the constitutive P1 promoter independent of p53. This 75 kDa form lacks the N-terminus of Mdm2 due to initiation of translation at two different internal AUG codons (AA 62 and 102) rendering Mdm2 incapable of binding to p53. PTEN has been shown to inhibit p75 Mdm2 transcription indirectly by modulating the activity of unknown transcription factor(38). Meanwhile, the only transcription factor that has been shown to induce expression from the P1 promoter is NF- κ B (39). The biological relevance for p75 Mdm2 is currently under investigation. Interestingly *mdm2* transcripts initiated from P1 undergo removal of exon 2 by splicing and retain exon 1; meanwhile p2 transcripts lack exon 1, and retain exon 2 (Figure 3).

The Mdm2 protein is highly modified by multiple site phosphorylation events that can alter its protein interactions, localization, stability, and its functions as an ubiquitin ligase. These modifications are clustered into three groups (Figure 4). The first group is around the nuclear localization/export signals, which are stimulated in response to growth factor and mitogenic signaling. The second is a group of eight sites that are found

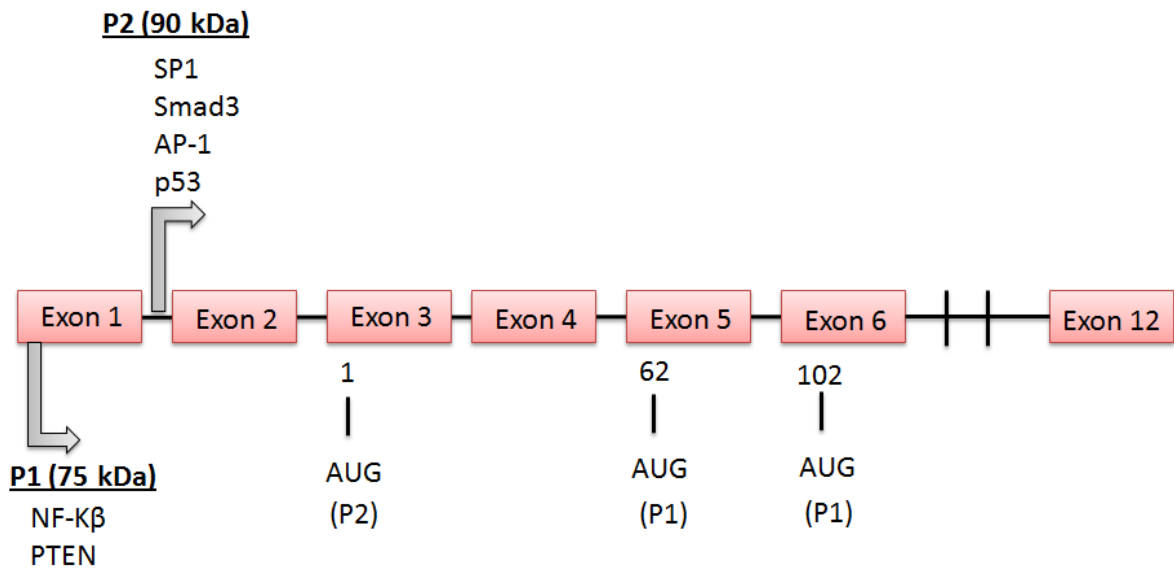


Figure 3: Organization of the human *mdm2* gene

The *mdm2* gene contains two unique promoters. P1 is a constitutive promoter, and P2 is the p53-responsive promoter. The translation start codons are indicated for each promoter. Initiation of translation from the P1 promoter results in an N-terminal truncated Mdm2 protein.

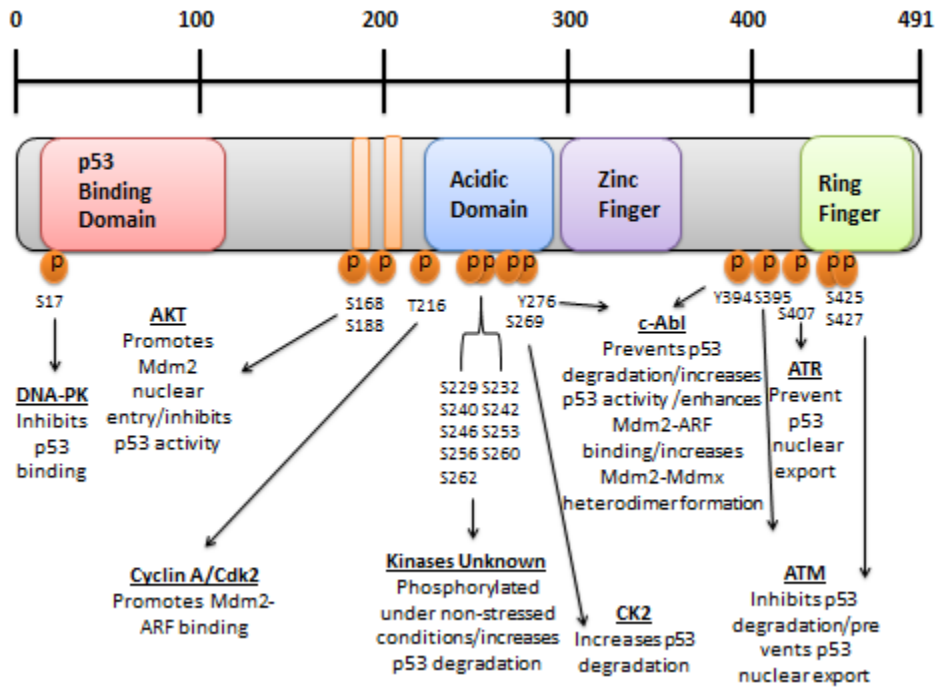


Figure 4: Known phosphorylation sites on Mdm2

Phosphorylation sites are indicated by (P). Protein kinases (if known) and the effects of phosphorylation events are indicated.

between amino acids 240-269. The final group is mostly clustered at the carboxyl-terminus and becomes phosphorylated in response to DNA damage. The phosphorylation sites around the bipartite NLS contain two Protein Kinase B (AKT/PKB) sites at 166 and 186. This phosphorylation event is triggered by insulin growth factor (IGF) and results in the nuclear accumulation of Mdm2, which binds p53 and inhibits its transcriptional activity (40). In the acidic domain, T216 of murine Mdm2 has been shown to be phosphorylated by cyclinA/cdk. This modification results in stabilization of p53 and is permissive of p19ARF binding (41, 42), a negative regulator of Mdm2. Casein Kinase 2 (CK2) phosphorylation of Mdm2 at S269 impairs Mdm2/Retinoblastoma (Rb) interaction and allows the binding of Mdm2 to the basal transcription factor TFII250 (43). Also under basal growth conditions, it has been suggested, that a group of serines located in the acidic domain are phosphorylated. Through use of mutation analysis it has been suggested that these phosphorylated serines promote Mdm2-mediated p53 turnover, although the kinases responsible for these events are still undefined (Figure 4).

Many studies have focused on Mdm2 phosphorylation in response to genotoxic stress. Ataxia telangiectasia mutated (ATM) has been shown to phosphorylate Mdm2 in response to DNA damage at S395 and block nuclear export of p53 (44). Additional ATM sites at S386, S425, and S428 all inhibit p53 degradation by preventing Mdm2 E3 oligomerization (45). Ataxia telangiectasia and Rad3-related protein (ATR) phosphorylates Mdm2 at S407 and also prevents p53 nuclear export under certain stress conditions (46). An additional phosphorylation site triggered by DNA damage at serine 17 is phosphorylated by DNA protein kinase (DNA-PK), an enzyme activated in

response to DNA double strand breaks. This phosphorylation event prevents Mdm2 interaction with p53 *in vitro* and activates p53 transcriptional activity (Figure 4) (47).

Interestingly there are only two known tyrosine kinases for Mdm2. The first, c-Abl, phosphorylates Mdm2 at Y394 and results in an increase of apoptosis by enhanced stability of p53. This increase in p53 stability is due to a c-Abl dependent promotion of Mdm2-Mdmx heterodimers, which enhances the degradation of both Mdm2 and Mdmx (48). c-Abl also phosphorylates Mdm2 at Y276 and results in enhanced p19ARF binding, sequestering Mdm2 from p53 (49). The other tyrosine kinase is ErbB-4. Phosphorylation of Mdm2 by ErbB-4 results in stabilization of p53 and increases Mdm2 ubiquitination (50). However the tyrosine(s) in Mdm2 have yet to be identified (Figure 4).

While the most studied function of Mdm2 is attributed to its regulation of p53, Mdm2 has been shown to engage in many p53 independent activities. Mdm2 has been implicated in cell cycle control, differentiation, DNA repair, basal transcription, and other processes. Some of Mdm2 p53-independent protein-protein interactions are detailed in Table 1.

1.2 c-Src

v-Src was originally isolated as the transforming agent in the Rous sarcoma virus (21). Its cellular counterpart c-Src is a member of the Src Family Kinase, a family of membrane associated non-receptor tyrosine kinases including: c-Src, c-Yes, Fyn, Lyn, Lck, Hck, Blk, Fgr, and Yrk. While most of the family members are expressed in the hematopoietic origin, c-Src shows more ubiquitous expression and is involved in many

Mdm2 Binding

Partner	Results of Mdm2 Binding
p73	Inhibits p73 transcriptional activity (does not degrade)(51, 52)
p19(ARF)	Blocks Mdm2/p53 binding(42)
Rb	Inhibits Mdm2-E2F1 binding(53)
E2F1	Stabilizes E2F1 protein levels (54)
PCAF	Ubiquitinates and degrades Mdm2(55)
JMY	Transcriptional activator that is degraded by Mdm2 (56)
Histone H2B	Mdm2 mono-ubiquitinates H2B
L5	Inhibits Mdm2 ligase activity (57)
L11	Inhibits Mdm2 ligase activity (58)
L23	Inhibits Mdm2 ligase activity (59)
PML	Sequesters Mdm2 to nucleolus (60)
Nbs1	Mdm2/Nbs1 binding inhibits onset of DNA repair(61)
DNA Polymerase ϵ	Stimulates DNA Polymerase ϵ enzymatic activity(62)
E-Cadherin	Mdm2 ubiquitinates and degrades E-cadherin (63)
HIF-1 α	Enhances HIF-1 α transcriptional activity(64)
NUMB	Mdm2 ubiquitinates and degrades Numb(65)
SCF(beta-TRCP)	Ubiquitinates and degrades Mdm2(66)

Table 1: Mdm2 binding partners

cellular processes including proliferation, survival, motility, invasiveness, and angiogenesis (22).

c-Src contains an amino-terminal membrane localization sequence in the SH4 domain that requires myristylation for localization. c-Src also contains Src homology domain 2 (SH2) and Src homology 3 domain (SH3) that mediate protein-protein interactions, a tyrosine kinase domain, and a regulatory sequence at the carboxyl-terminal end (Figure 4). SH3 domains generally bind to proline rich motifs with the minimal consensus P-x-x-P (23), while SH2 domains bind phosphorylated tyrosines (24). c-Src activity is regulated through phosphorylation and intra-molecular interactions. Phosphorylation of c-Src by C-terminal Src Kinase (CSK) at Y530 results in inactivation due to intermolecular binding between phosphorylated Y530 and the SH2 domain, resulting in a “closed” conformation of the protein (25, 26) (Figure 5). The v-Src protein has a C-terminal deletion resulting in loss of inhibitory phosphorylation on Y530.

Activation of c-Src can result from dephosphorylation of the Y530 by a protein phosphatase. Protein tyrosine phosphatase (PTP)-alpha, PTP1, PTP1B, and SH2-containing protein tyrosine phosphatase-1 (SHP-1) have all been implicated in c-Src activation (27, 28). c-Src activity can be augmented by higher intermolecular binding of the SH2 and SH3 between cellular ligands, such as platelet-derived growth factor receptor (PDGFR) or focal adhesion kinase (1) (29, 30). This activation of c-Src results in its open conformation with greater access to the SH2 and SH3 binding domains. For full activation, c-Src must undergo auto-phosphorylation at Y419 in its catalytic domain.

c-Src is rarely mutated in human cancers. Only a small set of colon cancer patients have been found to have an activating mutation similar to v-Src. Elevated levels

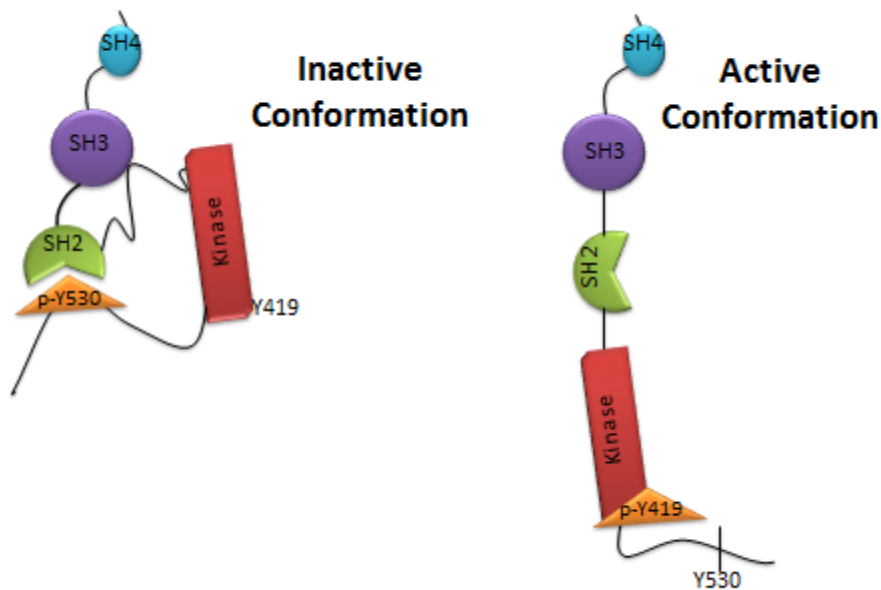


Figure 5: Structure and activation of c-Src

c-Src contains four homologous domains. The SH4 contains a myristoylation sequence and supports plasma membrane binding. The SH3 domain is a proline rich sequence that binds and interacts with other proteins. The SH2 domain recognizes phosphorylated tyrosine residues and regulates binding to other proteins. The SH3 and SH2 domains also function in intra-molecular interactions. The Y419 is located in the kinase domain and is auto-phosphorylated during activation. c-Src activation is regulated by the phosphorylation status of Y530. When phosphorylated, c-Src is in an inactive conformation due to p-Y530 binding to the internal SH2 domain. When dephosphorylated the conformation of c-Src opens allowing for activation.

of c-Src protein or an increase in activity are more commonly observed in human cancers. This is seen in cancers of the lung, breast, colon, and skin (67-69). Even though c-Src is involved in multiple pathways important for tumorigenesis and is seen at elevated levels in human cancers, c-Src itself is not a strong transforming oncogene (70). This has led to the hypothesis that c-Src can help facilitate the oncogenic roles of other proteins rather than being a strong autonomous transforming agent. To aid in tumorigenesis c-Src interacts with numerous tyrosine receptor kinases and other proteins implemented in cancer progression including PDGFR, vascular endothelial growth factor (VEGFR), epidermal growth factor receptor (EGFR), human epidermal growth factor receptor 2 (HER2), human epidermal growth factor receptor 3 (HER3), signal transducer and activator of transcription (STATs), heteromeric G proteins, cyclin D and E, and FAK (71). This diverse list shows c-Src integration in numerous cellular processes and how many different pathways c-Src may augment for cancer development.

1.3 Cancer Metastasis

Metastasis is a multi-staged process that cancerous cells undergo to relocate from their primary location to a distant site. Metastasis usually correlates with a poor prognosis and often results in death due to lack of treatment options. For metastasis to occur, tumor cells must first invade into the surrounding tissue of the primary site. This is followed by entrance into the circulation system, either through the lymph nodes or blood, where the tumor cell must survive until it can find a distal site suitable for growth (Figure 6).

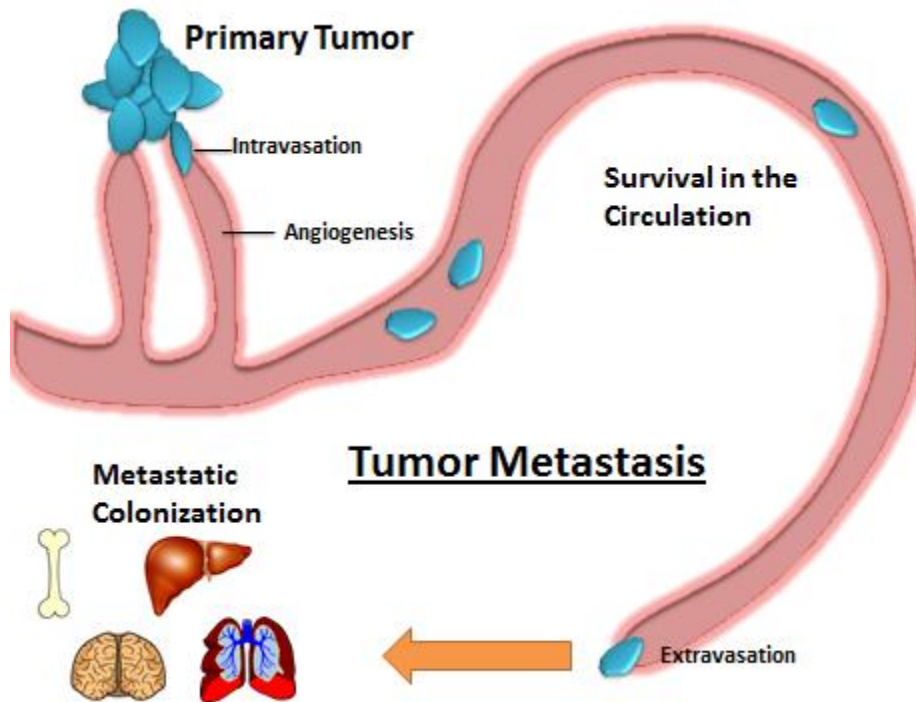


Figure 6: The tumor metastatic process

Metastasis of a tumor to a distal tissue involves a three-step process: First, tumor cells must be able to leave the primary tumor site and invade the vasculature. Second, they must survive in the bloodstream until they can arrest and extravasate into surrounding tissue. Finally they must interact with the microenvironment to establish metastatic colonization.

For a tumor cell to enter into the primary site around the tissue, it must lose contact from its surrounding cells and to the extra-cellular matrix. The contacts between cells are usually mediated by the cell attachment proteins of the cadherin family, which bind cells together through their extracellular domains (72). Loss of E-cadherin is a hallmark of epithelial-mesenchymal transition (EMT), which is defined by loss of epithelial characteristics including apical-basal polarity, tight junctions, expression of E-cadherin, and decreased cell mobility. The loss of these characteristics are combined with the gain of mesenchymal phenotype markers such as increases in vimentin and myosin expression, loss of polarity, and an increase in cellular mobility (73). Tumor cells are bound to the extra cellular matrix (ECM) through heterodimers of one alpha and one beta integrin protein. The alpha family consists of 18 members while the beta has 8. Each heterodimer binds to a specific protein of the ECM (74). For a tumor cell to begin to invade into surrounding tissues it must release its attachment to cells and ECM. This is accomplished through the use of proteases that degrade the ECM and attachments. The family of matrixmetalloproteinases (MMPs) is responsible for the breakdown of extracellular matrix. MMPs are normally secreted in an inactive form and are activated upon cleavage by extracellular enzymes (75).

Tumors first need to recruit a blood supply to aid in the metastatic process. The formation of new blood vessels from pre-existing ones is termed angiogenesis. Angiogenesis is required in order to support the growth and survival of tumors by delivering oxygen and other nutrients and metabolites to the tumor cells (76). Angiogenesis is simulated by pro-angiogenic factors that must counteract anti-angiogenic factors. Thus, the angiogenic switch will commence when the pro-angiogenic factors

outnumber the inhibitors. Important to this thesis are the roles of the pro-angiogenic molecule vascular endothelial growth factor (VEGF) and the anti-angiogenic molecule Maspin. The VEGF and the VEGF receptor (VEGF-R) pathway is one of the most studied pro-angiogenic factors. Multiple signaling networks are activated in response to VEGF/VEGF-R signaling and result in endothelial cell survival, mitogenesis, migration, and differentiation. VEGF also increases vascular permeability and initiates the mobilization of endothelial progenitor cells from the bone marrow into the peripheral circulation. The permeability induced by VEGF leads to access for the pro-angiogenic factors to enter the vessels and facilitate angiogenesis. VEGF activates its angiogenic switch through binding to one of three VEGF receptors. VEGF-R1 is responsible for most physiologic and developmental neo-vascularization (77). VEGF-R2, meanwhile, mediates the majority of the downstream effects of VEGF in angiogenesis, including microvascular permeability, endothelial cell proliferation, invasion, migration, and survival (78). VEGF-R3 is a receptor tyrosine kinase that is expressed mainly during development in the embryonic vasculature but is only expressed in lymphatic endothelial cells in adults (79). Due to its role in numerous cancers and angiogenesis, the VEGF/VEGFR pathway has been targeted clinically with drugs that inhibit both VEGF and VEGF-R.

Due to the prominent role VEGF plays in angiogenesis, understanding VEGF regulation is very important. VEGF is regulated in numerous ways including by oncogenes/tumor suppressor, transcription factors, and environmental factors. Important for this thesis is the regulation of VEGF by decreases in oxygen concentration, termed hypoxia, and the transcription factor hypoxia inducible factor 1-alpha (HIF-1 α). In

response to hypoxic conditions, cells must adapt by changing metabolic, bioenergetic, and redox demands for oxygen. To support these changes, cells must lower demands for growth, conserve energy, and induce survival and pro-angiogenic factors. While many pathways regulate the hypoxic response, including mammalian target of rapamycin (mTOR) and the unfolded protein response, the main transcription factor to mediate a transcriptional response to hypoxic conditions is HIF-1 α . The transcriptional response driven by HIF-1 α is dependent on its ability to bind canonical DNA sequences, called hypoxia response elements (HRE), in the promoter of target genes. HIF-1 α is a member of the bHLH-PAS family of transcription factors. The active transcription factor consists of a dimer combining a HIF- α and HIF- β subunit. The regulation of the HIF transcription factor resides in the stability of the α -subunit, of which 3 are known. The α -subunit is constitutively expressed but in the presence of oxygen the α -subunit is ubiquitinated and degraded by the von Hippel Lindau (VHL) protein through the 26S proteasome. This degradation takes place due to hydroxylation of HIF-1 α under normal oxygen conditions. These hydroxylation events, performed by specific prolyl hydroxylases (PHD), occur on proline 402 and 564 in the oxygen dependent degradation domain of HIF-1 α (80). These proline modifications allow for the binding of VHL, which serves as the substrate recognition component of an E3 ubiquitin ligase complex (Figure 7) (81). Under oxygen deprivation, the proline hydroxylases are inactive resulting in a stabilization of the HIF-1 α subunit. Once stabilized HIF-1 α subunits travel to the nucleus and dimerize with the HIF- β subunits and transcribe at least 150 genes that regulate cell metabolism, survival, motility, basement membrane integrity, angiogenesis, hematopoiesis, and other cellular functions (Figure 6) (82).

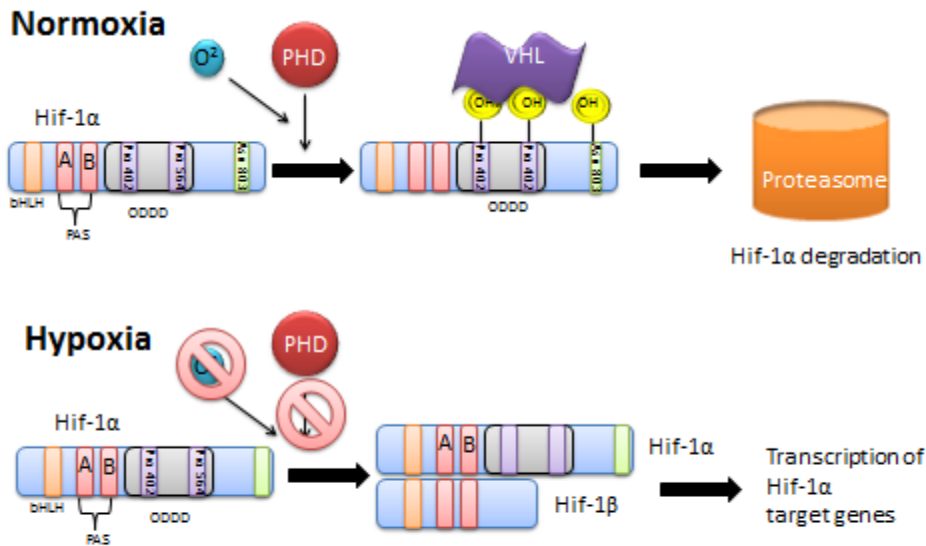


Figure 7: HIF-1 α /VHL pathway

Under normoxic conditions HIF-1 α is hydroxylated on proline 402 and 564 by prolyl-hydroxylases (PHD). This allows for the binding of VHL which ubiquitinates and degrades HIF-1 α . Under hypoxic conditions, PHD's are not active resulting in stable HIF-1 α , which can interact with HIF-1 β and activate hypoxic response genes.

One anti-angiogenic factor counteracting VEGF is the p53 induced tumor suppressor Maspin. The *maspin* gene was discovered by subtractive hybridization by its expression of mRNA in normal but not tumor-derived mammary epithelial cells (83). It has been classified as a member of the serpin protease inhibitors family and further defined as a member of the ov-serpin subfamily. This subfamily consists of thirteen members, including plasminogen activator inhibitor 1 and 2, which are involved in angiogenesis, apoptosis, and embryogenesis. All ov-serpin proteins have serine protease inhibitor function, except for maspin (84). This inhibition is accomplished through a conformational change in the serpin reactive site loop (RSL) upon binding to the protease resulting in a covalent bond between the RSL and the catalytic site of the protease. Maspin however does not appear to be a protease inhibitor. Maspin RSL is not conserved and is shorter than all other family members and does not undergo conformational changes (85). Interestingly, maspin is the only ov-serpin whose deficiency is embryonic lethal in mice (86).

The tumor suppressor functions of Maspin are attributed to its roles in cell migration/invasion, angiogenesis, and apoptosis (87-89). For angiogenesis to occur, vessel endothelial cells must be activated by factors (such as VEGF) that allow it to escape from the vessel walls. Once free, these endothelial cells can participate in the formation of new vasculature in tumors. Cell adhesion and migration regulate the release of endothelial cells from the original vessel. Maspin regulates this process by increasing endothelial adhesion to fibronectin, laminin, and collagen. This binding is increased through upregulation of integrin-linked kinase (90) and FAK signal transduction pathways that regulate attachment and focal adhesion disassembly (87). This prevents the

release and migration of endothelial cells from established vasculature. This is validated *in vivo* as treatment with recombinant Maspin resulted in a loss of vessel formation, as determined by CD31 staining, in tumors of nude mice. Also, Maspin effectively blocked neovascularization mediated by basic fibroblast growth factor (bFGF) in rat corneas (91). For its role in apoptosis, maspin mainly functions through the down-regulation of the anti-apoptotic protein Bcl-2, although the exact mechanism is still unknown. This downregulation of Bcl-2 allows Bax, an apoptotic inducing protein, to become active thus increasing mitochondria membrane permeability (92, 93).

Once angiogenesis has taken place and the tumor cells are able to access the vasculature, they must be able to survive in this new environment. This survival requires evading immune cells and avoiding anoikis, cell death due to detachment from a substratum. Beyond survival, tumor cells must at some point stop circulating (arrest) to allow them to escape from the vessels. Arrest is mediated by tumor cells through regulation of their own integrins and also by binding to coagulation factors (94, 95). It has been proposed that vessel endothelial cell selectin molecules may also aid in tumor cell arrest (96). Also, some cancer cells arrest due to size restriction of the capillaries.

The final stage of metastasis involves the colonization of a distal site. Interestingly, most cancers show a predisposition to metastasize to certain organs. This observation has led researchers to search for genes that identify specific organ metastasis (97). One example is the multitude of work that has been done on the requirements for breast cancer to bone metastasis. Breast cancer cells form osteolytic metastases through the regulation of osteoclast activating factors parathyroid hormone-related protein (PTHrP), interleukin (IL)-11, IL-6, tumor necrosis factor (TNF)- α , granulocyte-

macrophage colony-stimulating factor (GM-CSF), and receptor activator of nuclear factor kappa-B ligand (RANK-L). These factors are essential for the growth of osteolytic lesions in the bone environment, but would offer no advantage to another metastatic site or the tumor (98). Interestingly, c-Src has also been implicated in breast to bone metastasis through its regulation of bone remodeling. c-Src knockout mice develop osteopetrosis due to deficiency in bone remodeling (99). Mice injected with MDA-231 breast cancer cells overexpressing c-Src have more osteolytic bone metastases than control mice, linking c-Src to bone colonization (100).

2. Materials & Methods

2.1 Cell Culture

All mammalian cells were cultured at 37 °C in a humidified incubator with 5% CO₂ in Dulbecco's modified Eagle's medium (DMEM) high glucose supplemented with 10% fetal bovine serum and penicillin-streptomycin solution. shGFP and shMdm2 TMD-231 cells were kept under constant selection with puromycin (2 µg/ml).

2.2 Transfection

Cells were transfected using the calcium phosphate method or Lipofectamine (Invitrogen). For calcium phosphate method plasmid DNA (1-5 µg), water (130 µl), and 2M CaCl₂ (17 µl) were mixed to a total volume of 150 µl. This mixture was then added dropwise to 150 µl of 2X HBS (275 mM NaCl, 1.5 mM Na₂HPO₄, 50 mM HEPES, pH 7.0) while vortexing. Solution was incubated for 30 min at RT before adding dropwise to cells. This (300 µl) amount is used for an individual well of a 6 well plate. For 10 cm dishes volumes are raised to 500 µl each, for a total of 1 ml transfection reagent. DNA concentration was also raised to 5 µg. Lipofectamine transfections were done according to manufacturer's protocol.

2.3 Generation of shGFP and shMdm2 TMD-231 cell lines

Retroviruses encoding shRNA to GFP and Mdm2 (pLKO.1 vector) were packaged in 293T cells together with second-generation packaging constructs, pCMV-dR8.74 and pMD2G. Supernatant media containing virus were collected at 36 to 48 hours, supplemented with 4 µg/mL polybrene, filtered through a 0.45-µm filter, and

added to cells overnight. Uninfected cells were removed by selection with puromycin (2 $\mu\text{g}/\text{mL}$).

2.4 Luciferase Assays

For the luciferase assays, H1299 and MCF7 cells were transfected with PG13-Luc, Mdm2-P2-Luc, Maspin-Luc, Mutant Maspin-Luc (MT1) or HRE-Luc along with Myc-LacZ for determination of β -galactosidase activity, using the calcium phosphate method. Reporter activity was normalized to β -galactosidase activity. Data generated were done in triplicate and standard deviation was calculated from the mean.

2.5 Glutathione S-Transferase-pull down assay

GST-SH3-Src and GST alone for control were incubated with glutathione-sepharose beads that had been pre-washed in TEN100 Buffer (20 mM Tris, pH 7.4, 0.1 mM EDTA and 100 mM NaCl) for 1 hr at 4° C. After GST-proteins were immobilized the complexes were spun down and washed four times for 15 min each with TEN100. After washing, recombinant His-Mdm2 was incubated with immobilized GST-SH3-Src or GST for 1 hr at 4° C. After complexes formed, they were spun down and were washed four times in NTEN Buffer (.5% NP40, 1 mM EDTA, 20 mM Tris, pH 7.4, 1 M NaCl). The bound proteins were eluted in SDS-Loading Buffer and western blot analysis was performed.

2.6 Cloning of Mdm2 mutants

2.6.1 Wild-Type Mdm2

Wild-type Mdm2 was subcloned from a pCDNA 3.1 expression plasmid into the pRSETA vector for protein purification using BamHI and PstI restriction enzyme sites (Figure 8).

2.6.2 Mdm2 90-383

90-383 deletion mutant of Mdm2 was cloned using two internal HindIII site in wild-type Mdm2. The 90-383 piece liberated from WT Mdm2 was cloned into the pRSETA vector for protein purification using the HindIII site. Sequence analysis was performed to ensure proper orientation, as this was a non-directional cloning procedure (Figure 8).

2.6.3 Mdm2 4-268

The 4-268 deletion mutant of Mdm2 was sub-cloned from the PGEX 4T3 vector using EcoRI and subcloned into the pRSETB vector using the same site. Sequence analysis was performed to ensure proper orientation, as this was a non-directional cloning procedure (Figure 8).

2.6.4 Mdm2 102-491

The 102-491 deletion mutant of Mdm2 was generated by PCR amplification. The DNA fragment was cloned into pRSETA for protein purification using BamHI and PstI restriction sites (Figure 8).

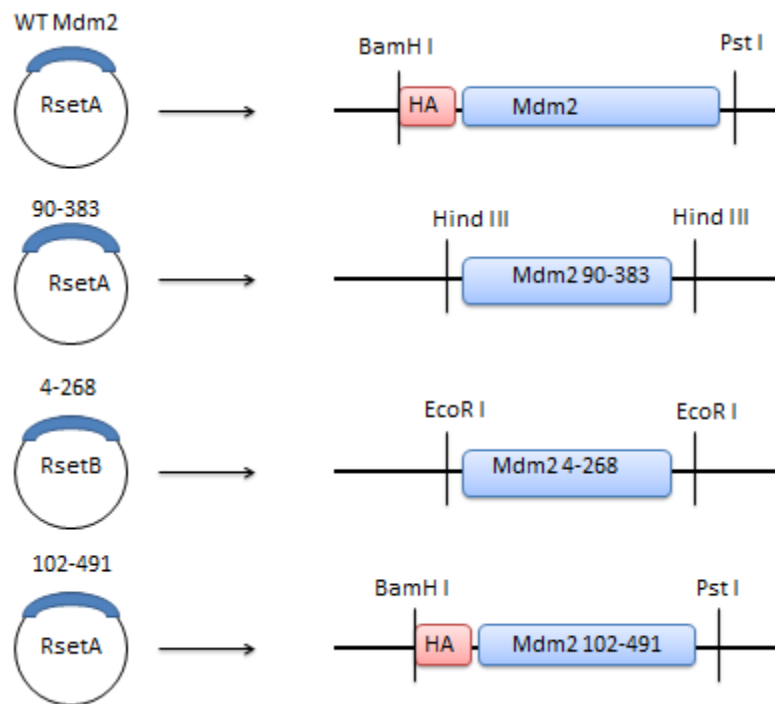


Figure 8: Restriction sites used for cloning of Mdm2 truncation mutants
 All mutants were cloned in the designated pRSET vector for protein purification. HA represents a human influenza hemagglutinin tag.

2.7 His-ubiquitin and His-Nedd8 pulldowns

H1299 cells were transfected with His-ubiquitin or His-nedd8 and other plasmids using calcium phosphate method. Forty-eight hr after transfection cells were lysed in 1 ml of 6 M guanidinium-HCl, 0.1 M Na₂HPO₄/NaH₂PO₄, 0.01 M Tris-HCl pH 8.0 plus 5 mM imidazole and 10 mM β-mercaptoethanol. After sonication, the lysates were mixed with 30 μl of Ni²⁺-NTA-agarose beads (Qiagen) prewashed with lysis buffer and incubated for 2 hr at room temperature. The beads were successively washed for 15 min in each of the following: 6 M guanidinium-HCl, 0.1 M Na₂HPO₄/NaH₂PO₄, 0.01 M Tris-HCl pH 8.0 plus 10 mM β-mercaptoethanol; 8 M urea, 0.1 M Na₂HPO₄/NaH₂PO₄, 0.01 M Tris-HCl pH 8.0, 10 mM β-mercaptoethanol; 8 M urea, 0.1 M Na₂HPO₄/NaH₂PO₄, 0.01 M Tris-HCl pH 6.3, 10 mM β-mercaptoethanol (Buffer A) plus 0.2% Triton X-100; buffer A and then buffer A plus 0.1% Triton X-100. After the last wash with buffer A the beads were eluted with 200 mM imidazole in 5% SDS, 0.15 M Tris-HCl pH 6.7, 30% glycerol, 0.72 M β-mercaptoethanol. Elutes were subjected to sodium dodecyl sulfate polyacrylamide gel electrophoresis (SDS-PAGE) and western blotting.

2.8 Purification of recombinant proteins

For purification of His-tagged proteins a 50 ml culture of BL-21 *Escherichia coli* was grown overnight at 37° C at 25,000 rpm. On the day of purification the culture was reseeded in 200 ml of Lysogeny broth (LB) to a 0.1 optical density (OD) value. The bacteria were allowed to grow to 0.6 OD before the induction with 100 mM of Isopropyl-β-D-thio-galactoside (IPTG). Induction was performed at 24° C for four hr. After

induction cells were spun down at 6000 rpm for 10 min and resuspended in Buffer A (25 mM Hepes, 0.2% TX-100, 5 mM DTT, 1 M KCL) and sonicated 4 times for 30 sec on ice. After centrifugation at 10,000 rpm for 25 min at 4° C, the supernatant was removed and 40 µl of pre-washed (Buffer A) Ni-NTA slurry (Qiagen) was added. Binding was allowed to occur for 30 min at 4° C. Complexes were spun down at 1500 rpm for 5 min and then washed six times for 15 min in Buffer B (Buffer A+10 mM imidazole). Proteins were then for eluted in Buffer C (Buffer A+300 mM imidazole) and dialyzed into Dialysis Buffer (50 mM HEPES pH 7.5, 100 mM NaCl, 10% glycerol, 1 mM DTT).

2.9 In vitro kinase reactions

Src and Abl kinase reactions were performed at 37 °C for 30 min in kinase buffer (25 mM Tris, pH 7.4, 10 mM MgCl₂, 1 mM MnCl₂, 0.5 mM DTT, 10 µM ATP) using 0.1 µg of Src (Calbiochem) or Abl (Invitrogen).

2.10 In vitro ubiquitination reactions

For *in vitro* ubiquitination assays; 500 ng of p53 was incubated with 50 ng E1 (Boston Biochem), 200 ng Ubch5a (Boston Biochem), and 1 µg ubiquitin (Boston Biochem) in the presence of 500 ng phosphorylated or unphosphorylated Mdm2. Reactions were performed for 2 hr at 37° C.

2.11 Protein analysis, immunoprecipitation, and Western blotting

Whole cell extracts lysates were prepared in Nonidet P-40 lysis buffer (25 mM Tris, pH 8.0, 150 mM NaCl, 0.5 mM EDTA, 0.5 mM EGTA, 1% Nonidet P-40, 1 mM

sodium orthovanadate, 1 mM dithiothreitol (DTT)) and supplemented with protease inhibitor mixture set III (Calbiochem) at 1:100 and incubated on ice for 30 min. Debris was collected by centrifugation, and supernatant collected. Protein concentration was determined using Bradford assay. For immunoprecipitation assays 500 µg of lysates were incubated over night with antibody at 4 °C in 700 µl of PBS. 20 µl of pre-washed Protein A/G Plus Agarose (Santa Cruz Biotechnology) was added to the mixture and incubated an additional 4 hr at 4 °C, precipitates were washed three times in PBS, and samples were resuspended in SDS loading buffer.

2.12 Cell cycle analysis

TMD-231 shGFP or shMdm2 cells were serum starved for 24 hr. After serum starvation, cells were given 1% serum for 0, 8 and 24 hr. Cells were then harvested and resuspended in 1.2 mL of PBS. 3 mL of 100% ethanol was then added dropwise to cells, while vortexing. The cells were then fixed in this 70% ethanol solution for 30 min. After fixing, cells were spun at 2200 rpm for 10 min and washed twice in 15 mL of PBS. Pellets were resuspended in 4.5 mL of PBS and 0.5 mL RNase stock (1 mg Rnase/1 mL H₂O) and incubated for 30 min at 37° C. After incubation cells were washed twice in PBS and resuspended in 2 mL propidium iodide (PI) stain solution (10 mg PI/100 mL PBS) at a final concentration of 1×10^6 cells/mL. The cells were analyzed on a flow cytometer. ModFit analysis determined the percentage of cells in a specific stage of the cell cycle.

2.13 Plating Efficiency

TMD-231 shGFP and shMdm2 cells were counted and plated from a single cell suspension for clonogenic survival. Cells grew for 14-21 days at 37°C. Cells were then fixed with a 3:1 methanol/acetic acid mixture and stained with crystal violet. Colonies with ≥ 50 cells were included in the survival analysis. Plating efficiency (PE) was determined by number of colonies counted divided by number of cells plated.

2.14 Cell Attachment Assay

Six-well plates were coated with 5 $\mu\text{g/ml}$ fibronectin at 37 °C for 1 hr, washed twice with PBS, and then incubated with 1% bovine serum albumin at 37 °C for 1 hr. Plates were then washed twice with PBS. 2×10^4 TMD-231 shGFP or shMdm2 cells were plated with 2 ml of culture medium per well and incubated in the 37 °C, incubator for 30 min. The culture medium was removed and cells were washed twice with PBS, trypsinized and counted on a Beckman Coulter Cell Analyzer.

2.15 Matrigel Invasion Assay

2.5×10^4 cells were seeded in into each well of matrigel chambers. 5% serum was used as the chemoattractant. The chambers were incubated for 22 hr in a humidified tissue culture incubator, at 37° C, 5% CO₂. After incubation the media was removed and the surface of the membrane was scrubbed using a cotton tip swab, to ensure removal of non-invading cells. After scrubbing, the membranes were removed from the chambers and stained in methanol for 2 min followed by 1% toluidine blue for 2 min. The chambers were counted at magnification of 20X. Multiple fields for each set were counted and the

experiment was done in triplicate. Percent invasion was calculated using the following equation.

$$\% \text{ Invasion} = \frac{\text{Mean \# of cells invading through Matrigel insert membrane}}{\text{Mean \# of cell migrating through control insert membrane}} \times 100$$

2.16 Assessment of tumorigenicity *in vivo*

The Indiana University *In Vivo* Therapeutics Core was responsible for all animal work. 7.5×10^5 cells of either TMD-231 shGFP or ShMdm2 cells were injected into the mammary fat pad of γ -null NOD-SCID mice (n=10 per group). All mice developed tumors. Tumor growth was calculated by volumetric analysis using calipers. The tumors were allowed to grow to an average volume of 600 mm.

2.17 Tissue preparation and staining

The Indiana University Pathology Core performed all tumor preparation and staining for hematoxylin & eosin (H&E) and CD31.

2.18 Lung metastasis evaluation

The right and left lobe of the lungs from each mouse was stained with H&E and mounted on a slide. The entire lung of each mouse was scored for metastases. A metastatic legion was defined as ≥ 5 tumor cells.

3. c-Src phosphorylates and switches Mdm2 to a neddylation enzyme

3.1 Introduction

As previously described, c-Src is one of the 9 members of the Src-family kinases. It is a cytoplasmic non-receptor tyrosine kinase that is a critical initiation site for multiple signal transduction pathways and interactions.

One of the downstream effectors of c-Src is the survival factor Akt. Akt has been shown to phosphorylate many substrates to promote cell survival including Mdm2 (40, 101). Mdm2 undergoes nuclear translocation in response to Akt phosphorylation at serine 166 and 186 (40). Once in the nucleus Mdm2 binds to the tumor suppressor p53 and inhibits its transcriptional activity along with functioning as an E3 ubiquitin ligase to signal nuclear export and proteasomal degradation. While normally kept at low levels, p53 is stabilized through post-translational modifications to both itself and Mdm2 in response to genotoxic stress (102). While the ubiquitin ligase activity of Mdm2 is important for regulating p53 activity, other mechanisms are currently under investigation. Interestingly Mdm2 can regulate p53 function by conjugation of nedd8. This modification results in a transcriptionally inactive p53 but what regulates Mdm2 neddylation activity is still unknown (22).

In the tumor microenvironment there are numerous growth factors and cytokines secreted from various invading cells and the stroma. This signaling leads to p53 levels that are generally not lower but elevated. This suggests that the Mdm2-mediated destabilization of p53 was not functional. Here we examined if Mdm2 neddylation activity could be regulated in response to growth factor activated signaling cascades. Here we show a novel Mdm2/c-Src interaction that results in the phosphorylation of

Mdm2 at Y281 and Y302. These phosphorylation sites are distinct from the previously reported sites for c-Abl. This novel phosphorylation event increases the half-life of Mdm2. Analysis of the enzymatic activity of Mdm2 shows that Mdm2 is unable to be loaded with ubiquitin and thus did not conjugate ubiquitin to p53. In contrast, Src-phosphorylated Mdm2 resulted in loading of nedd8 to itself and to p53. This switch of Mdm2 enzymatic activity results in inactive but elevated levels of p53. This Src-mediated activation of the neddylation activity of Mdm2 provides a mechanism for inactive-stable p53 in cultured cells and tumor cells.

3.2 Results

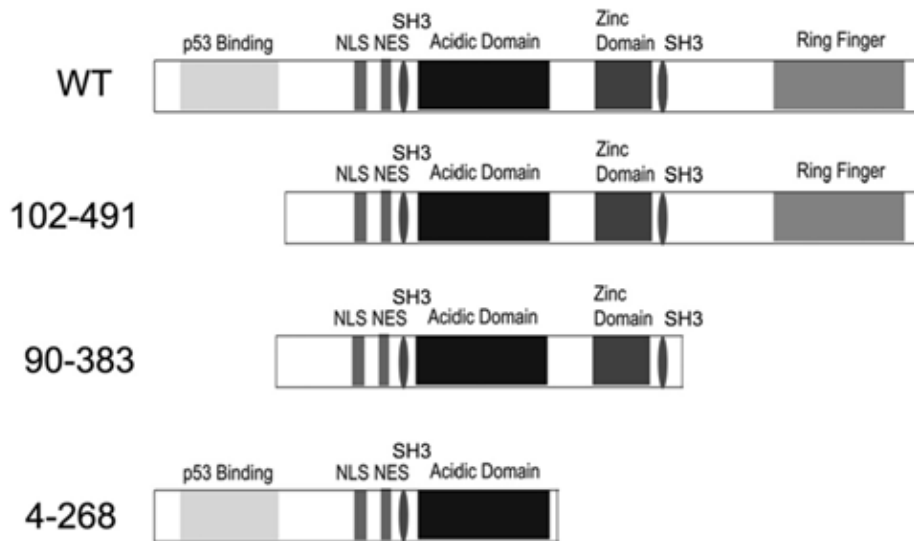
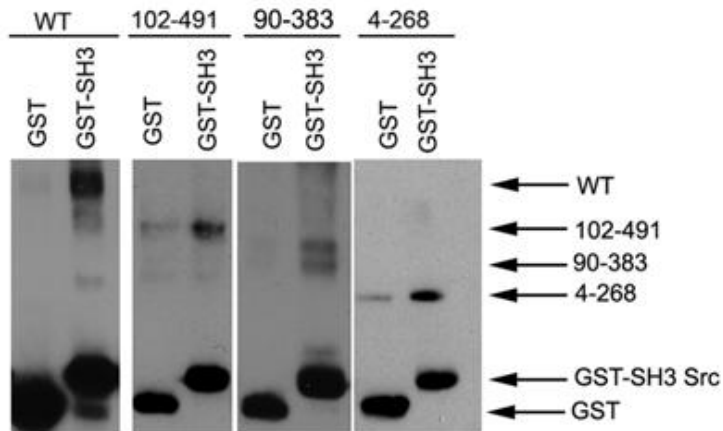
Mdm2 is a substrate for the non-receptor kinase c-Abl under genotoxic stress conditions (103). c-Abl contains an SH3 domain, which binds to partner proteins containing an SH3 binding domain (P-x-x-P). Mdm2 contains two SH3 P-x-x-P binding domains, so we investigated whether Mdm2 could bind to other tyrosine kinases that have an SH3 domain. Recombinant Mdm2 was incubated on a SH3 domain array from Panomics. Mdm2 bound to c-Abl, Abl2, c-Src and Hck-specific SH3 domains (Table 2).

Due to the prominent role of c-Src in tumorigenesis, we pursued this interaction with Mdm2 further. To define specific Mdm2 domains required for SH3-Src binding, a series of His-tagged recombinant Mdm2 truncation mutants were made (Figure 9A). These Mdm2 mutants were incubated in a GST-pulldown assay with either GST or the GST-SH3 domain of Src (SH3-Src). All Mdm2 mutants bound the SH3-Src domain, but not by GST alone, revealing the portion of Mdm2 needed for the Src interaction is

Symbol	Name	Mdm2 bound
Abl	Ableson Tyrosine kinase	+
Abl2	Ableson-related Protein (ARG)	+
BLK	B lymphocyte specific Protein tyrosine Kinase	
BTK	Burton's Tyrosine kinase	
HCK	Hematopoietic cell kinase	+
IHK	Interleukin 2 inducible T-cell kinase	
LCK	Human T-lymphocyte specific tyrosine kinase	
cSrc	Cellular Rous Sarcoma viral oncogene homolog	+
SLK	Proto-oncogene tyrosine protein kinase FYN	
TXK	Tyrosine-protein kinase	

Table 2: SH3 domain array

Recombinant Mdm2 was incubated with an SH3 domain array (Panomics) containing SH3 domains of indicated proteins. Unbound Mdm2 was washed away and western analysis performed for Mdm2. (+) indicates a positive interaction.

A**B****Figure 9: c-Src binds Mdm2 between aa90-268**

(A) Schematic of recombinant Mdm2 truncation mutants. (B) Western blot analysis of GST and Mdm2. GST-pull-down assay was done using recombinant GST or GST-SH3-Src and recombinant Mdm2 proteins.

between residues 102-268 (Figure 9B). This is a region that contains an SH3 binding domain. To further validate this interaction and determine if it would occur *in vivo*, an immunoprecipitation of endogenous Src from MCF7 cells was performed and shows that Mdm2 and c-Src are in a complex (Figure 10).

Since our data indicate that the non-receptor tyrosine kinase c-Src interacts with Mdm2, we hypothesized that Mdm2 could be a substrate for tyrosine phosphorylation by c-Src. Mdm2 is a highly phosphorylated protein and yet only two tyrosine kinases have been identified to phosphorylate Mdm2 (49, 50, 103). The Mdm2 protein has 14 tyrosines residues, 3 of which are already identified as c-Abl sites (Figure 11). To determine if c-Src could phosphorylate Mdm2 an *in vitro* kinase reaction was performed using ^{32}P γ -labeled ATP. Mdm2 was incubated alone, with c-Src or with c-Abl as a positive control. As expected, Mdm2 was phosphorylated by c-Abl. Interestingly c-Src also phosphorylated Mdm2, providing evidence that Mdm2 is a substrate for Src. (Figure 12).

To determine which tyrosine(s) is targeted for phosphorylation by c-Src another *in vitro* kinase reaction was performed using the Mdm2 truncation mutants (Figure 9A). The different mutants were incubated with c-Src and then immunoblot analysis was performed using an anti-phosphotyrosine antibody (4G10). The blot was then stripped and re-probed for Mdm2 (SMP14). Comparison of the blots revealed that the WT, 102-491, and 90-383 were all effectively phosphorylated by c-Src (Figure 13A.). However, the Mdm2 truncation mutant 4-268 was unable to be phosphorylated by c-Src as shown by the outline squares (Figure 13A). Of note the 4-268 mutant of Mdm2 still contains a SH3 binding domain and was able to bind to SH3-Src, thereby eliminating the possibility that the loss of tyrosine phosphorylation was a result of Src not binding to Mdm2. Thus,

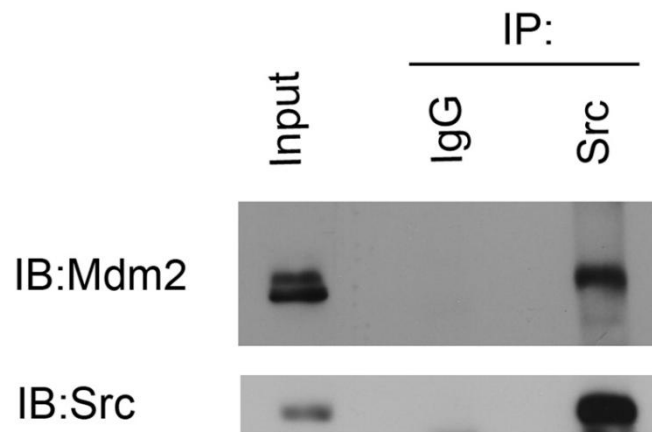


Figure 10: Mdm2 and c-Src interact *in vivo*

Western blot of immunoprecipitation of endogenous c-Src from MCF7 cell extracts was followed by western blot analysis of c-Src and Mdm2.

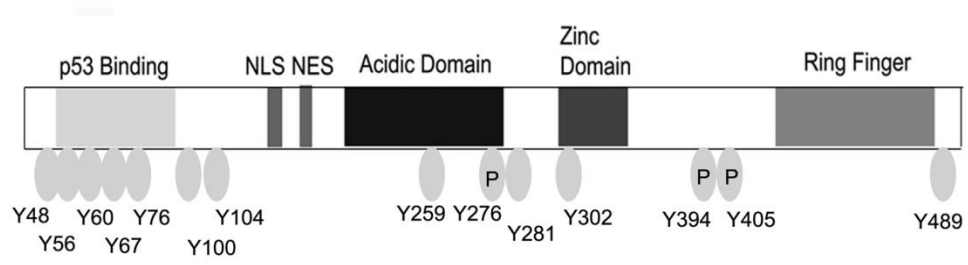


Figure 11: Schematic of tyrosines in Mdm2

Mdm2 contains 14 tyrosines. There are three known c-Abl phosphorylation sites (P) in Mdm2.

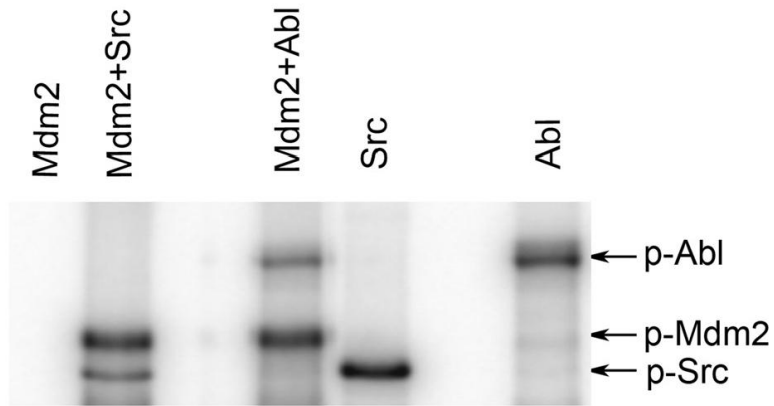


Figure 12: c-Src phosphorylates Mdm2 *in vitro*

Autoradiograph of ^{32}P incorporation in an *in vitro* kinase reaction of Mdm2 (p-Mdm2) by c-Src. c-Abl phosphorylation of Mdm2 and c-Abl/c-Src autophosphorylation were used as positive control.

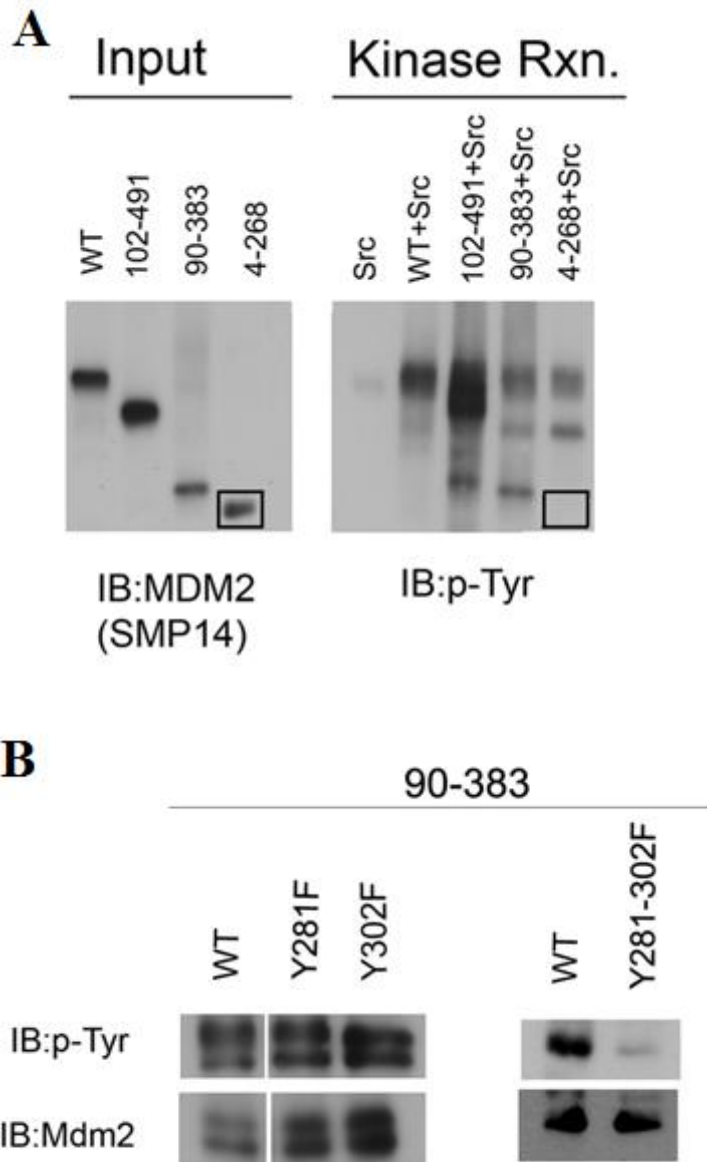


Figure 13: c-Src phosphorylates Mdm2 at Y281 and Y302

(A) Western blot analysis of Mdm2 and phospho-tyrosine (pTyr) of *in vitro* phosphorylation reaction on truncated Mdm2 proteins. Square outline highlights the inability of truncation mutant 4-268 to be phosphorylated by c-Src. (B) Tyrosine to phenylalanine mutants to each site Y281F and Y302F or in combination, Y281-302F, were generated in the 90-383 Mdm2 background. *In vitro* kinase reaction was performed with c-Src using Mdm2 point mutants followed by western blotting as performed in (A).

the *in vitro* kinase reaction narrowed down the potential c-Src phosphorylation site(s) to amino acids 268-393, which incorporates Y276, Y281, and Y302. Since c-Src and c-Abl are predicted to have different recognition sequences (104) and Y276 is already a known c-Abl phosphorylation site, this left Y281 and Y302 as potential c-Src phosphorylation sites. To establish which site is necessary for c-Src phosphorylation, site-directed mutagenesis was performed. Y281F, Y302F, and an Y281-302F double mutant were created in the 90-383 truncated form of Mdm2. The mutants were used as substrates for an *in vitro* kinase reaction with c-Src. As shown in Figure 13B, the Y281-302F mutant was not phosphorylated by c-Src, while the single mutants were phosphorylated.

Since we mapped the phosphorylation sites on Mdm2 to Y281 and Y302, it was necessary to determine if Mdm2 could be a substrate *in vivo*. This was tested by two approaches. First, H1299 cells were transfected with HA-tagged Mdm2 (HA-Mdm2) with either constitutively active c-Src (CA-Src) or a kinase dead Src (KD-Src). The CA-Src has a point mutation, Y530F, that prevents the normal down regulation of kinase activity and the KD-Src has a point mutation, K297R, which results in catalytically inactive c-Src. An immunoprecipitation was then performed using the HA-tag followed by immunoblot analysis using anti-phosphotyrosine antibody (4G10). Tyrosine phosphorylation of Mdm2 was observed in the presence of CA-Src, but not KD-Src (Figure 14A). Along with overexpression, it was crucial to determine if c-Src could phosphorylate endogenous Mdm2. For this second approach pharmacologic inhibition of c-Src was used. MCF7 cells were pretreated with the c-Src selective inhibitor PP1 for 16 hr followed by immunoprecipitation with Mdm2. Immunoblot analysis for phosphorylated tyrosine revealed that c-Src inhibition resulted in a loss of endogenous

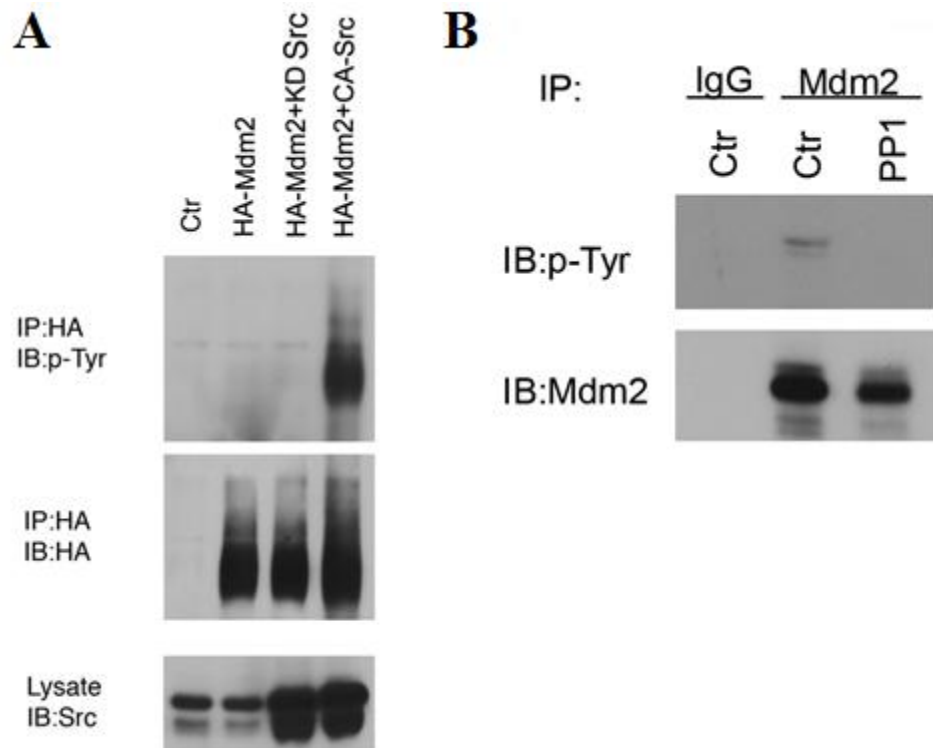


Figure 14: Mdm2 is phosphorylated by c-Src *in vivo*

(A) Immunoprecipitation of HA-tag from transient transfections of H1299 cells with HA-Mdm2, KD-Src, or CA-Src. Immunoprecipitation was followed by western blot of p-Tyr and HA. Western analyses of lysate show c-Src expression. (B) Western blot of Mdm2 and p-Tyr. Mdm2 was immunoprecipitated from MCF7 extracts after treatment with 10 μ M of the c-Src inhibitor PP1 for 16 hr.

Mdm2 tyrosine phosphorylation (Figure 14B). Mdm2 levels were observed after the immunoblot was re-probed for Mdm2. Thus, our *in vitro* and *in vivo* data shows that Mdm2 is a substrate for c-Src.

Since we have previously shown that Mdm2 is rapidly degraded following DNA damage induced c-Abl phosphorylation (48), we examined the possibility that c-Src phosphorylation would also decrease the levels of Mdm2. H1299 cells were transfected with Mdm2, Mdm2 + CA-Src, or Mdm2 + KD-Src. Conversely, western blot analysis showed an induction of Mdm2 protein levels in the presence of CA-Src, but not in the presence of KD-Src (Figure 15A). To examine if an increase in c-Src activity would result in a dose-dependent increase in Mdm2 protein levels, H1299 cells were transfected with Mdm2 and with increasing concentrations of CA-Src. As expected, Mdm2 protein levels increased concomitantly as c-Src levels increased (Figure 15B). It is noteworthy that the observed increases in Mdm2 protein levels are independent of p53 as H1299 cells are devoid of p53. To verify that c-Src tyrosine phosphorylation of Mdm2 is required for the increase in Mdm2 protein levels, the Y281-302F Src-phosphorylation mutant of Mdm2 was used in transient transfection of H1299 cells. Overexpression of the Y281-302F Mdm2 mutant, with or without CA-Src, in H1299 cells did not change Mdm2 protein levels (Figure 16).

To examine how c-Src regulates endogenous Mdm2 protein levels, we activated c-Src through epidermal growth factor (EGF) stimulation of MCF7 cells. MCF7 cells were serum-starved for 48 hr and then treated with 200 ng/mL of EGF for a time course of 2 hr. EGF stimulation resulted in an increase of Mdm2 protein levels with a peak achieved by 1 hr (Figure 17A). To ensure that this increase of Mdm2 by EGF

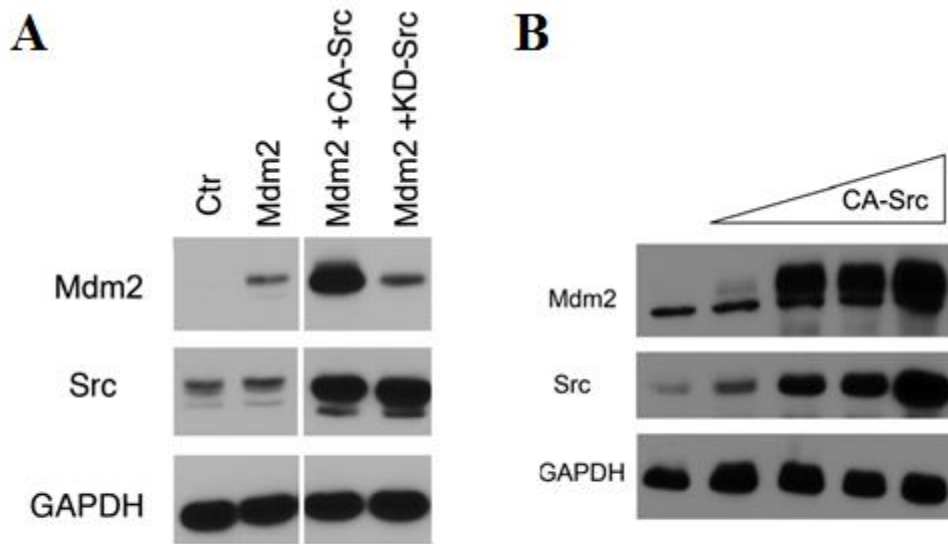


Figure 15: Overexpression of CA-Src increases Mdm2 protein levels
 (A) Western blot of Mdm2, Src, and GAPDH from extracts of H1299 cells ectopically expressing Mdm2, CA-Src, or KD-Src. (B) Western analysis of H1299 cells overexpressing Mdm2 and increasing concentrations (0.5, 1, 5, 10μg) of CA-Src.

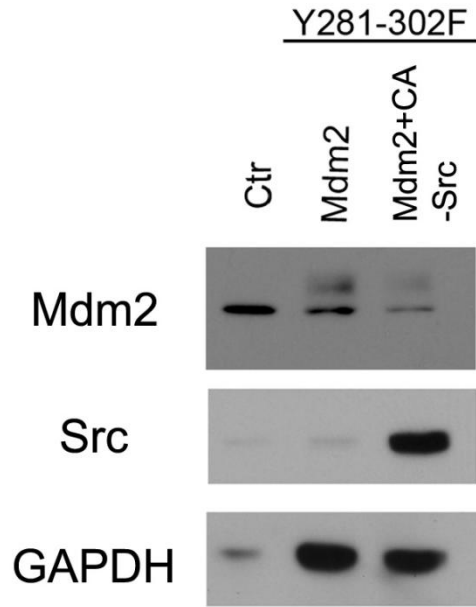


Figure 16: Increases in Mdm2 protein levels by c-Src is dependent on c-Src phosphorylation sites Y281 and Y302 of Mdm2

H1299 cells ectopically expressing Mdm2 Y281-302F and CA-Src. Western blot analysis was performed for Mdm2, c-Src, and GAPDH as indicated.

was due to c-Src activity, serum starved MCF7 cells were pre-treated with the c-Src inhibitor, PP1 or DMSO control for 1 hr before addition of EGF. While EGF alone resulted in an increase of Mdm2, exposure of cells to the c-Src inhibitor PP1 showed no apparent increase in Mdm2 (Figure 17B). Since Mdm2 levels are increased due to c-Src activation, then it would be anticipated that inhibition of c-Src should result in a decrease in Mdm2 levels. This observation was validated, as treatment of MCF7 cells with increasing PP1 concentrations resulted in a dose-dependent decrease in Mdm2 levels (Figure 17C). Thus, the increase in Mdm2 protein level is due to activated c-Src and the phosphorylation of Mdm2.

While Mdm2 is a substrate for c-Src we could not exclude the possibility that the increased levels of Mdm2 was dependent on gene expression. To test if c-Src altered *mdm2* gene expression, we conducted reporter assays using the *mdm2* P2 promoter attached to luciferase. As anticipated, no difference was seen by overexpression of c-Src in H1299 cells or with inhibition of endogenous c-Src using PP1 treatment in MCF7 cells on the *mdm2* promoter as determined by luciferase (Figure 18 A&B).

Since we eliminated the contribution of gene expression to increasing Mdm2 levels, we examined if c-Src would alter the half-life of Mdm2. To test the effect c-Src has on Mdm2 protein half-life, H1299 cells were transfected with Mdm2 plus Myc-LacZ for internal control and either CA-Src, KD-Src, or pUSE (Src vector control). After transfection (24 hr) the cells were treated with cyclohexamide to stop protein synthesis. The cells were then harvested at the indicated time points and subjected to immunoblotting to determine Mdm2 levels (Figure 19A). The protein levels were

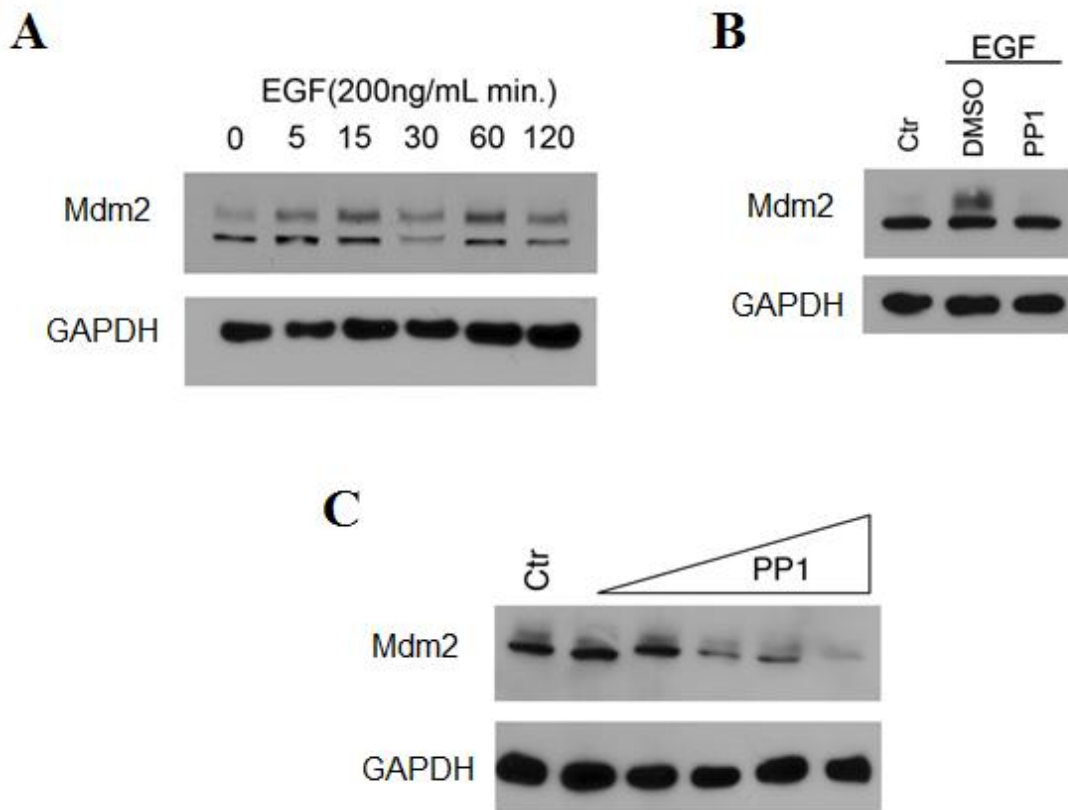
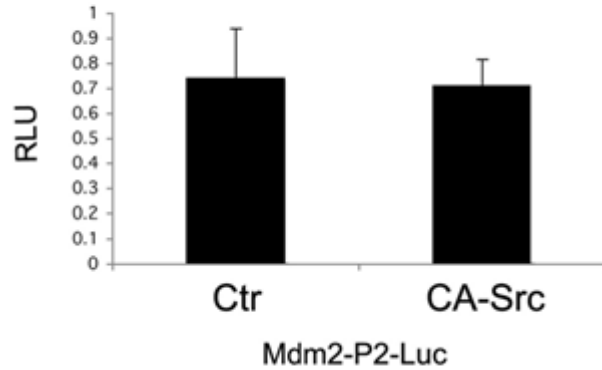
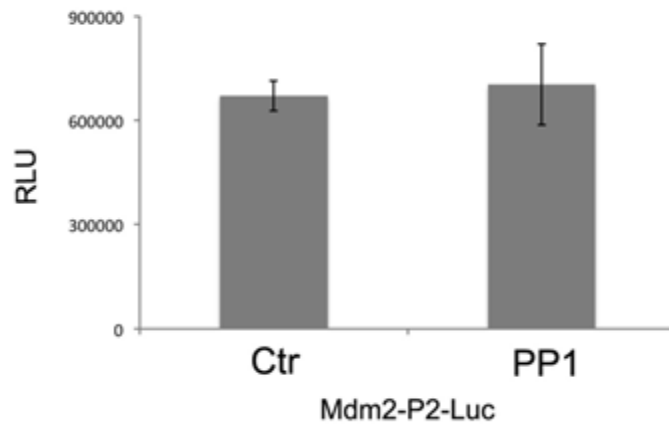


Figure 17: Activation/inhibition of endogenous c-Src regulates endogenous Mdm2 protein levels

(A) MCF7 cells were serum-starved for 48 hr and then treated with 200 ng/mL of EGF for times indicated. Endogenous Mdm2 and GAPDH were analyzed by western blot. (B) MCF7 cells were serum starved for 48 hr and then pre-treated with either DMSO or PP1 (10 μM) for 1 hr prior to addition of EGF (200 ng/mL). EGF treatment was for 1 hr followed by western analysis for Mdm2 and GAPDH. (C) MCF7 cells were treated with increasing concentrations (1, 5, 10, 15, and 20 μM) of PP1 for 16 hr and western blot was performed for Mdm2 and GAPDH.

A**B****Figure 18: c-Src does not induce Mdm2 transcription from the P2-promoter**

(A) Luciferase assay of the *mdm2*-P2-Luc with Myc-LacZ in H1299 cells alone or expressing CA-Src. (B) Luciferase activity was measured from of the *mdm2*-P2-Luc and Myc-LacZ in MCF7 cells after treatment with 10 μ M of PP1 or DMSO for 16 hr. Y-axis measurements are relative luciferase units (RLU), calculated from the ratio of luciferase/ β -gal activity. Error bars represent standard deviation.

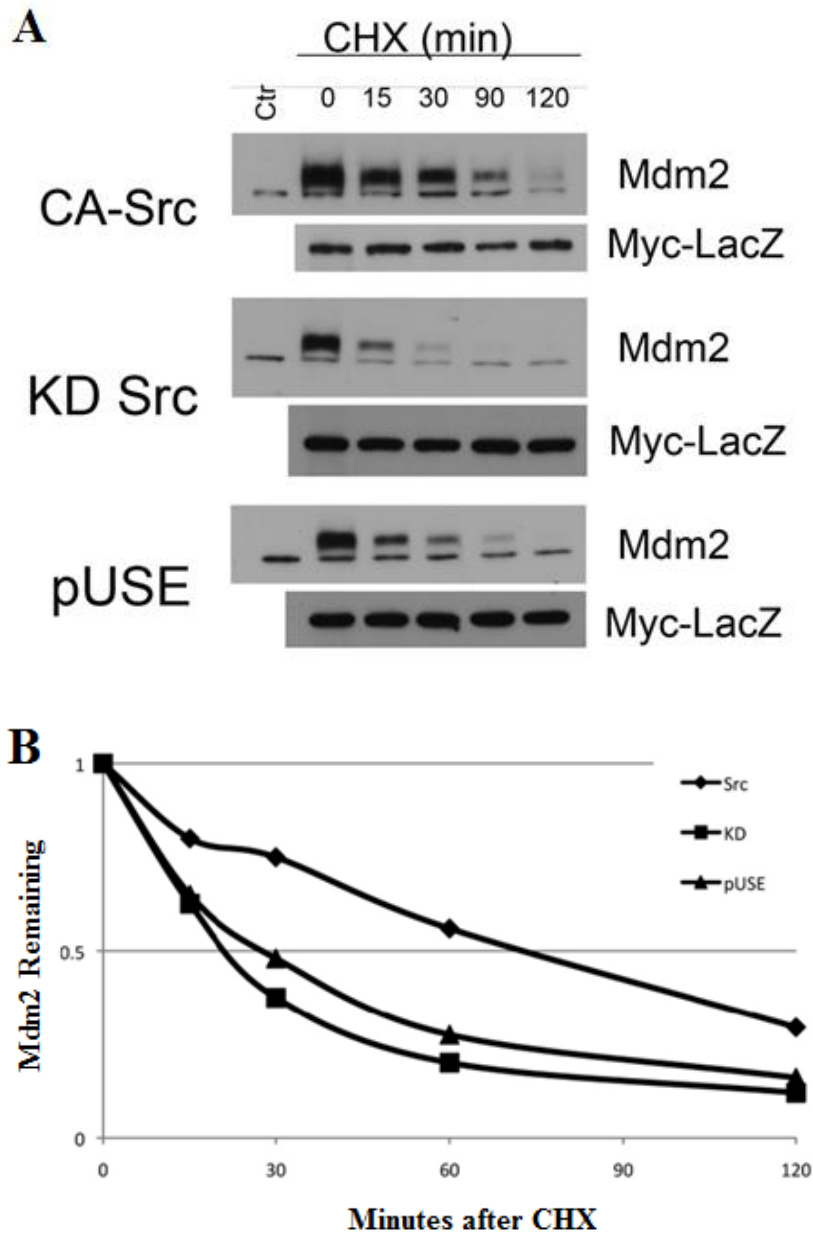


Figure 19: c-Src increases Mdm2 protein half-life

(A) H1299 cells were transfected with Mdm2 and CA-Src, KD-Src or empty vector (pUSE) in the presence of Myc-LacZ vector. Twenty-four hr post-transfection the cells were treated with 50 μ g/ml cyclohexamide (CHX) and harvested at different time points as indicated. The cell lysates were immunoblotted with anti-Mdm2 and anti-Myc antibodies as indicated. (B) The density of Mdm2 in each lane was quantified against the level of Myc-LacZ and plotted in a graph.

quantitated and graphed as a ratio of Mdm2/LacZ by measuring the intensity of each band. In the presence of KD-Src the half-life of Mdm2 was 25 min, which is consistent with published reports of Mdm2 half-life. Interestingly, in the presence of CA-Src the half-life of Mdm2 increased to 70 min (Figure 19B). However when the Mdm2 Y281-302F mutant was co-expressed with CA-Src, the half-life remained at 25 min, the same as WT Mdm2 in the presence of KD-Src (Figure 20 A&B). Thus, c-Src phosphorylation of Mdm2 more than doubled the half-life of Mdm2.

Since Mdm2 possesses the ability to function as an ubiquitin ligase, we wondered if c-Src phosphorylation might inhibit the ability of Mdm2 to be loaded with ubiquitin, which would contribute to the increase in protein stability. A transient assay was employed utilizing overexpressed and purified his-tagged ubiquitin protein conjugates. We found that in the presence of CA-Src that Mdm2 ubiquitination is greatly reduced (Figure 21). These experiments show that the increase in Mdm2 protein levels is due the lack of ubiquitin being loaded to Mdm2, subsequently resulting in stabilization of Mdm2.

Since phosphorylation of Mdm2 by c-Src reduced loading of ubiquitin, we questioned whether it could still serve as an E3 ubiquitin ligase towards p53. To this end, an *in vitro* ubiquitination assay of p53 was performed using untreated or phosphorylated Mdm2. Phosphorylation was done with c-Src or c-Abl. c-Abl is known to inhibit Mdm2 ubiquitination of p53, and thus served as a positive control. As shown in Figure 22, phosphorylation with c-Src inhibited the ubiquitination of p53 to the same extent as c-Abl. Since Mdm2 was unable to ubiquitinate p53 *in vitro*, we tested for p53 protein levels in cells. H1299 cells were transfected with different combinations of p53, Mdm2, CA-Src, and KD-Src. As expected, addition of Mdm2 resulted in a decrease of p53, but CA-

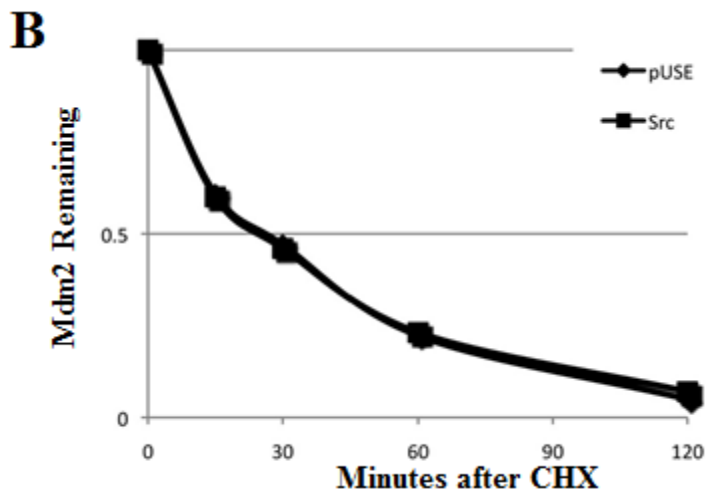
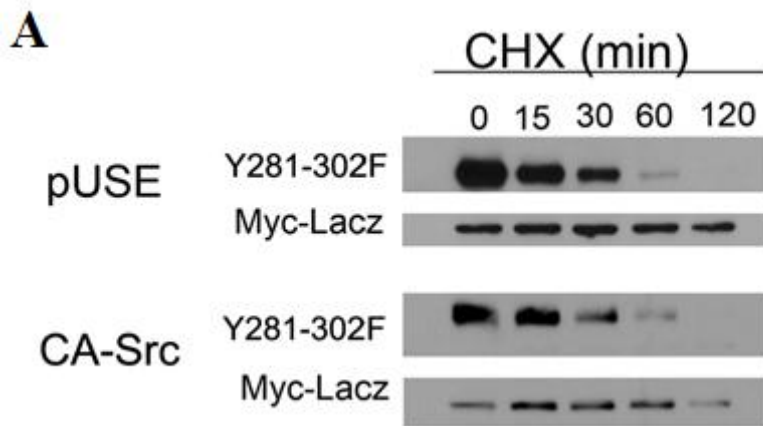


Figure 20: Y281 and Y302 of Mdm2 are required for c-Src mediated increase of Mdm2 half-life

(A) H1299 cells were transfected with Y281-302F of Mdm2 and CA-Src, or KD-Src in the presence of Myc-LacZ vector. Twenty-four hr post-transfection the cells were treated with 50 μ g/ml cyclohexamide (CHX) and harvested at different time points as indicated. The cell lysates were immunoblotted with anti-Mdm2 and anti-Myc antibodies as indicated. (B) The density of Mdm2 in each lane was quantified against the level of Myc-LacZ and plotted in a graph.

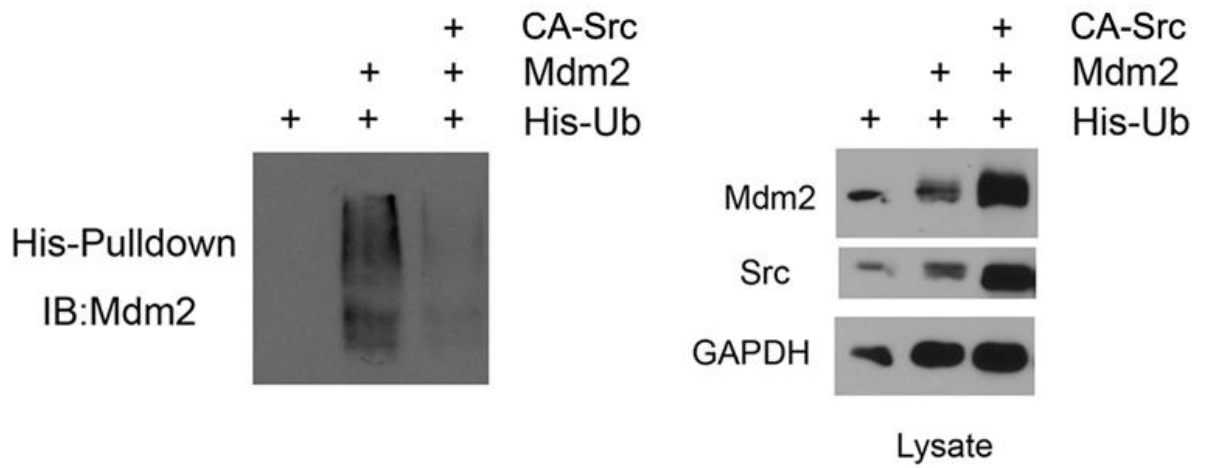


Figure 21: Loss of Mdm2 ubiquitination by CA-Src

(A) Western blot analysis of Mdm2 from a his-ubiquitin pull-down assay. His-ubiquitin conjugates were purified from H1299 cells transfected with Mdm2, CA-Src and His-ubiquitin (left). Western blotting from lysates shows expression of Mdm2, Src and GAPDH.

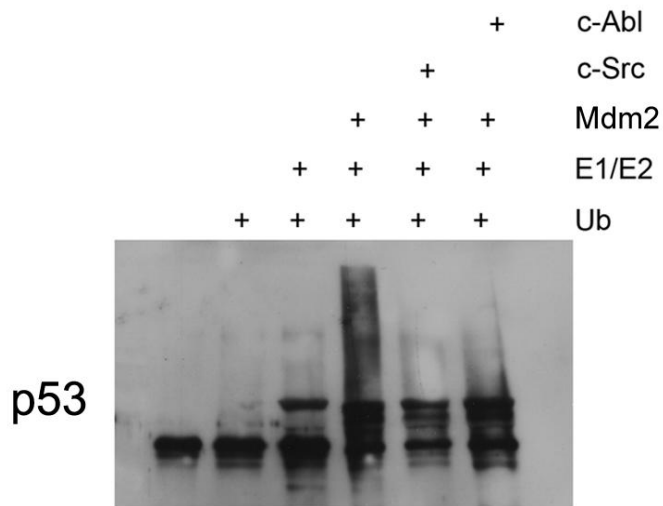


Figure 22: c-Src inhibits Mdm2 mediated ubiquitination of p53

In vitro ubiquitination assay of recombinant p53 using Mdm2 or Mdm2 phosphorylated by c-Src or c-Abl. Western blot was probed for p53. E1, E2, and ubiquitin were added as indicated.

Src prevented Mdm2-mediated degradation of p53, while KD-Src had no such effect (Figure 23A). To examine endogenous p53 levels, MCF 7 cells were transfected with increasing amounts of CA-Src. As seen with the overexpression, endogenous levels of p53 increased with c-Src expression and this increase of p53 correlated directly with the increase of Mdm2 (Figure 23B). Furthermore, activation of endogenous c-Src by EGF over a 1 hr time course resulted in a similar increase in p53 that mimics the increases of c-Src and Mdm2 protein levels (Figure 24A). Additionally, inhibition of endogenous c-Src with PP1 resulted in a dose dependent decrease in p53 levels (Figure 24B). These results support the observation that c-Src phosphorylation of Mdm2 results in stabilization of p53 levels due to Mdm2 inability to function as an ubiquitin ligase. Since Mdm2 could not ubiquitinate p53, we needed to determine if this stability would coincide with an increase in p53 activity. Using the PG13-Luc, which is an artificial p53 promoter attached to luciferase, along with combinations of p53, Mdm2, CA-Src and KD-Src we observed that p53 activity was decreased in the presence of Mdm2 as expected. However, p53 activity was further decreased by an additional 60% in the presence of CA-Src and reverted to the same level of Mdm2 alone in the presence of KD-Src. These data show that Mdm2 inhibition of p53 is further enhanced in the presence of CA-Src (Figure 25A), even though p53 protein levels are stabilized.

Mdm2 can inhibit p53 just through binding, yet the c-Src-phosphorylation sites suggest that this inhibition is not dependent on increasing the p53-Mdm2 complex. To test if this was evident, we conducted a luciferase assay using the ligase dead mutant C464S of Mdm2. H1299 cells were again transfected with the PG-13-Luc along with p53, C464S, and CA-Src. The luciferase assay showed that p53 activity was decreased in

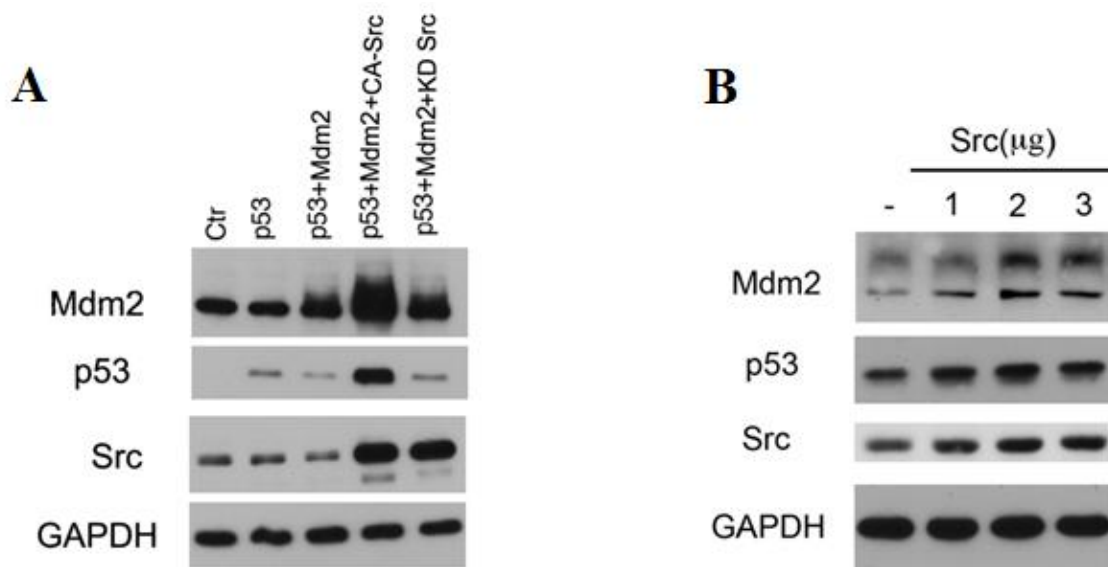


Figure 23: Exogenous CA-Src elevates p53 protein levels

(A) Western blot analysis of lysates from H1299 cells overexpressing p53, Mdm2, CA-Src, and KD-Src. (B) Western blot was performed to examine endogenous levels of Mdm2, p53, GAPDH, and expression of Src from lysates of MCF7 cells ectopically expressing CA-Src.

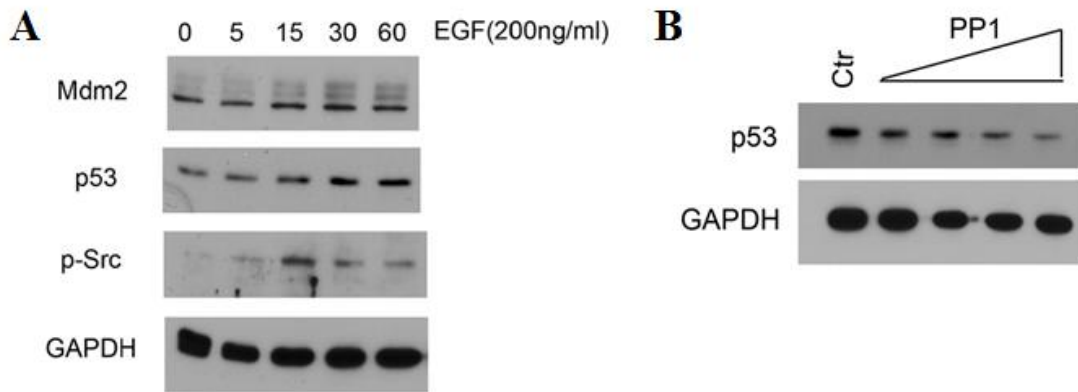


Figure 24: Activation/Inhibition of endogenous c-Src regulates endogenous p53 protein levels

(A) Western blot analysis was performed for Mdm2, p53, activated Src (p-Src Y419) and GAPDH from MCF7 cells serum starved for 48 hr and incubated with EGF over a time course of 1hr. (B) Western blot of p53 from MCF7 cell extracts treated for 16 hr with increasing concentrations of PP1 (1, 5, 10, 15, 20 μ M).

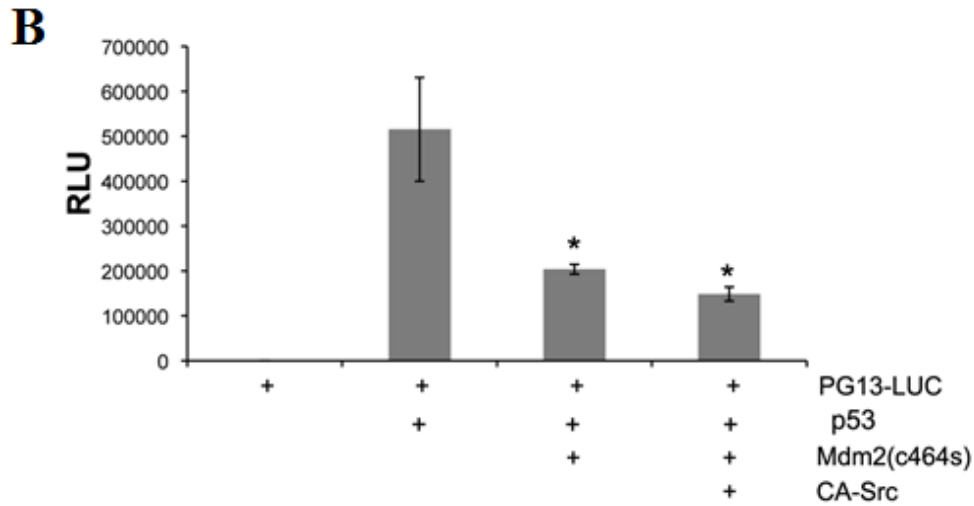
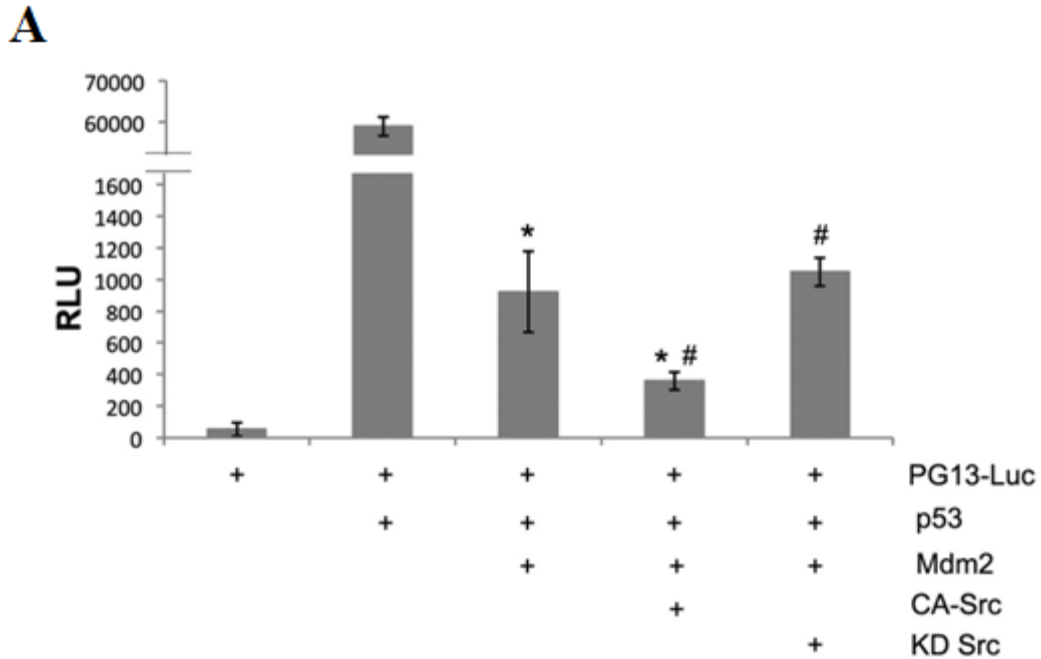


Figure 25: c-Src inhibits p53 transcriptional activity dependent on Mdm2 ligase activity

(A) Luciferase assay of the PG13-sythetic promoter and Myc-LacZ in H1299 cells transfected with p53, Mdm2, CA-Src, and KD-Src. (B) Luciferase assay using PG-13-Luc and Myc-LacZ in H1299 cells transfected with p53, Mdm2 C464S, and CA-Src. *,# represents statistical significance of $p < 0.05$. Y-axis measurements are relative luciferase units (RLU). The RLU was calculated from the ratio of luciferase/ β -gal activity. Error bars represent standard deviation of at least three experiments.

the presence of C464S Mdm2 but was not dramatically increased with CA-Src (Figure 25B). This experiment provides direct evidence that there is a dependence on the RING domain of Mdm2 for c-Src to fully inactivate p53.

We have shown that p53 protein levels are stabilized but transcriptionally inactive and that this inhibition is dependent on an intact Mdm2 RING finger and c-Src phosphorylation. Because of these observations, we examined if c-Src phosphorylated Mdm2 could still function as a neddylation enzyme. To test this, H1299 cells were transfected with a His-nedd8 construct along with p53, Mdm2, and CA-Src or KD-Src. A nickel pulldown assay was used to isolate neddylated proteins. Figure 25A illustrates that in the presence of CA-Src, neddylated p53 dramatically increases. When the immunoblot was stripped and re-probed with anti-Mdm2 antibodies, we were able to detect an increase in Mdm2-nedd8 conjugates in the presence of CA-Src. Interestingly, nedd8 conjugated to p53 or Mdm2 was absent when KD-Src was present (Figure 26A). This indicates that c-Src phosphorylation of Mdm2 is activating the neddylation activity of Mdm2.

To provide further evidence that this switch of Mdm2 activity was dependent on Src-phosphorylation Mdm2, a His-nedd8 pulldown assay using the phosphorylation deficient mutant Y281-302F was performed. This result shows that p53 neddylation increases dramatically in the presence of WT Mdm2 and CA-Src, but there was no change in p53 neddylation in the presence of Y281-302F and CA-Src (Figure 26B).

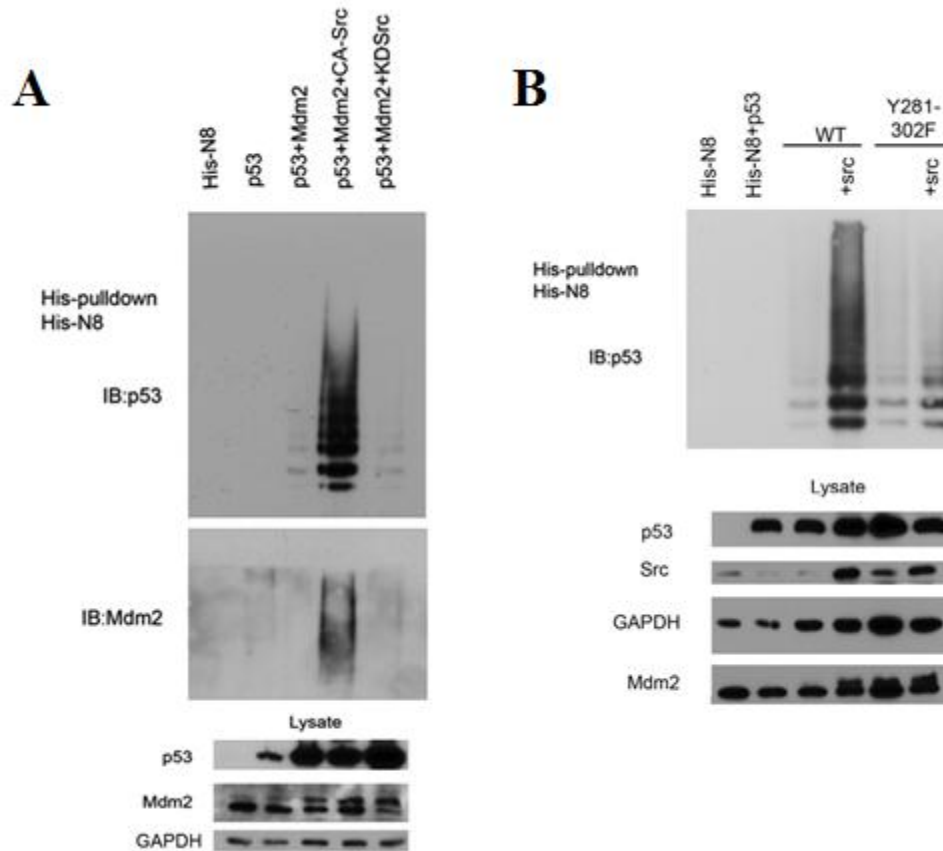


Figure 26: c-Src activates Mdm2 neddylation activity, dependent on Y281 and Y302
 (A) Western blot of p53 and Mdm2 from His-nedd8 pull-down assay of H1299 cells expressing His-nedd8, p53, WT-Mdm2, CA-Src, and KD-Src. To verify expression, lysates were subjected to western analysis as indicated. (B) His-nedd8 pull-down was performed as in (A), but with the use of Mdm2 Y281-302F as indicated.

Since our transient transfection data indicated that Mdm2 can function as a neddylation enzyme, we examined the effect of inhibiting neddylation by pharmacological agents. H1299 cells transfected with p53, Mdm2, and CA-Src and treated with the neddylation inhibitor, MLN4924, showed a loss of neddylated p53 (Figure 27). This result would be anticipated as c-Src directs Mdm2 to switch and become a neddylation enzyme, and nedd8 would not be loaded to Mdm2. To integrate the role of c-Src on endogenous neddylation of p53, the c-Src inhibitor PP1 was used. MCF7 cells were treated with PP1, and p53 was immunoprecipitated from cell extracts. Immunoblot analysis was done using anti-nedd8. Figure 28 shows that inhibition of c-Src using PP1 results in a decrease in endogenous neddylated p53. Since Mdm2 ligase activity is specified by which E2 (ubiquitin or neddylation) it binds, we hypothesized that c-Src phosphorylation of Mdm2 might inhibit or enhance interactions with a specific E2. Recombinant GST-Ubc5 (ubiquitin E2) and GST-Ubc12 (neddylation E2) were incubated with Mdm2 or phosphorylated Mdm2 and a GST pulldown assay performed. As shown in Figure 29, c-Src phosphorylation of Mdm2 resulted in a substantial decrease in the Ubc5/Mdm2 interaction compared to unphosphorylated Mdm2. Meanwhile the Ubc12/Mdm2 interaction showed a slight increase after Mdm2 phosphorylation. This experiment provides evidence that the mechanism of c-Src activation of Mdm2 neddylation activity may involve changes in specific E2 recruitment. Taken together, these results show that c-Src phosphorylation of Mdm2 activates the neddylation activity of Mdm2.

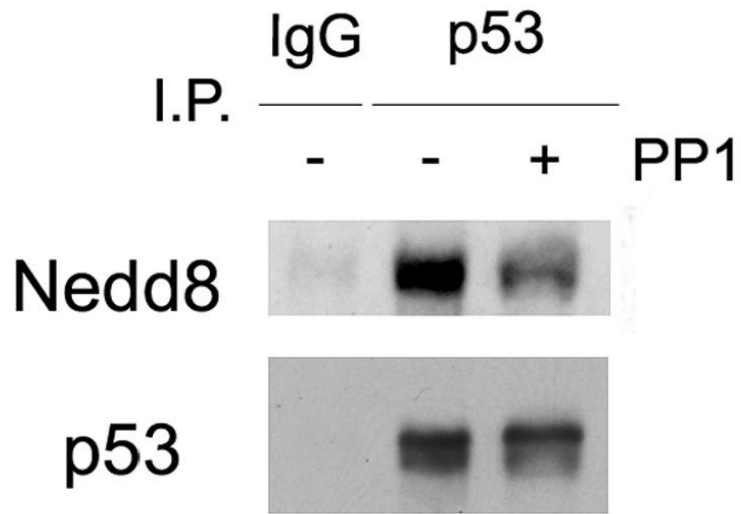


Figure 28: Inhibition of c-Src results in loss of endogenous neddylated p53
 Western blot of p53 immunoprecipitated from MCF7 cells after treatment with PP1 or DMSO for 16 hr. Western blot analysis for nedd8 was done to determine amount of nedd8-conjugated p53.

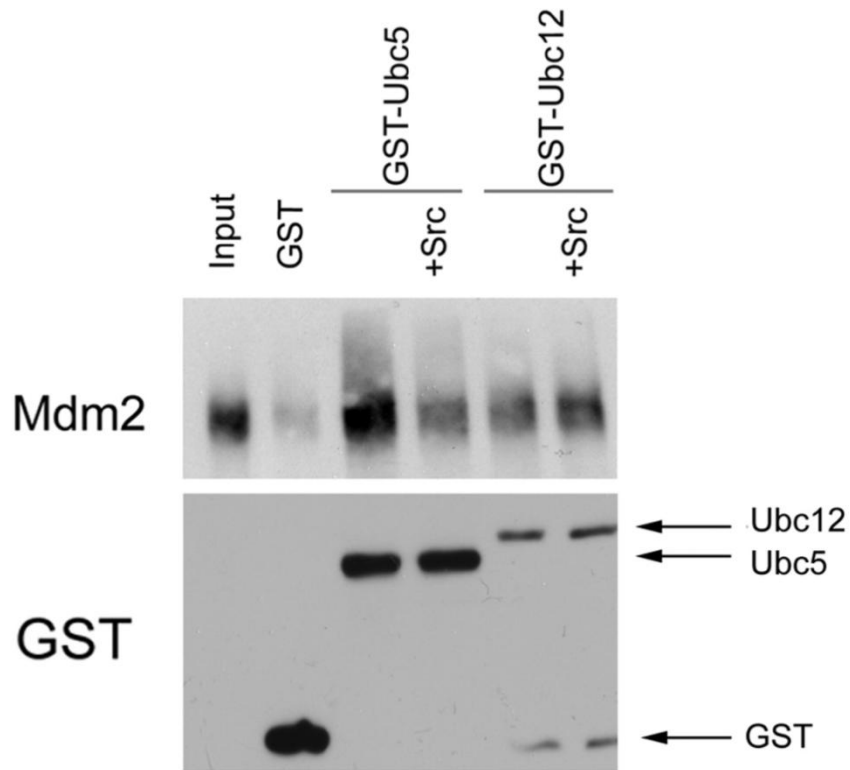


Figure 29: Specific *in vitro* E2 requirement to Mdm2 by c-Src phosphorylation
 Western blot of GST-pulldown of GST-Ubc5 and GST-Ubc12 with Mdm2 or c-Src phosphorylated Mdm2. GST alone was used as negative control.

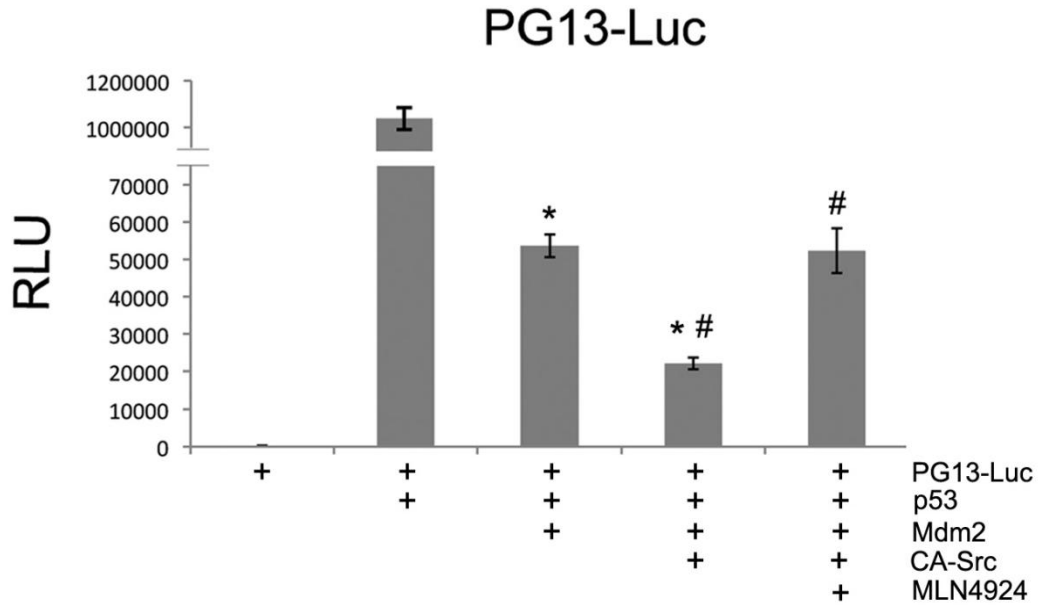


Figure 30: Inhibition of neddylation reverses c-Src downregulation of p53 transcriptional activity

PG13-Luc activity was assayed using H1299 cells transfected with Myc-LacZ, p53, Mdm2, and CA-Src. 24 hr post-transfection cells were treated with DMSO or 0.3 μ M of the NAE inhibitor MLN4924 for 16 hr. *, # represent statistical significance of $p < 0.05$. Y-axis measurements are relative luciferase units (RLU). The RLU was calculated from the ratio of luciferase/ β -gal activity. Error bars represent standard deviation.

Since c-Src phosphorylation of Mdm2 directs ligase activity towards neddylation, we tested what effect inhibition of neddylation would have on p53 activity. H1299 cells were transfected with the PG-13-Luc, p53, Mdm2 and CA-Src. Reduction in p53 activity by Mdm2 was further increased in the presence of c-Src as expected. Treatment of H1299 cells with MLN4924 restores p53 activity to levels observed with Mdm2 alone, thereby supporting an Src-Mdm2-nedd8 pathway that inactivates p53 (Figure 30). Since the PG13-Luc is a synthetic construct we wanted to find a more relevant physiological promoter. Since both c-Src and Mdm2 are intimately linked to regulation of angiogenic processes, such as the positive regulation of VEGF (64, 106), we next determined what effect c-Src phosphorylation of Mdm2 would have on an anti-angiogenic target. The tumor suppressor *maspin* is a p53 target that plays an important role in regulating tumor cell invasion and metastasis (107). We have previously shown that p53 is required for the upregulation of Maspin protein levels under hypoxic conditions in glioblastoma cell lines (108). To assess Src-phosphorylated Mdm2 effect on p53-induced *maspin*, a luciferase assay utilizing the *maspin* promoter was performed. As shown in Figure 31A, H1299 cells transfected with the *maspin* promoter attached to the luciferase gene (*maspin*-Luc) shows that p53 drives the expression of luciferase from the *maspin* promoter and that a decrease is seen with Mdm2 overexpression. Just like with the PG13-Luc, expression of CA-Src further inhibits p53 activity on the *maspin* promoter and the inhibition is dependent on neddylation. To ensure that the decrease seen on the *maspin* promoter was due to c-Src phosphorylation of Mdm2, another luciferase assay was done using the Y281-302F Mdm2 and CA-Src. Here the *maspin* promoter luciferase decreased with the addition of Mdm2 Y281-Y302F, but the addition of CA-Src did not result in an increase

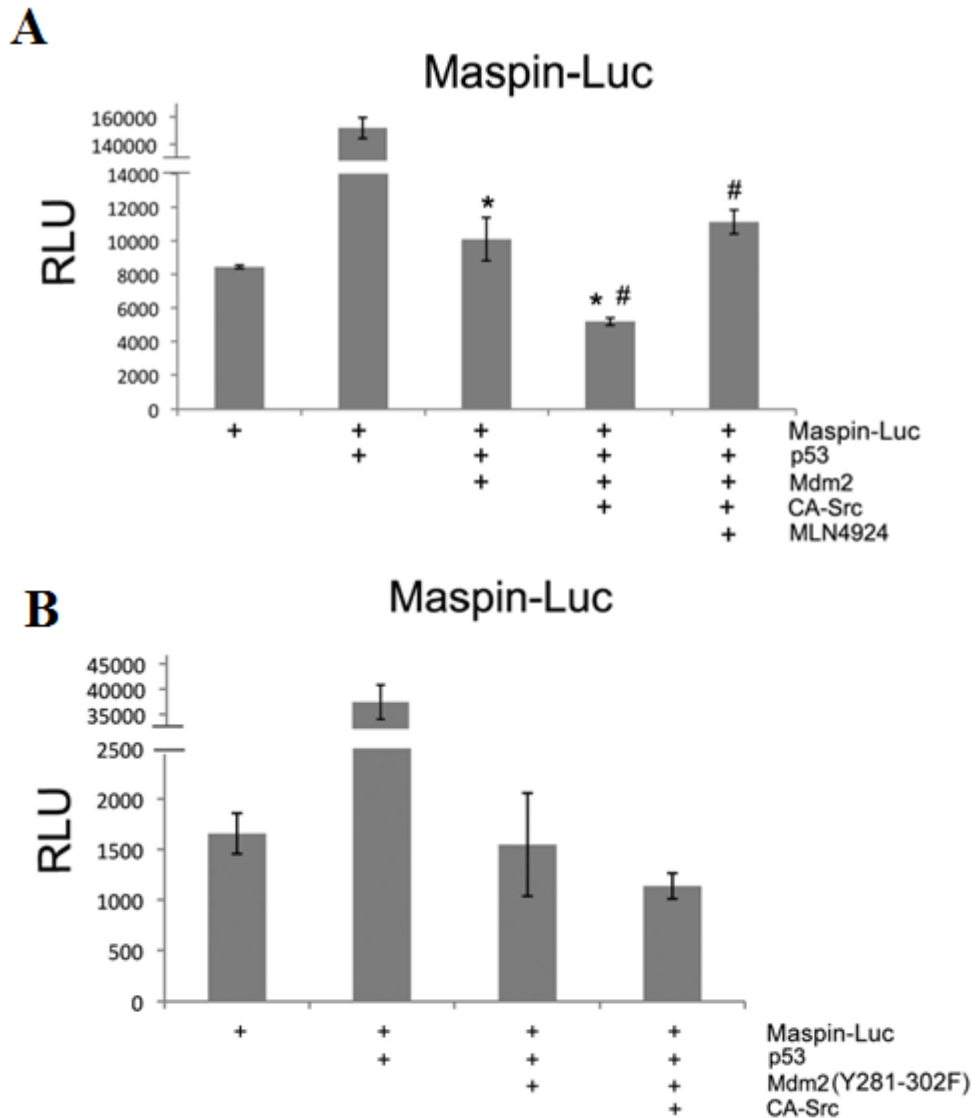


Figure 31: Inhibition of *maspin* promoter by c-Src is dependent on neddylation and Mdm2 Y281/Y302

(A) *Maspin*-Luc activity was assayed using H1299 cells transfected with Myc-LacZ, p53, Mdm2, and CA-Src. Post-transfection (24 hr) cells were treated with DMSO or 0.3 μ M of the NAE inhibitor MLN4924 for 16 hr. (B) Luciferase assay of *maspin*-Luc in H1299 cells using p53, Mdm2 Y281-302F, and CA-Src. *, # represents statistical significance of $p < 0.05$. Y-axis measurements are relative luciferase units (RLU). The RLU was calculated from the ratio of luciferase/ β -gal activity. Error bars represent standard deviation.

of inhibition as seen with WT Mdm2 (Figure 31B). This shows that the enhancement of inhibition seen on the *maspin* promoter by c-Src is dependent on Mdm2 Y281 and Y302. For further insight on how endogenous neddylation of p53 would affect *maspin* levels, MCF7 cells were transfected with the *maspin*-Luc construct or a mutant *maspin*-Luc (MT1) that is unresponsive to p53, to insure luciferase activity was dependent on p53. c-Src was then inhibited for 16 hr using PP1 and a luciferase assay performed. Inactivation of c-Src allowed for an increase of p53 activity on the *maspin*-Luc construct (Figure 32A). This increase of p53 activity was also seen at the protein level, as Maspin protein was increased following inhibition of c-Src (Figure 32B). These findings provide insight into the regulation of c-Src-induced neddylation of p53. This neddylation event is responsible for the further reduction in p53 activity on both the PG-13-Luc and on its ability to activate the tumor suppressor Maspin.

3.3 Discussion

Understanding how Mdm2 functions in tumor progression is of critical importance since Mdm2 protein levels are detectable in 40-80% of high-grade human malignances and 10% show *mdm2* gene amplification (4). The current paradigm is that Mdm2 upregulation would inhibit the p53 tumor suppressor, through destabilization, resulting in tumor progression. However there are many human cancers, including breast, gliomas, oral, renal, and cervical, that have elevated levels of Mdm2 and wild-type p53 (109-113). This correlation of high Mdm2 and p53 levels indicate that Mdm2 may have other possible mechanisms for the inactivation of p53, besides destabilization. The Mdm2 protein has been shown to conjugate a nedd8 molecule to p53 that inactivates its

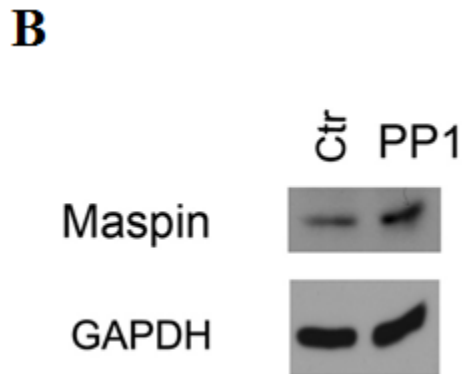
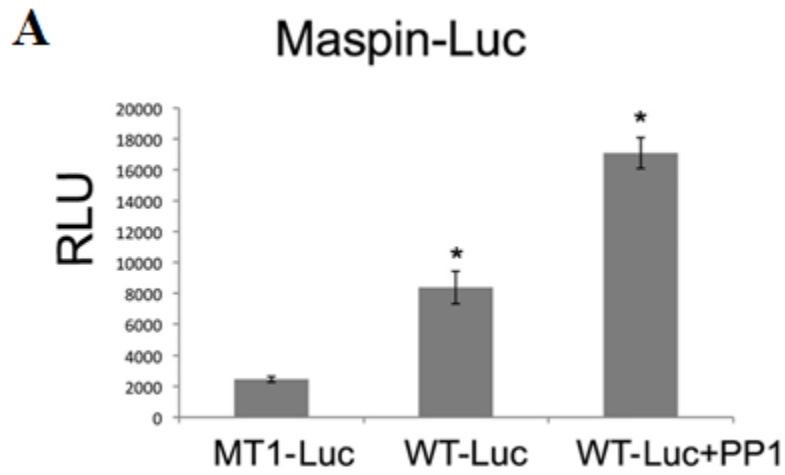


Figure 32: Inhibition of c-Src upregulates maspin transcription and protein levels
 (A) Luciferase assay of MCF7 transfected with either *maspin*-Luc or mutant *maspin*-Luc (MT1) and Myc-LacZ. After transfection (24 hr) cells were treated with DMSO or 10 μ M PP1 for 16 hr. (B) Western blot analysis of MCF7 cells treated with DMSO or 10 μ M PP1 for 16 hr.

transcriptional activity without affecting its protein stability, but the mechanism has remained elusive (22).

The non-receptor tyrosine kinase c-Src regulates a number of normal and pathological processes including proliferation, survival, motility, and angiogenesis (71). c-Src functions poorly as an oncogenic factor on its own and activating mutations of c-Src in human cancer are rare. This has led to the view that c-Src may facilitate and promote the activity of other proteins, as opposed to being an autonomous dominant transforming agent on its own. One c-Src interacting protein that has been extensively studied is EGFR. This interaction results in phosphorylation of EGFR at Y845, and is c-Src dependent (114). This pathway activates STAT5b (115) and mediates proliferation and promotes cell survival through cyclooxygenase 2 (COXII) (116). FAK also interacts with c-Src. FAK mediates cancer metastasis by regulating focal adhesion formation and turnover. c-Src phosphorylation activates FAK kinase activity and generates docking sites for Grb2 and other signaling molecules that regulate signaling pathways (117). In this study we provide evidence that c-Src cooperates with Mdm2 to enhance oncogenic activities.

Our data shows that Mdm2 interacts with and is phosphorylated by c-Src (Figures 9A, 10, 12, 14A&B). We demonstrate through *in vitro* GST pull-down assays and an immunoprecipitation from MCF7 cells that the Mdm2/Src interaction takes place both *in vitro* and *in vivo*. c-Src uses its SH3 protein domain for many of its protein-protein interactions including those with paxillin and p85. Here the c-Src SH3 domain is sufficient for binding to Mdm2. Also, through the use of truncation mutants of Mdm2 we narrowed down the c-Src binding to amino acids 90-268 of Mdm2 (Figure 9B).

Interestingly, this truncation of Mdm2 encompasses the acidic domain, which is known to contain many serine residues that are normally phosphorylated under non-stress conditions (118). One hypothesis is that these modifications could enhance c-Src binding of Mdm2. Hence any alteration to these modifications, such as dephosphorylation of by PP2A (119), or any other protein interactions driven by cellular stresses could represent a mechanism to regulate the c-Src-Mdm2 interaction. The phosphorylation of Mdm2 by c-Src occurs on tyrosine 281 and 302. *In vitro* kinase reactions revealed that both Y281 and Y302 have to be mutated to phenylalanine to inhibit c-Src mediated phosphorylation of Mdm2 (Figure 13). Through the use of ectopically expressed c-Src or activation by EGF, we show that c-Src phosphorylation of Mdm2 results in an increase in Mdm2 protein levels (Figure 15 A&B, 17 A-C). These c-Src phosphorylation sites are within or near the zinc finger domain of Mdm2. Recent work has shown that a mutation in the zinc finger domain (C305F) has an enhanced half-life compared to wild-type (120). Interestingly, c-Src phosphorylation of Mdm2 showed similar results (Figure 19 A&B) and mutation of the two c-Src sites resulted in no change in half-life (Figure 20 A&B). Taken together these results could hint that alteration of the Mdm2 zinc finger domain could have great implication for protein stability.

The E3 ubiquitin ligase activity of Mdm2 has been extensively studied, especially in regard to p53 degradation. We have previously shown that after DNA damage c-Abl phosphorylation of Mdm2 at Y276 and Y394 enhances complex formation with Mdmx. This complex leads to degradation of both Mdm2 and Mdmx and results in the stabilization of p53 (48). Yet how growth factor activated tyrosine kinases affects Mdm2 ubiquitin ligase activity has not been determined. Utilizing an *in vitro* ubiquitin ligase

assay, c-Src inhibited Mdm2 mediated ubiquitination of p53 to the same extent as c-Abl (Figure 22). This decrease in ubiquitination translated into p53 protein stability in H1299 cells ectopically expressing p53 (Figure 23 A). Treatment with EGF also revealed a stabilization of p53 that correlated directly with increases in Mdm2 and activated c-Src protein (Figure 24A). To compensate for this increase in p53 protein levels, c-Src phosphorylation of Mdm2 further reduced p53 transcriptional activity in an Mdm2 RING finger dependent manner (Figure 25 A&B). These results are in direct opposition of the effect c-Abl phosphorylation signaling to Mdm2 has on p53 transcriptional activity. This provides evidence that tyrosine phosphorylation of Mdm2 under different conditions, may have different effects on p53 transcriptional activity, while maintaining protein levels. Interestingly, this induction of protein levels coupled with concurrent inhibition of transcriptional activity is not unheard of in the p53 family. It has been reported that p73 when bound to Mdm2 results in p73 stabilization, but leads to inhibition of its transcriptional activity (51). Similarly, the c-Src family member Hck, has been shown to phosphorylate p73 resulting in protein stability but decreases in its activity (121). These findings support the notion that increases in p53 protein levels do not guarantee transcriptional activation.

The decrease in p53 transcriptional activity by c-Src could be explained by the increase of Mdm2 protein and half-life. Even without the ability to degrade p53 by ubiquitin ligase activity, Mdm2 is still capable of inhibition by masking p53's N-terminal transactivation domain (122). This is evident as the RING finger dead mutant of Mdm2, C464S, is still efficient at inhibiting p53 transcriptional activity. Our data illustrate that the RING domain of Mdm2 is required for a more dramatic reduction in p53 activity in

the presence of CA-Src (Figure 25B). The Mdm2 protein has dual ligase activity capable of conjugating ubiquitin and nedd8. A previous report has shown that the histone acetyl transferase Tip60 can inhibit Mdm2 mediated neddylation of p53, but not ubiquitination (123). Also the original study showing p53 neddylation showed that CHO-TS-41 cells, which have a temperature sensitive mutation in the APP-BP1 gene inhibiting neddylation, still have ubiquitinated p53 even in the absence of neddylation (22). These studies taken together reveal that Mdm2 ligase activities can be both separately and individually regulated. However, signaling events regulating the activation of Mdm2 neddylation activity have yet to be identified. Our data reveal that c-Src phosphorylation of Mdm2 results in increased neddylated p53 and Mdm2. This increase in neddylation of p53 is dependent on the c-Src phosphorylation, as the Y281-302F Mdm2 mutant did not increase neddylated p53 and inhibition of c-Src by PP1 resulted in less nedd8 bound to p53 endogenously (Figure 26 A&B, 28). It appears that c-Src may regulate this switch by determining which E2 is able to bind to Mdm2 (Figure 29). Furthermore, using the inhibitor of neddylation, MLN4924, the inhibition on both the PG13-Luc promoter and the *maspin*-Luc promoter by Mdm2 in the presence of Src was reversed (Figure 30, 31). The effect on the *maspin* promoter is especially interesting due to the role of Maspin as a tumor suppressor in breast cancer. Maspin is normally highly expressed in normal breast epithelial cells, but is down regulated in invasive and metastatic breast carcinoma cells (83). Maspin tumor suppressor activity was validated as stable transfection of *maspin* in breast cancer cell lines led to an inhibition of tumor cell invasion *in vitro* and a decrease in tumor metastasis in mice (124, 125). The ability of Maspin to inhibit tumor growth was linked to its inhibition of tumor-induced angiogenesis. Maspin protein blocked

endothelial cell migration in response to growth signals and inhibited endothelial tube formation *in vitro* (91). Also, Maspin expression correlated with decreased micro-vessel staining in human breast cancer samples (126). This is important as both Mdm2 and c-Src have been linked to angiogenesis and metastasis in breast cancer, and here we show that inhibition of c-Src using PP1 results in greater activity of the *maspin*-Luc and greater Maspin protein levels in the breast cancer cell line, MCF7 (Figure 32 A&B). Taken together, these experiments prove that neddylation is a key component in c-Src ability to inhibit the p53/maspin tumor suppressor network through Mdm2 (Figure 33).

The data presented here reveal a novel c-Src /Mdm2/p53/Maspin pathway. This signaling cascade could be responsible for the high levels of Mdm2 seen in numerous cancers that still maintain wild-type p53. We also show that this pathway has a direct influence on the levels of the tumor suppressor maspin and might have implications in tumor angiogenesis. Thus, future treatment options might benefit from inhibition of c-Src and/or neddylation to engage the p53/Maspin anti-angiogenic pathway.

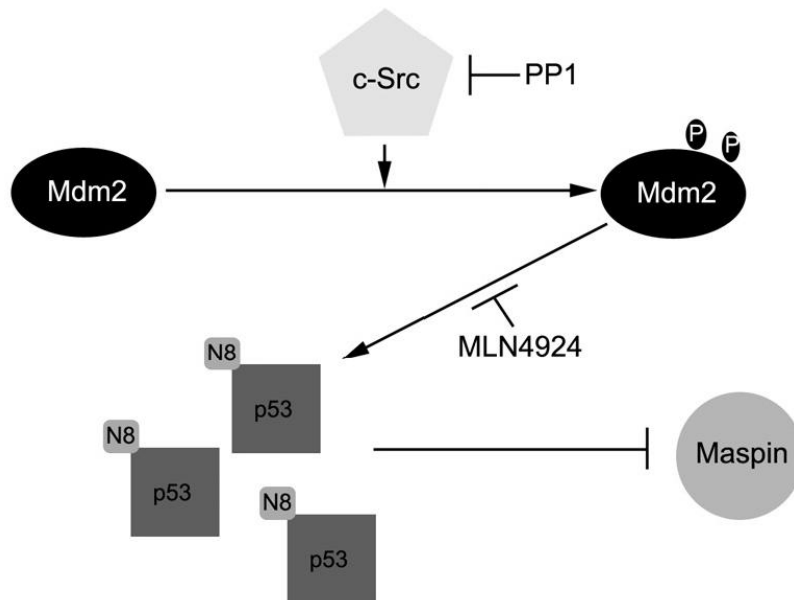


Figure 33: Model of c-Src phosphorylation of Mdm2 and its downstream effects
 Phosphorylation of Mdm2 by c-Src at Y281 and Y302 switches Mdm2 ligase activity to a neddylating enzyme, reducing p53 transcriptional activity on target genes, including Maspin. Inhibitors of both c-Src and neddylation can be used to inhibit this pathway.

4. Mdm2 enhances breast cancer metastasis

4.1 Introduction

In the United States, women will have a 1 in 8 chance of developing breast cancer in their lifetime (127). There are two main types of breast cancer. The first is ductal carcinoma, which starts in the ducts that move milk from the breast to the nipple. The other is lobular carcinoma and it starts in the lobules, which produce the milk. Breast cancer is a heterogeneous disease but has clinically distinct subtypes based on the expression of molecular markers. These markers include hormone receptor (HR), progesterone receptor (PR), and Her2. Another subtype of breast cancer termed, triple negative breast cancer, is diagnosed on the absence of all 3 of these markers, and carries the basal like molecular profile (128). Metastasis, the process by which tumor cells invade and colonize distal sites, is the leading cause of death, due to organ failure, for breast cancer patients. Breast cancer has five primary sites of metastasis including lung, bone, lymph nodes, liver and pleura. Metastatic tumors at these sites can be seen in over 50% of patients at autopsy, providing evidence of how frequently breast cancer is able to undergo metastasis (129).

While there are many factors that regulate tumor metastasis, recent work has implicated the Mdm2 network in this process. One study by Wang et al., illustrated how Mdm2, through wild-type 53, is responsible for the ubiquitination and degradation of Slug in lung cancer (130). Slug is a major transcriptional repressor of E-Cadherin, and can trigger EMT. Interestingly, it was also shown that E-Cadherin itself can interact with and undergo ubiquitination by Mdm2. Primary tumors from breast cancer patients had an inverse correlation between Mdm2 and E-cadherin protein levels as seen by

immunohistochemistry. These high Mdm2/low E-cadherin levels were associated with lymph node metastasis (63). We have reported that Mdm2 is upregulated in many late stage breast cancers, due to a tumor growth factor (TGF)- β /Smad3 signaling event that drives transcription of Mdm2. We demonstrated that approximately 65% of late-stage carcinomas were positive for activated Smad3 and Mdm2, indicating a strong correlation between TGF- β 1-mediated induction of Mdm2 and late-stage tumor progression. Furthermore 73% of the carcinomas that had known metastases stained for Mdm2 and activated Smad3, possibly linking Mdm2 to a role in breast cancer metastasis (11).

Two *in vivo* studies have also tried to elucidate the role of Mdm2 in metastasis. First, Zhang and Hill, showed that overexpression of Mdm2 in KHT cells resulted in more lung metastasis after tail vein injection (131). Meanwhile, an orthotopic pancreatic model using lentiviral knockdown of Mdm2, showed that tumor growth and metastasis was decreased in tumors with lower levels of Mdm2 (132). However, both studies concluded that the metastatic potential provided by Mdm2 was due to its regulation of wild-type p53. While Mdm2 main function is attributed to the regulation of p53, it has also been shown to promote tumorigenesis independent of p53. For example Mdm2 splice variants unable to bind p53 can still promote transformation and p53-null transgenic mice overexpressing Mdm2 have a higher incidence of tumors compared to littermate controls (133, 134). These experiments provide evidence that Mdm2 can promote tumor growth in the absence of p53. But the question remains if Mdm2 can facilitate metastasis in a p53-independent manner?

To answer this question we employed a known orthotopic mouse model of breast cancer metastasis. We used the TMD-231 cell line, which are derived from MDA-MB-

231 cells that had been grown in the mammary fat pad of mice. The MDA-MB-231 is the most widely used and characterized cell line for tissue specific metastasis of human breast cancer. The MDA-MB-231 cell is derived from the pleural effusion of a late stage breast cancer patient who died with multiple metastases (135). We chose these cells, as they are known to metastasize to the lung and also contain mutant p53. The mutation is R280K and is located in the DNA binding domain and inactivates p53 DNA binding activity. Thus, this allows us to study Mdm2's role in metastasis independent of p53 activity. To this end, we used a lentiviral construct harboring shRNA to knockdown Mdm2 in the TMD-231 cell line. We show that knockdown of Mdm2 has no effect on TMD-231 cellular growth *in vitro* or cell cycle progression, but knockdown of Mdm2 did result in decreased invasive potential. Interestingly, knockdown of Mdm2 did slow tumor growth *in vivo*, possible due to a decreased affinity for binding to fibronectin. Most importantly, we found that knockdown of Mdm2 showed a dramatic loss in breast to lung metastasis. This loss of metastatic potential was due to a reduction in HIF-1 α and VEGF protein levels leading to a loss of primary tumor vascularization. Here we provide definitive evidence Mdm2 can enhance tumor metastasis, independent of p53.

4.2 Results

Mdm2 expression correlates with metastasis in both pancreatic and breast cancer models (131, 132). However all studies to date have determined that the role of Mdm2 in metastasis is due to the regulation of wild-type p53. No studies however, have determined if Mdm2 plays a role in metastasis independent of p53. To determine if Mdm2 has a p53-independent role in this process, we used the TMD-231 cell line, which harbors mutant p53 (R280K), and generated a knockdown of Mdm2 using a lentiviral

vector harboring shRNA. Western blot analysis in Figure 34A shows that Mdm2 was knockeddown in the shMdm2 compared to shGFP control cells. While Mdm2 is the main E3 ubiquitin ligase for the wild-type p53, it has also been shown to ubiquitinate mutant p53 (136). It has been established that mutant p53 can promote metastasis through its gain of function properties, including interacting with p63 and p73, and inhibiting their tumor suppressor functions (137). To ensure that any changes in metastatic potential in cells with shMdm2 was not due to mutant p53 levels, western analysis for mutant p53 was performed. ShMdm2 had no detectable increases in mutant p53 levels compared to shGFP cells ensuring that any changes in metastasis would not be due to levels of mutant p53 (Figure 34B).

Mdm2 has been shown to promote positive effects on cell proliferation, through its binding to Rb, and Cyclin A (54, 138). Thus, it was necessary to determine if knockdown of Mdm2 would inhibit TMD-231 cell proliferation and cell cycle progression. First, shGFP and shMdm2 TMD-231 cells were plated and grown for 96 hr. Knockdown of Mdm2 did not show any inhibition of proliferation of TMD-231 cells up to 96 hr, when normalized to the 24 hr time point (Figure 35A). For cell cycle analysis, shGFP and shMdm2 TMD-231 cells were serum starved for 24 hr. After the addition of serum no changes in cell cycle was seen at any time point (Figure 35B). Since no differences in proliferation were observed, we hypothesized that knockdown of Mdm2 in TMD-231 cells would lead to inhibition of their ability to migrate and invade, as has been reported in other cell lines (63, 139). A Matrigel Invasion Assay was employed, using serum as a chemoattractant, and showed that 70% of shGFP cells were able to migrate

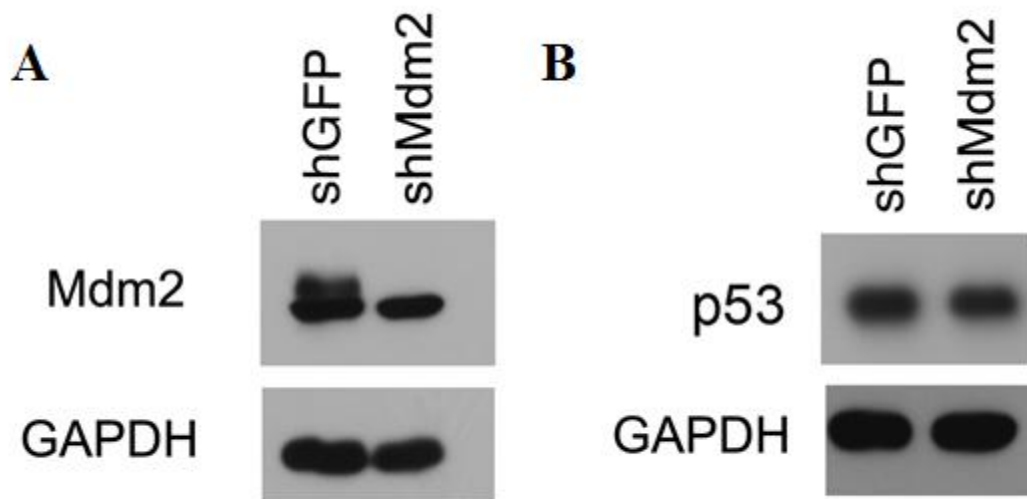


Figure 34: Analysis of Mdm2 and p53 protein levels in shGFP and shMdm2 TMD-231 cells

(A) Western blot analysis of Mdm2 and GAPDH in shGFP and shMdm2 TMD-231 cells.

(B) Western blot analysis of p53 and GAPDH in shGFP and shMdm2 TMD-231 cells.

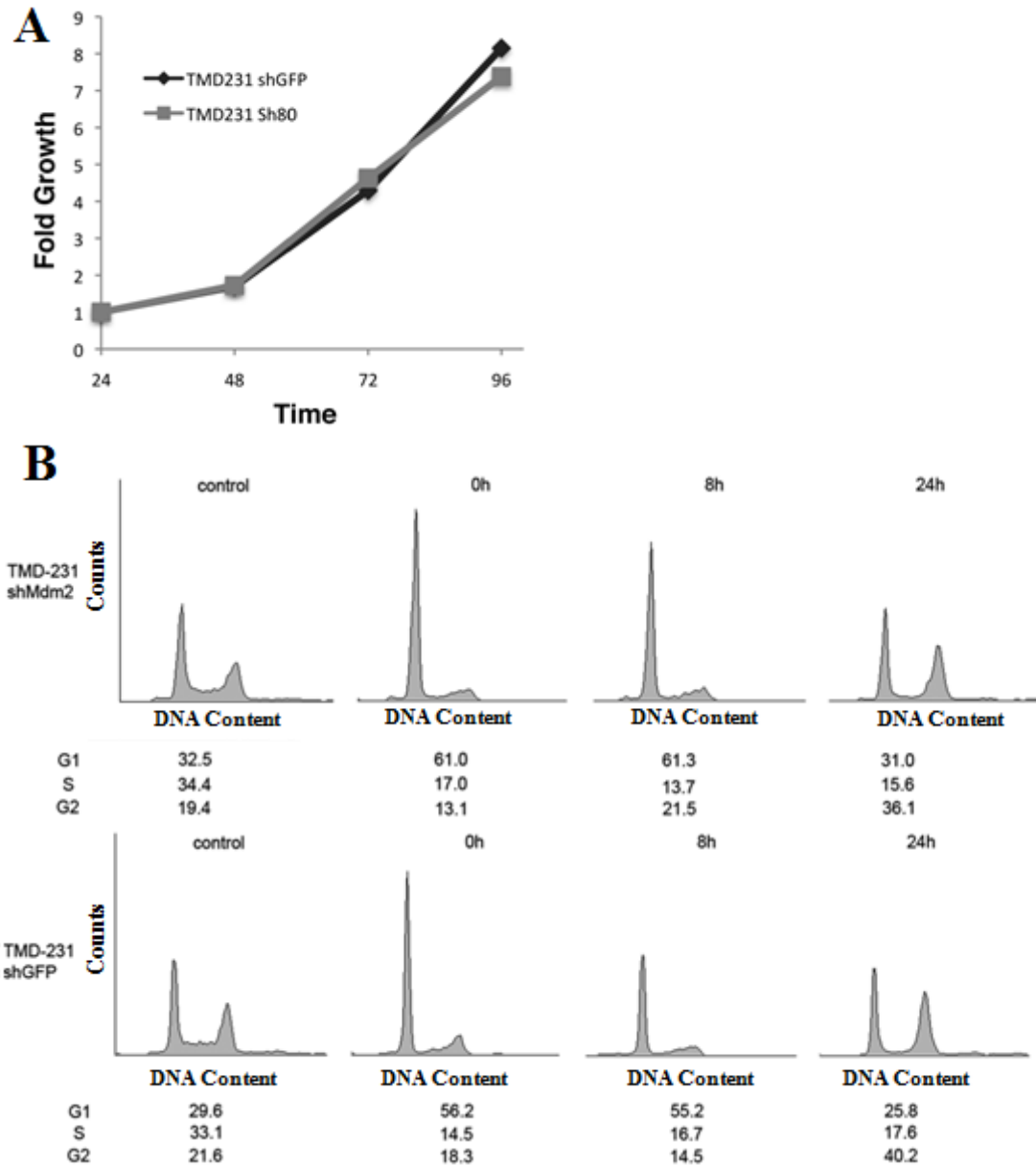


Figure 35: Growth and cell cycle analysis of TMD-231 shGFP and shMdm2 cells
 (A) TMD-231 cells were grown for 96 hr with cell counts taken at 24 hr intervals. Cell counts are normalized to 24 hr time point, to account for differences in plating efficiencies. (B) Cell cycle analysis of TMD-231 cells that were serum starved for 24 hr followed by addition of 1% serum for times indicated.

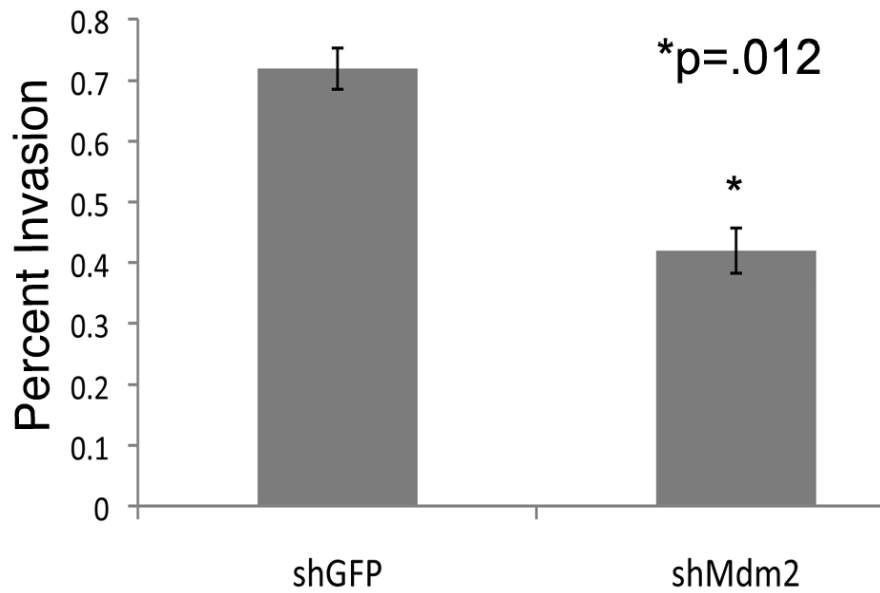


Figure 36: *In vitro* invasion potential of shGFP and shMdm2 TMD-231 cells
shGFP and shMdm2 cells were plated in 8 μ m Matrigel chambers and allowed to invade for 22 hr using serum as a chemoattractant. Cells were counted in three random 25X fields and experiments were done in triplicate. Percent invasion was determined as defined in Materials and Methods. Error bars represent standard deviation.

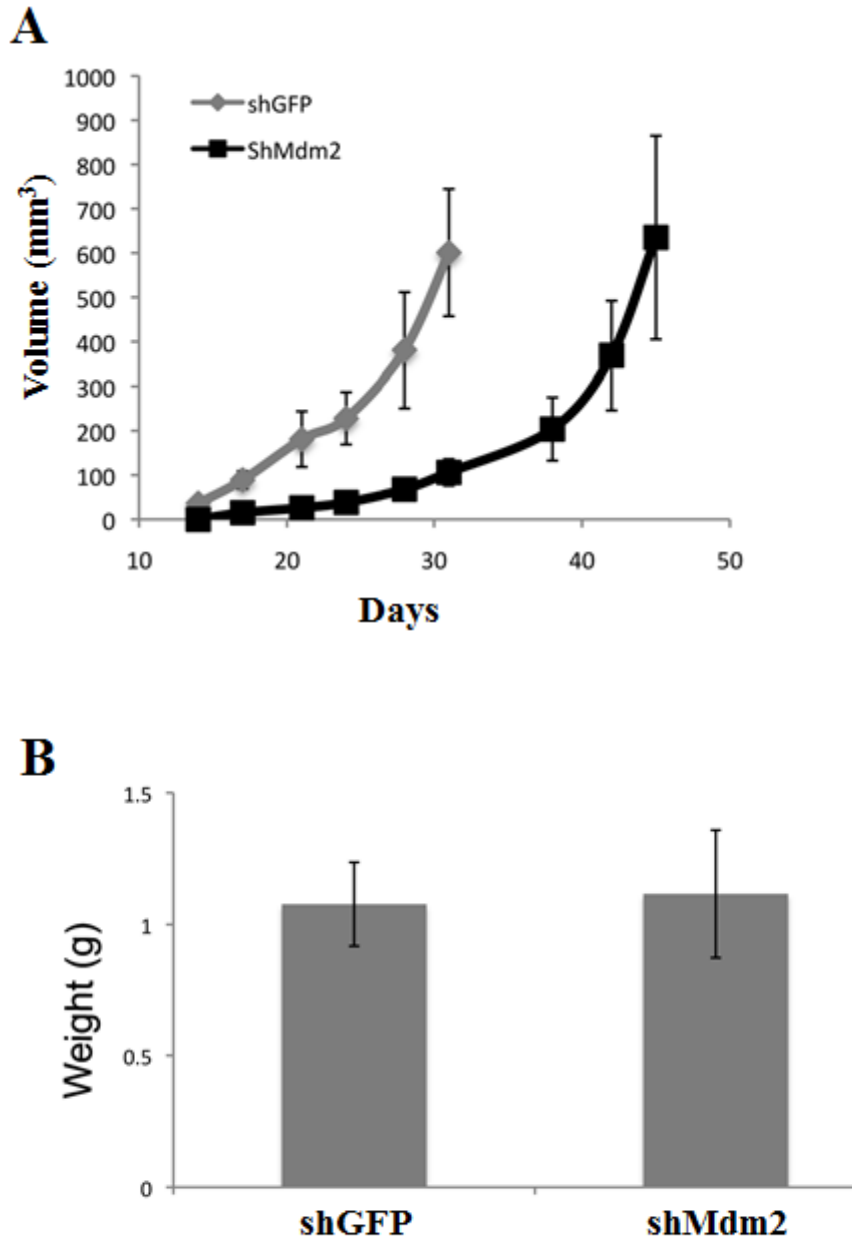


Figure 37: *In vivo* tumor growth and final tumor weights

(A) Graph of tumor volumes over time of shGFP and shMdm2 TMD-231 cells implanted into the mammary fat pad of mice. Tumors were harvested when average volume of group was 600 mm. (B) Final tumor weights after harvest from both TMD-231 tumor groups. Error bars represent standard deviation.

through the chamber compared to only 42% of the shMdm2 cells (Figure 36). These experiments indicate that knockdown of Mdm2 in TMD-231 cells does not affect their proliferation or cell cycle progression, but does hinder the ability of the cells to migrate and invade through Matrigel.

Since knockdown of Mdm2 reduced the ability of TMD-231 cells to migrate through the Matrigel, we were interested to determine if Mdm2 would affect invasion and metastasis *in vivo*. To this end, we implanted shGFP and shMdm2 TMD-231 cells into the mammary fat pad of 6 week old γ -null NOD-SCID mice. To ensure that any differences seen in metastasis were due to Mdm2 loss and not tumor size or weight, each group was harvested when they reached an average final volume of 600mm. At the time of harvest the average tumor weight from each group was identical (1.1g) (Figure 37B). Interestingly the shMdm2 tumors grew at a slower rate, requiring an extra 2 weeks to reach the final volume (Figure 37A). However we noted that the delayed in growth appeared to occur in the initial time after implantation, thus we wondered if the shMdm2 cells may have a problem seeding in an *in vivo* environment. It has been shown that Mdm2 can have effects on extracellular proteins involved with cell attachment (140, 141). Interestingly, shMdm2 cells ability to bind to plates coated with fibronectin was decreased by 40% (Figure 38). This provides evidence that the shMdm2 cells may take longer to adhere in the mammary fat pad and could explain the delayed growth *in vivo*.

The TMD-2331 cell line is a model of breast cancer metastasis to the lung (142). To determine if Mdm2 had any role in this metastatic process we harvested the lungs from both shGFP (n=10) and shMdm2 (N=10) and H&E was performed. All metastases were counted in both the right and left lobe of the lung. The shGFP lungs had an average

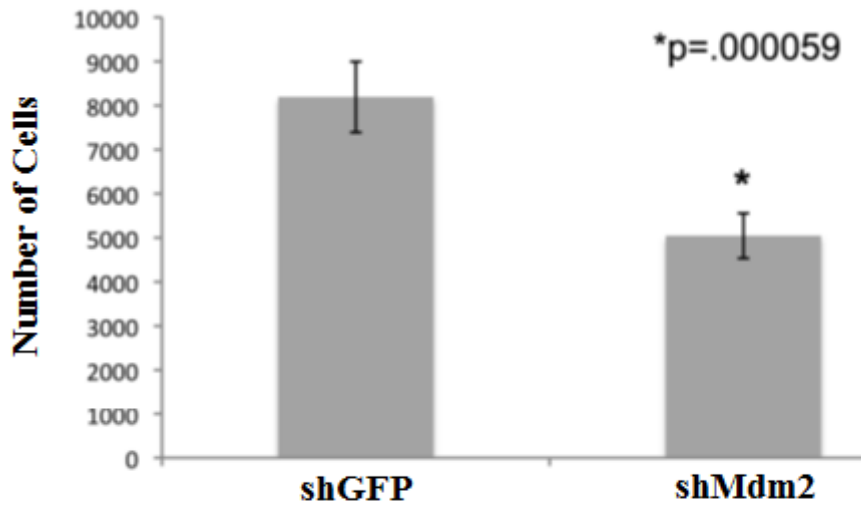


Figure 38: shMdm2 cells have diminished ability to bind fibronectin

shGFP and shMdm2 cells were plated on cell culture dishes that were coated with 5 μ g/ml fibronectin. Cells were incubated for 30 min and then removed and counted. Error bars represent standard deviation.

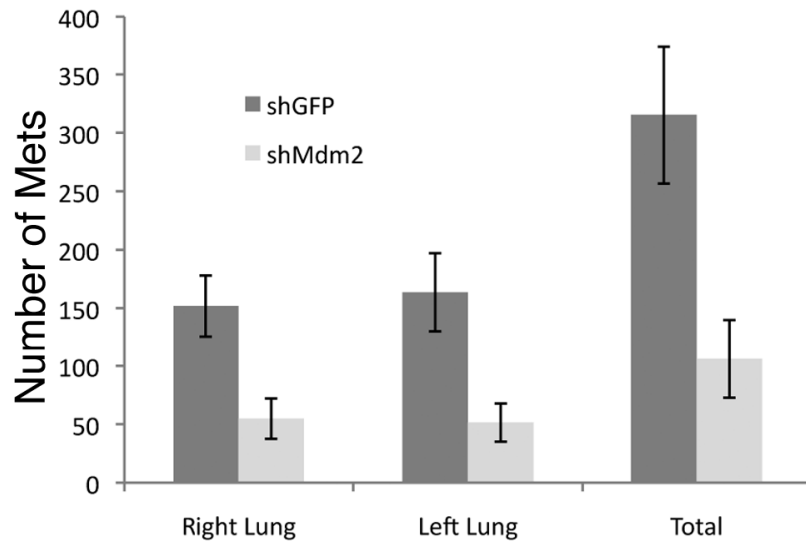


Figure 39: Lung metastatic potential of shGFP and shMdm2 tumors

Lung metastatic lesions from both tumor groups were counted as described in Materials & Methods.

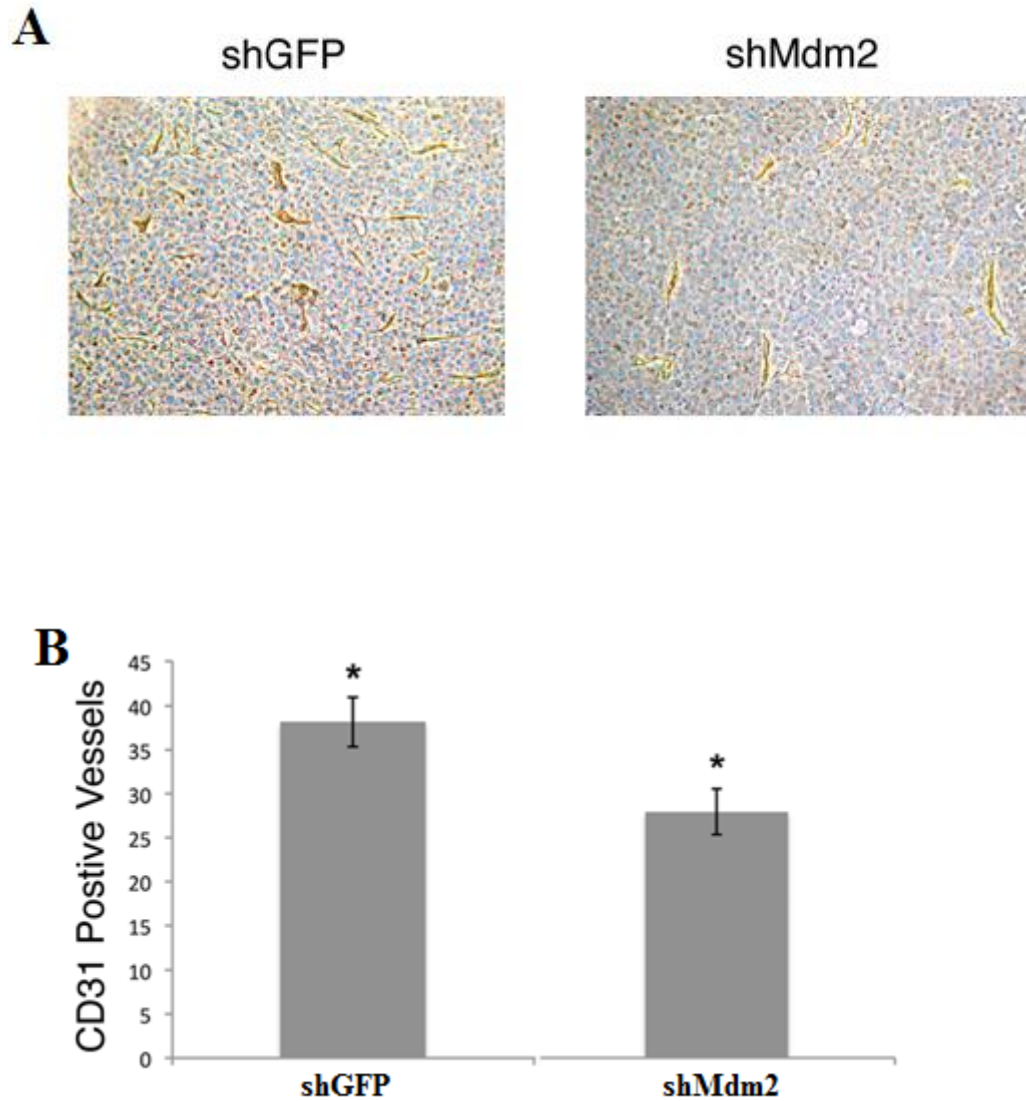


Figure 40: Loss of CD-31 staining in shMdm2 tumors

(A) Tumors from shGFP and shMdm2 were stained for CD-31 using immunohistochemistry. (B) Bar graph representing quantification of CD-31 staining in shGFP and shMdm2 tumors. Three separate 25x fields from 4 different tumors were counted. Error bars represent standard deviation. * represents statistical significance of $p < 0.05$.

of 315 metastases per lung, with each lobe accounting for about half the total number. However the shMdm2 had only an average of 130 metastases per lung, a statistically significant decrease of 60% compared to the shGFP (Figure 39). While the Mdm2 knockdown affected the total number of metastatic foci, it did not affect the size of the lesions, as both small and large metastases were noted in both the shGFP and shMdm2 groups. These results definitively show that Mdm2 is involved in breast cancer metastases to the lung.

Angiogenesis, the formation of new blood vessels from pre-existing ones, is essential in helping tumor cells metastasize. Interestingly Mdm2 has been shown to have numerous angiogenic functions. We have previously shown that Mdm2 can bind to HIF-1 α resulting in the up regulation of the pro-angiogenic factor VEGF (64). Mdm2 can also stabilize VEGF mRNA levels promoting angiogenesis (143). In light of this evidence, we wondered if the tumors harboring knockdown of Mdm2 would be less vascularized. The vessels of the primary tumors were stained with CD-31 and the numbers of blood vessels were counted in multiple fields (Figure 40A). The shGFP showed an average of 38 vessels per field while the shMdm2 tumors only had an average of 28, a significant reduction in the amount of blood vessels by 25% (Figure 40B) from four tumors. To verify that the decrease seen in vascularization was due to changes in HIF-1 α and VEGF protein levels, western blot analysis of both cell lines and tumors were performed. Figure 41A shows that HIF-1 α protein levels are higher in shGFP cells compared to shMdm2 cells under both normoxic and hypoxic conditions. The same results were seen with VEGF protein levels (Figure 41B). As expected, HIF-1 α protein levels in the tumors correlated exactly with the results from tissue culture. Four primary tumors from both

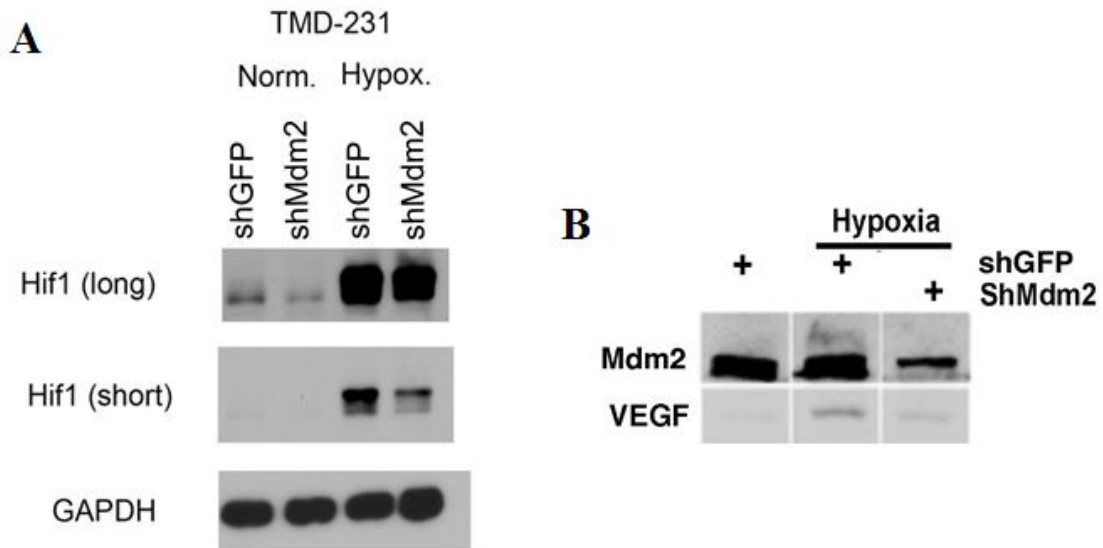


Figure 41: Mdm2 increases HIF-1 α and VEGF protein levels *in vitro*

(A) TMD-231 cells were placed under normoxic or hypoxic conditions and western blot analysis was performed for HIF-1 α and GAPDH. (B) Western analysis of Mdm2 and VEGF from shGFP and shMdm2 TMD-231 cells, under normoxic or hypoxic conditions.

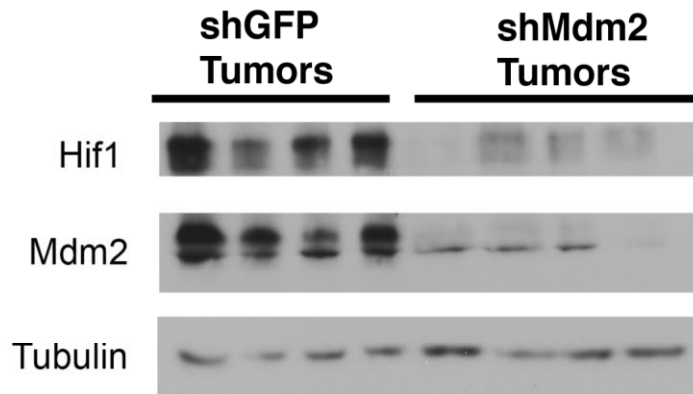


Figure 42: Mdm2 increases HIF-1 α protein levels in tumors

Tumors excised from the mammary fat pad of mice were lysed and western blotting performed for HIF-1 α , Mdm2, and Tubulin.

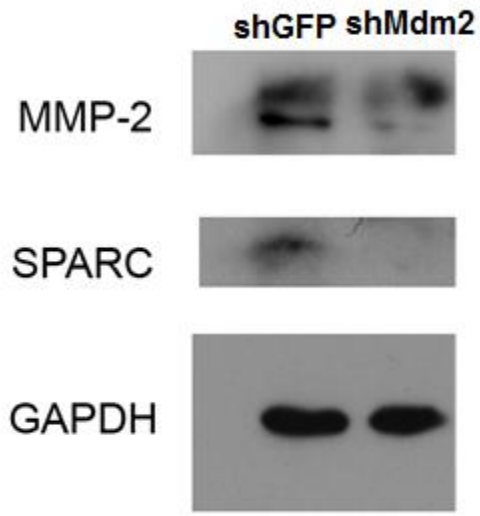


Figure 43: Mdm2 augments protein levels of lung metastasis genes
Western blot analyses of MMP-2, SPARC, and GAPDH from shGFP and shMdm2 TMD-231 cells.

shGFP and shMdm2 showed that Mdm2 and HIF-1 α are all lower in the shMdm2 tumors (Figure 42). These results show that knockdown of Mdm2 results in lower levels of HIF-1 α and VEGF. This loss of pro-angiogenic factors lowers tumor vascularization, thus leading to a decrease in lung metastasis.

Since Mdm2 facilitates many functions in the cell, we hypothesized that Mdm2 could be regulating other pro-metastatic proteins or pathways. Minn et al. recently performed gene-array analysis and generated a list of gene candidates that could mediate breast cancer to lung metastasis (144). From this list we found that both MMP-2 and SPARC protein levels were down regulated in shMdm2 cells compared with shGFP, hinting that Mdm2 could be promoting or regulating a pro-metastatic gene profile for lung metastases (Figure 43). Further work is needed to determine the mechanism by which Mdm2 is regulating these genes.

4.3 Discussion

The Mdm2 onco-protein is implicated in a variety of p53-independent cellular processes including transcription regulation, translation control, DNA repair, and cell cycle regulation, all in addition to its role as the primary regulator of p53. Understanding how Mdm2 is regulating different tumorigenic properties is important treatment of malignancies in the clinic. Mdm2 overexpression correlates with poor patient prognosis and is seen in a variety of human cancers including 1/3 of sarcomas and cancers of the brain, breast, ovary cervix, lung, colon, and prostate (4, 5). The role for Mdm2 in promoting tumorigenesis is well established in both p53 dependent and independent

manner. Recent studies have also implicated Mdm2 in the process of tumor metastasis, but it has not been determined if this role is dependent on p53 (63, 132).

To address this issue we generated a TMD-231 cell line with knockdown of Mdm2 in the background of mutant p53 to use as a model for breast to lung metastasis. This mutation in p53 occurs as a point mutation, R280K. This mutation resides within the DNA binding domain of p53 and renders it incapable of functioning as a transcription factor. This mutation allows us to determine if Mdm2 can promote metastasis independent of wild-type p53 function. Mdm2 has been implemented in cell growth and cell cycle progression not only by inhibiting p53 function, but also through p53-independent mechanisms. Due to this role of Mdm2, we needed to ascertain if knockdown of Mdm2 would affect TMD-231 cell growth and cell cycle progression. Knockdown of Mdm2 in SW1990 pancreatic cells has been shown to reduce cellular proliferation (132). In contrast, however the growth rates of p53^{-/-} MEFS and p53^{-/-}, Mdm2^{-/-} MEFS are nearly identical (145). Furthermore, expression of Mdm2 splice variants incapable of binding p53 can actually inhibit cellular proliferation *in vitro* (146). The knockdown of Mdm2 in our TMD-231 cells did not affect cell growth, providing evidence that Mdm2's role for cell proliferation in cell culture may be cell type specific (Figure 35A).

Mutant p53 can acquire gain of function attributes that aid in cell survival advantages, such as increased proliferation, evasion of apoptosis, and chemoresistance. These gain of function attributes are seen as the use of shRNA to mutant p53 in MDA-MB-231 cells results in decreased cell proliferation, reduced invasion in boyden chambers, and lower tumor weight in nude mice (147). Important to the scope of this

study is the gain of function ability of mutant p53 to enhance tumor metastasis. Mutant p53 enhancement of metastatic potential is shown by the observation that p53 knockout mice develop tumors at a high frequency, but have a low occurrence of metastasis or invasive growth. In contrast, transgenic mice knocked-in with mutant p53 develop highly metastatic tumors (148). Furthermore, mutant p53 was found to promote EMT by facilitating the function of the key transcriptional regulators of this process, TWIST1 and SLUG, and inhibit cell invasion via the inhibition of p63 (130, 149). Since we were interested in the role of Mdm2 in metastasis in a p53-independent background, we had to be sure that mutant p53 levels were not affected by Mdm2 knockdown. Mdm2 still retains the ability to degrade mutant p53 (136), but our results indicated that knockdown of Mdm2 had no bearing on mutant p53 protein levels (Figure 34 A&B). If Mdm2 was regulating mutant p53 in TMD-231 cells, knockdown of Mdm2 should have resulted in an increase of mutant p53 levels. Our result that mutant p53 levels are not altered is in agreement with recent findings that suggest mutant p53 cannot interact with Mdm2 in cancer cells. (147).

Comparing our *in vitro* cell proliferation data to *in vivo* tumor growth, we note that knockdown of Mdm2 does slow *in vivo* tumor growth (Figure 37A). These differing observations hint that Mdm2 may play a role in TMD-231 cells ability to adhere on different growth substrates. Mdm2 has been implemented in regulation of cell adhesion molecules such as E-cadherin and Syntaxin 6. Thus, loss of Mdm2 may interfere with the ability of TMD-231 cells to seed in an *in vivo* environment. This hypothesis is attractive as knockdown of Mdm2 significantly reduces the ability of cells to adhere to fibronectin-

coated plates (Figure 38). This reasoning would explain why the tumors after an initial growth lag were able to eventually seed and grow to the same size as control tumors.

The ability of the shMdm2 tumors to grow to the same size as control tumors was imperative, as we wanted to assure ourselves that the tumor size would have no bearing on the ability of the tumors to metastasize. All tumors were harvested when the average volume was 600 mm³. The average tumor weight for each group was 1.1g (Figure 37 B). This allowed us to ensure that the difference seen in metastases was not due to a greater tumor weight and volume in the shGFP group, and was solely due to differences in Mdm2 expression. This scenario was observed, as knockdown of Mdm2 resulted in drastic loss of metastases to the lung. A 60% reduction of lungs metastases was seen in the shMdm2 group (Figure 39). Overall the size of the metastases between the two groups was similar suggesting that Mdm2 did not have an effect on the ability of the tumor cells to grow once they have seeded at a new site. Therefore, Mdm2 may also have a role in the intravasation stage of metastasis. The ability of tumor cells to escape into the blood stream is dependent on the capacity of the tumor to recruit new vasculature through angiogenesis. Mdm2 has been described as having pro-angiogenic properties through its regulation of HIF-1 α and VEGF. We have shown that Mdm2 can bind HIF-1 α and enhance VEGF transcription as determined by luciferase activity assays (64). This enhancement of HIF-1 α transcriptional activity is from an increase in p300 recruitment through an Mdm2 dependent process that inhibits hydroxylation of Asn803 in HIF-1 α both *in vivo* and *in vitro* (150). Interestingly, recent work has also shown an Mdm2 dependent increase of VEGF mRNA stability and translation through Mdm2 binding to the AU-rich sequence within the 3' untranslated region of VEGF mRNA (143). Due to

Mdm2's defined role in regulating these pro-angiogenic targets, it was logical to assume that our cells and tumors would yield similar experimental results. As expected, knockdown of Mdm2 resulted in the loss of HIF-1 α and VEGF protein levels in both cell culture and tumor lysates (Figure 41 & 42). This loss of angiogenic factors correlates with a decrease in vascular endothelial cells in the tumor (Figure 40 A&B), as the knockdown of Mdm2 prevented the formation of new vasculature in the tumor. These results provide evidence that Mdm2 may enhance tumor metastasis through the recruitment of angiogenic factors and allow vascularization of the primary tumor.

Metastasis is a multi-step process including tumor cell intravasation, survival in circulation, extravasation into a distant organ, angiogenesis and uninhibited cellular growth. Due to the role of Mdm2 in numerous cellular processes we could not eliminate the possibility that Mdm2 could be functioning in other ways to promote lung metastasis than just through regulating pro-angiogenic factors. Recent work by Minn and colleagues using MDA-MB-231 cells and transcriptomic analysis identified a set of genes that mediates breast cancer metastasis to the lungs (144). Their results showed a subset of four genes (SPARC, IL13RA2, VCAM1 and MMP2) whose expression, as determined by northern blot was generally seen in aggressive lung-metastatic populations. We show that knockdown of Mdm2 results in lower levels of both MMP2 and SPARC (Figure 43). Normally SPARC functions as a modulator of the extracellular matrix, but deregulation has been linked to an invasive tumor cell phenotype and poor outcome in human melanomas. Recent work has shown that SPARC augments tumor growth by stabilizing Mdm2 levels through AKT phosphorylation at serine 166. This phosphorylation allows Mdm2 to translocate to the nucleus and inactivate p53 in human melanomas (141). This

work, along with ours, could support a Mdm2/SPARC network to support tumor growth and metastasis.

Here we show that Mdm2 is involved in tumor metastasis through multiple p53 independent functions including a role in tumor cell adherence, regulation of the pro-angiogenic factors HIF-1 α and VEGF, and perpetrating a lung metastatic gene signature through increases in the protein levels of SPARC and MMP2. Understanding how Mdm2 regulates metastasis is important as metastatic disease is usually the terminal step in cancer development, so understanding and prevention is critical. Here we present evidence that Mdm2 can be a primary component of breast cancer to lung metastasis and thus could be a viable clinical target.

5. Summary/Future Directions

Mdm2 serves many diverse functions in a variety of cellular processes and has a well-established role in tumorigenesis. Here we have shown that Mdm2, through c-Src mediated phosphorylation, can inhibit p53 activity through neddylation while maintaining p53 protein levels. We have also confirmed that Mdm2 has a positive role in cancer metastasis, thus adding more complex functions to Mdm2 regulation of tumorigenesis. Since roles for Mdm2 in cancer are continuing to be identified, a sustained effort to find Mdm2 inhibitors for clinical use is urgently needed. Most Mdm2 inhibitors developed thus far have focused on inhibiting the p53-Mdm2 interaction in an attempt to re-activate p53. The interaction between p53 and Mdm2 involves four residues in p53 (Phe 19, Leu 22, Trp 23, Leu 26) and a hydrophobic pocket in the N-terminal region of Mdm2. The most studied inhibitor has been Nutlin-3a, which inhibits Mdm2-p53 binding by binding to the Mdm2 hydrophobic pocket resulting in activation of p53 and leading to cell cycle arrest, apoptosis, and growth inhibition of human tumor xenografts in nude mice (151). It was first assumed that Nutlin would only function in wild-type p53 tumors, but recent work has shown that Nutlin can inhibit angiogenesis through inhibition of the Mdm2/HIF-1 α interaction, independent of p53 (64, 150). Furthermore, it was recently demonstrated that Nutlin-3a can upregulate apoptotic genes independent of p53, by blocking the p73/Mdm2 interaction (152). These studies show that inhibition of Mdm2 can still have advantageous results even in absence of wild-type p53 and lends support to the developmental ideology for inhibitors that target alternative domains outside of the p53-binding region. Inhibition of the Mdm2 RING E3 ligase is an attractive target and has been shown to activate p53, which is accomplished through inhibition of p53

ubiquitination and neddylation (153). Mdm2 specifies its ligase activity through the recruitment of specific E2 enzymes, thus specific inhibitors for each interaction, could be an invaluable tool depending on a specific tumor genetic makeup. For tumors with high Mdm2/low p53 a Mdm2/Ubc5 inhibitor could be used to inhibit p53 ubiquitination. While tumors with high Mdm2/high p53, would benefit from inhibition of Mdm2/Ubc12, which would inhibit neddylation, thus personalizing cancer care by specifically targeting Mdm2 function. This could be even more advantageous for mutant p53 tumors as Mdm2 has been shown to ubiquitinate and degrade mutant p53. Interestingly, work has not been performed on neddylation of mutant p53 and the downstream signaling consequences. It could be envisioned that neddylation of mutant p53 could enhance mutant p53 gain of function status. Therefore, inhibition of neddylation, but not ubiquitination could be clinically relevant in the treatment of certain cancers.

Angiogenesis facilitates tumor growth and metastasis. We show here that Mdm2 has a role in regulating cancer metastasis partly through controlling HIF-1 α /VEGF levels and promoting vascularization of the tumor. Additionally, we also show that c-Src phosphorylation of Mdm2 affects the angiogenic pathway through inhibiting the expression of p53-mediated transcription of *maspin*.

This lead us to hypothesize if c-Src and Mdm2 together could be leading the angiogenic switch, since both proteins have been implemented in the positive regulation of HIF-1 α and VEGF. Since we have shown that c-Src can phosphorylate Mdm2, we

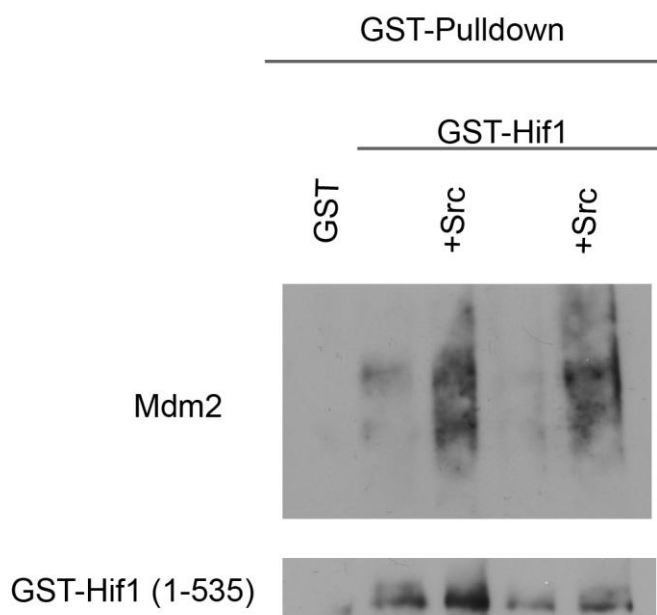


Figure 44: c-Src phosphorylation of Mdm2 increases Mdm2/HIF-1 α binding

In vitro GST-pulldown assay using GST-HIF-1 α (1-535) and Mdm2. Mdm2 was left unphosphorylated or was phosphorylated by c-Src before incubation with GST-HIF-1 α . GST alone was used a negative control. Experiment was performed in duplicate.

wondered if this event might enhance the pro-angiogenic phenotype. Through the use of *in vitro* GST-pulldown assays we have data showing that c-Src phosphorylated Mdm2 binds HIF-1 α to a greater degree than unphosphorylated Mdm2, allowing for greater transcriptional activity of HIF-1 α (Figure 44). Recent work has shown that HIF-1 α itself is also neddylated, leading to an increase in the protein half-life (154). However the E3 ligase responsible for this neddylation has yet to be determined. Due to Mdm2 ability to bind HIF-1 α and function as a neddyating enzyme we wondered if this interaction could result in neddylated HIF-1 α . Through the use of overexpression, and immunoprecipitation of HA-nedd8, our data shows that HIF-1 α is neddylated in the presence Mdm2, but not in the presence of the ligase dead C464S (Figure 45). Thus c-Src phosphorylation of Mdm2 results in an increased binding to HIF-1 α , which enables Mdm2 to neddylate HIF-1 α . This neddylation event would result in an increase of HIF-1 α half-life, allowing for increased HIF-1 α transcriptional activity. If this hypothesis is correct, then inhibiting c-Src activity should result in the loss of Mdm2 ability to activate HIF-1 α transcriptional activity. This is shown as treatment with the c-Src inhibitor PP1 decreases the positive effect of Mdm2 on the HRE-Luc promoter as determined by a luciferase assay (Figure 46). These experiments provide evidence that c-Src and Mdm2 may be collaborating for a pro-angiogenic phenotype, and support future endeavors into determining its regulation.

In conclusion, we have shown novel regulation and activities of the oncogene Mdm2. First we have provided evidence that c-Src phosphorylation of Mdm2 can switch its E3 ligase activity from ubiquitin to neddylation resulting in stable, but

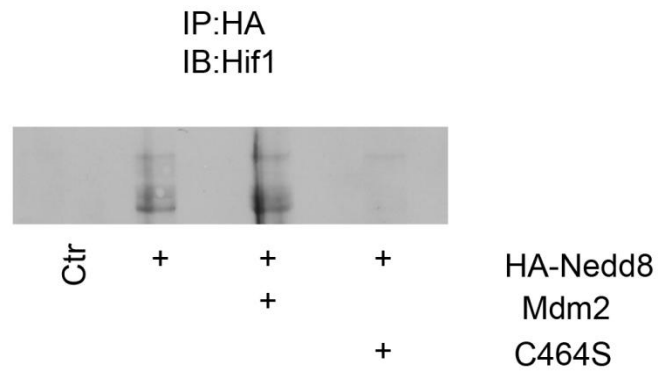


Figure 45: Neddylation of HIF-1 α by Mdm2

H1299 cells, overexpressing HA-Nedd8 plus Mdm2 or C464S, were exposed to hypoxic conditions for 16 hr, before the immunoprecipitation of HA-tag. Following immunoprecipitation western blot analysis was performed for HIF-1 α . Bands represent neddylated HIF-1 α .

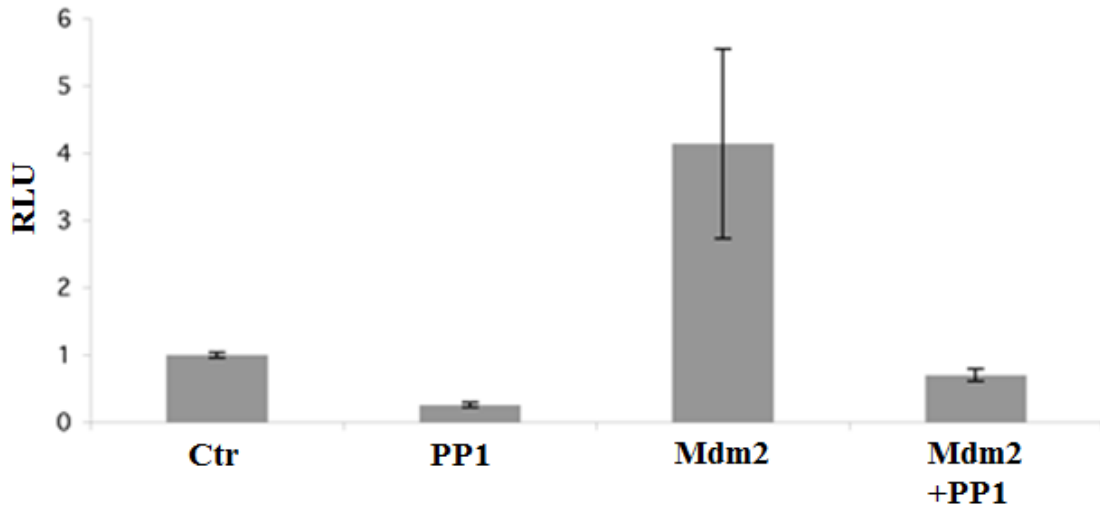


Figure 46: Inhibition of c-Src impairs Mdm2's ability to enhance HIF-1 α transcriptional activity

H1299 cells overexpressing HRE-Luc, myc-LacZ, and Mdm2. Cells were treated with 10 μ M PP1 for 16 hr before determination of luciferase activity. Y-axis measurements are relative luciferase units (RLU). The RLU was calculated from the ratio of luciferase/ β -gal activity. Error bars represent standard deviation.

transcriptionally inactive p53. We have also definitively shown that Mdm2 can enhance breast cancer metastasis, independent of p53 status. Taken together, my data provide novel insights into important p53-dependent and independent functions of Mdm2 and provide potential novel avenues for therapeutic intervention.

References

1. Fakharzadeh SS, Trusko SP, George DL. Tumorigenic potential associated with enhanced expression of a gene that is amplified in a mouse tumor cell line. *EMBO J* 1991; 10: 1565-9.
2. Finlay CA. The mdm-2 oncogene can overcome wild-type p53 suppression of transformed cell growth. *Mol Cell Biol* 1993; 13: 301-6.
3. Cahilly-Snyder L, Yang-Feng T, Francke U, George DL. Molecular analysis and chromosomal mapping of amplified genes isolated from a transformed mouse 3T3 cell line. *Somat Cell Mol Genet* 1987; 13: 235-44.
4. Rayburn E, Zhang R, He J, Wang H. MDM2 and human malignancies: expression, clinical pathology, prognostic markers, and implications for chemotherapy. *Curr Cancer Drug Targets* 2005; 5: 27-41.
5. Momand J, Jung D, Wilczynski S, Niland J. The MDM2 gene amplification database. *Nucleic Acids Res* 1998; 26: 3453-9.
6. Chau V, Tobias JW, Bachmair A, et al. A multiubiquitin chain is confined to specific lysine in a targeted short-lived protein. *Science* 1989; 243: 1576-83.
7. Hicke L, Schubert HL, Hill CP. Ubiquitin-binding domains. *Nat Rev Mol Cell Biol* 2005; 6: 610-21.
8. Schulman BA, Harper JW. Ubiquitin-like protein activation by E1 enzymes: the apex for downstream signalling pathways. *Nat Rev Mol Cell Biol* 2009; 10: 319-31.
9. Wenzel DM, Stoll KE, Klevit RE. E2s: structurally economical and functionally replete. *Biochem J* 2011; 433: 31-42.
10. Deshaies RJ, Joazeiro CA. RING domain E3 ubiquitin ligases. *Annu Rev Biochem* 2009; 78: 399-434.
11. Araki S, Eitel JA, Batuello CN, et al. TGF-beta1-induced expression of human Mdm2 correlates with late-stage metastatic breast cancer. *J Clin Invest* 2010; 120: 290-302.
12. Haupt Y, Maya R, Kazaz A, Oren M. Mdm2 promotes the rapid degradation of p53. *Nature* 1997; 387: 296-9.
13. Kubbutat MH, Jones SN, Vousden KH. Regulation of p53 stability by Mdm2. *Nature* 1997; 387: 299-303.
14. Maki CG, Huibregtse JM, Howley PM. In vivo ubiquitination and proteasome-mediated degradation of p53(1). *Cancer Res* 1996; 56: 2649-54.
15. Menendez D, Inga A, Resnick MA. The expanding universe of p53 targets. *Nat Rev Cancer* 2009; 9: 724-37.
16. Kruse JP, Gu W. Modes of p53 regulation. *Cell* 2009; 137: 609-22.
17. Li M, Brooks CL, Wu-Baer F, Chen D, Baer R, Gu W. Mono- versus polyubiquitination: differential control of p53 fate by Mdm2. *Science* 2003; 302: 1972-5.
18. Ito A, Lai CH, Zhao X, et al. p300/CBP-mediated p53 acetylation is commonly induced by p53-activating agents and inhibited by MDM2. *EMBO J* 2001; 20: 1331-40.
19. Jones SN, Roe AE, Donehower LA, Bradley A. Rescue of embryonic lethality in Mdm2-deficient mice by absence of p53. *Nature* 1995; 378: 206-8.
20. Montes de Oca Luna R, Wagner DS, Lozano G. Rescue of early embryonic lethality in mdm2-deficient mice by deletion of p53. *Nature* 1995; 378: 203-6.

21. Itahana K, Mao H, Jin A, et al. Targeted inactivation of Mdm2 RING finger E3 ubiquitin ligase activity in the mouse reveals mechanistic insights into p53 regulation. *Cancer Cell* 2007; 12: 355-66.
22. Xirodimas DP, Saville MK, Bourdon JC, Hay RT, Lane DP. Mdm2-mediated NEDD8 conjugation of p53 inhibits its transcriptional activity. *Cell* 2004; 118: 83-97.
23. Lammer D, Mathias N, Laplaza JM, et al. Modification of yeast Cdc53p by the ubiquitin-related protein rub1p affects function of the SCFCdc4 complex. *Genes Dev* 1998; 12: 914-26.
24. Kurz T, Pintard L, Willis JH, et al. Cytoskeletal regulation by the Nedd8 ubiquitin-like protein modification pathway. *Science* 2002; 295: 1294-8.
25. Tateishi K, Omata M, Tanaka K, Chiba T. The NEDD8 system is essential for cell cycle progression and morphogenetic pathway in mice. *J Cell Biol* 2001; 155: 571-9.
26. Ohh M, Kim WY, Moslehi JJ, et al. An intact NEDD8 pathway is required for Cullin-dependent ubiquitylation in mammalian cells. *EMBO Rep* 2002; 3: 177-82.
27. Soucy TA, Smith PG, Milhollen MA, et al. An inhibitor of NEDD8-activating enzyme as a new approach to treat cancer. *Nature* 2009; 458: 732-6.
28. Kamura T, Conrad MN, Yan Q, Conaway RC, Conaway JW. The Rbx1 subunit of SCF and VHL E3 ubiquitin ligase activates Rub1 modification of cullins Cdc53 and Cul2. *Genes Dev* 1999; 13: 2928-33.
29. Duda DM, Borg LA, Scott DC, Hunt HW, Hammel M, Schulman BA. Structural insights into NEDD8 activation of cullin-RING ligases: conformational control of conjugation. *Cell* 2008; 134: 995-1006.
30. Pan ZQ, Kentsis A, Dias DC, Yamoah K, Wu K. Nedd8 on cullin: building an expressway to protein destruction. *Oncogene* 2004; 23: 1985-97.
31. Abida WM, Nikolaev A, Zhao W, Zhang W, Gu W. FBXO11 promotes the Neddylation of p53 and inhibits its transcriptional activity. *J Biol Chem* 2007; 282: 1797-804.
32. Carter S, Vousden KH. p53-Ubl fusions as models of ubiquitination, sumoylation and neddylation of p53. *Cell Cycle* 2008; 7: 2519-28.
33. Liu G, Xirodimas DP. NUB1 promotes cytoplasmic localization of p53 through cooperation of the NEDD8 and ubiquitin pathways. *Oncogene* 2010; 29: 2252-61.
34. Watson IR, Li BK, Roche O, Blanch A, Ohh M, Irwin MS. Chemotherapy induces NEDP1-mediated destabilization of MDM2. *Oncogene* 2010; 29: 297-304.
35. Bartel F, Taubert H, Harris LC. Alternative and aberrant splicing of MDM2 mRNA in human cancer. *Cancer Cell* 2002; 2: 9-15.
36. Bond GL, Hu W, Bond EE, et al. A single nucleotide polymorphism in the MDM2 promoter attenuates the p53 tumor suppressor pathway and accelerates tumor formation in humans. *Cell* 2004; 119: 591-602.
37. Phelps M, Darley M, Primrose JN, Blaydes JP. p53-independent activation of the hdm2-P2 promoter through multiple transcription factor response elements results in elevated hdm2 expression in estrogen receptor alpha-positive breast cancer cells. *Cancer Res* 2003; 63: 2616-23.
38. Chang CJ, Freeman DJ, Wu H. PTEN regulates Mdm2 expression through the P1 promoter. *J Biol Chem* 2004; 279: 29841-8.

39. Busuttill V, Droin N, McCormick L, et al. NF-kappaB inhibits T-cell activation-induced, p73-dependent cell death by induction of MDM2. *Proc Natl Acad Sci U S A* 2010; 107: 18061-6.
40. Mayo LD, Donner DB. A phosphatidylinositol 3-kinase/Akt pathway promotes translocation of Mdm2 from the cytoplasm to the nucleus. *Proc Natl Acad Sci U S A* 2001; 98: 11598-603.
41. Kamijo T, Weber JD, Zambetti G, Zindy F, Roussel MF, Sherr CJ. Functional and physical interactions of the ARF tumor suppressor with p53 and Mdm2. *Proc Natl Acad Sci U S A* 1998; 95: 8292-7.
42. Pomerantz J, Schreiber-Agus N, Liegeois NJ, et al. The Ink4a tumor suppressor gene product, p19Arf, interacts with MDM2 and neutralizes MDM2's inhibition of p53. *Cell* 1998; 92: 713-23.
43. Allende-Vega N, McKenzie L, Meek D. Transcription factor TAFII250 phosphorylates the acidic domain of Mdm2 through recruitment of protein kinase CK2. *Mol Cell Biochem* 2008; 316: 99-106.
44. Maya R, Balass M, Kim ST, et al. ATM-dependent phosphorylation of Mdm2 on serine 395: role in p53 activation by DNA damage. *Genes Dev* 2001; 15: 1067-77.
45. Cheng Q, Chen L, Li Z, Lane WS, Chen J. ATM activates p53 by regulating MDM2 oligomerization and E3 processivity. *EMBO J* 2009; 28: 3857-67.
46. Shinozaki T, Nota A, Taya Y, Okamoto K. Functional role of Mdm2 phosphorylation by ATR in attenuation of p53 nuclear export. *Oncogene* 2003; 22: 8870-80.
47. Mayo LD, Turchi JJ, Berberich SJ. Mdm-2 phosphorylation by DNA-dependent protein kinase prevents interaction with p53. *Cancer Res* 1997; 57: 5013-6.
48. Waning DL, Lehman JA, Batuello CN, Mayo LD. c-Abl phosphorylation of Mdm2 facilitates Mdm2-Mdmx complex formation. *J Biol Chem* 2011; 286: 216-22.
49. Dias SS, Milne DM, Meek DW. c-Abl phosphorylates Hdm2 at tyrosine 276 in response to DNA damage and regulates interaction with ARF. *Oncogene* 2006; 25: 6666-71.
50. Arasada RR, Carpenter G. Secretase-dependent tyrosine phosphorylation of Mdm2 by the ErbB-4 intracellular domain fragment. *J Biol Chem* 2005; 280: 30783-7.
51. Zeng X, Chen L, Jost CA, et al. MDM2 suppresses p73 function without promoting p73 degradation. *Mol Cell Biol* 1999; 19: 3257-66.
52. Minsky N, Oren M. The RING domain of Mdm2 mediates histone ubiquitylation and transcriptional repression. *Mol Cell* 2004; 16: 631-9.
53. Sdek P, Ying H, Zheng H, et al. The central acidic domain of MDM2 is critical in inhibition of retinoblastoma-mediated suppression of E2F and cell growth. *J Biol Chem* 2004; 279: 53317-22.
54. Uchida C, Miwa S, Kitagawa K, et al. Enhanced Mdm2 activity inhibits pRB function via ubiquitin-dependent degradation. *EMBO J* 2005; 24: 160-9.
55. Linares LK, Kiernan R, Triboulet R, et al. Intrinsic ubiquitination activity of PCAF controls the stability of the oncoprotein Hdm2. *Nat Cell Biol* 2007; 9: 331-8.
56. Coutts AS, Boulahbel H, Graham A, La Thangue NB. Mdm2 targets the p53 transcription cofactor JMY for degradation. *EMBO Rep* 2007; 8: 84-90.
57. Dai MS, Lu H. Inhibition of MDM2-mediated p53 ubiquitination and degradation by ribosomal protein L5. *J Biol Chem* 2004; 279: 44475-82.

58. Zhang Y, Wolf GW, Bhat K, et al. Ribosomal protein L11 negatively regulates oncoprotein MDM2 and mediates a p53-dependent ribosomal-stress checkpoint pathway. *Mol Cell Biol* 2003; 23: 8902-12.
59. Dai MS, Zeng SX, Jin Y, Sun XX, David L, Lu H. Ribosomal protein L23 activates p53 by inhibiting MDM2 function in response to ribosomal perturbation but not to translation inhibition. *Mol Cell Biol* 2004; 24: 7654-68.
60. Wei X, Yu ZK, Ramalingam A, et al. Physical and functional interactions between PML and MDM2. *J Biol Chem* 2003; 278: 29288-97.
61. Bouska A, Lushnikova T, Plaza S, Eischen CM. Mdm2 promotes genetic instability and transformation independent of p53. *Mol Cell Biol* 2008; 28: 4862-74.
62. Asahara H, Li Y, Fuss J, et al. Stimulation of human DNA polymerase epsilon by MDM2. *Nucleic Acids Res* 2003; 31: 2451-9.
63. Yang JY, Zong CS, Xia W, et al. MDM2 promotes cell motility and invasiveness by regulating E-cadherin degradation. *Mol Cell Biol* 2006; 26: 7269-82.
64. LaRusch GA, Jackson MW, Dunbar JD, Warren RS, Donner DB, Mayo LD. Nutlin3 blocks vascular endothelial growth factor induction by preventing the interaction between hypoxia inducible factor 1alpha and Hdm2. *Cancer Res* 2007; 67: 450-4.
65. Sczaniecka M, Gladstone K, Pettersson S, McLaren L, Huart AS, Wallace M. MDM2 protein-mediated ubiquitination of numb protein: identification of a second physiological substrate of MDM2 that employs a dual-site docking mechanism. *J Biol Chem* 2012; 287: 14052-68.
66. Inuzuka H, Tseng A, Gao D, et al. Phosphorylation by casein kinase I promotes the turnover of the Mdm2 oncoprotein via the SCF(beta-TRCP) ubiquitin ligase. *Cancer Cell* 2010; 18: 147-59.
67. Irby RB, Yeatman TJ. Role of Src expression and activation in human cancer. *Oncogene* 2000; 19: 5636-42.
68. Finn RS. Targeting Src in breast cancer. *Ann Oncol* 2008; 19: 1379-86.
69. Giaccone G, Zucali PA. Src as a potential therapeutic target in non-small-cell lung cancer. *Ann Oncol* 2008; 19: 1219-23.
70. Shalloway D, Coussens PM, Yaciuk P. Overexpression of the c-src protein does not induce transformation of NIH 3T3 cells. *Proc Natl Acad Sci U S A* 1984; 81: 7071-5.
71. Yeatman TJ. A renaissance for SRC. *Nat Rev Cancer* 2004; 4: 470-80.
72. Cavallaro U. N-cadherin as an invasion promoter: a novel target for antitumor therapy? *Curr Opin Investig Drugs* 2004; 5: 1274-8.
73. Savagner P. The epithelial-mesenchymal transition (EMT) phenomenon. *Ann Oncol* 2010; 21 Suppl 7: vii89-92.
74. Guo W, Giancotti FG. Integrin signalling during tumour progression. *Nat Rev Mol Cell Biol* 2004; 5: 816-26.
75. Overall CM, Kleinfeld O. Tumour microenvironment - opinion: validating matrix metalloproteinases as drug targets and anti-targets for cancer therapy. *Nat Rev Cancer* 2006; 6: 227-39.
76. Rak J, Yu JL. Oncogenes and tumor angiogenesis: the question of vascular "supply" and vascular "demand". *Semin Cancer Biol* 2004; 14: 93-104.
77. Fong GH, Rossant J, Gertsenstein M, Breitman ML. Role of the Flt-1 receptor tyrosine kinase in regulating the assembly of vascular endothelium. *Nature* 1995; 376: 66-70.

78. Millauer B, Wizigmann-Voos S, Schnurch H, et al. High affinity VEGF binding and developmental expression suggest Flk-1 as a major regulator of vasculogenesis and angiogenesis. *Cell* 1993; 72: 835-46.
79. Kaipainen A, Korhonen J, Mustonen T, et al. Expression of the fms-like tyrosine kinase 4 gene becomes restricted to lymphatic endothelium during development. *Proc Natl Acad Sci U S A* 1995; 92: 3566-70.
80. Schofield CJ, Ratcliffe PJ. Oxygen sensing by HIF hydroxylases. *Nat Rev Mol Cell Biol* 2004; 5: 343-54.
81. Kaelin WG, Jr., Ratcliffe PJ. Oxygen sensing by metazoans: the central role of the HIF hydroxylase pathway. *Mol Cell* 2008; 30: 393-402.
82. Brahimi-Horn MC, Pouyssegur J. The hypoxia-inducible factor and tumor progression along the angiogenic pathway. *Int Rev Cytol* 2005; 242: 157-213.
83. Zou Z, Anisowicz A, Hendrix MJ, et al. Maspin, a serpin with tumor-suppressing activity in human mammary epithelial cells. *Science* 1994; 263: 526-9.
84. Silverman GA, Bird PI, Carrell RW, et al. The serpins are an expanding superfamily of structurally similar but functionally diverse proteins. Evolution, mechanism of inhibition, novel functions, and a revised nomenclature. *J Biol Chem* 2001; 276: 33293-6.
85. Umekita Y, Hiipakka RA, Liao S. Rat and human maspins: structures, metastatic suppressor activity and mutation in prostate cancer cells. *Cancer Lett* 1997; 113: 87-93.
86. Gao F, Shi HY, Daughy C, Cella N, Zhang M. Maspin plays an essential role in early embryonic development. *Development* 2004; 131: 1479-89.
87. Qin L, Zhang M. Maspin regulates endothelial cell adhesion and migration through an integrin signaling pathway. *J Biol Chem* 2010; 285: 32360-9.
88. Endsley MP, Hu Y, Deng Y, et al. Maspin, the molecular bridge between the plasminogen activator system and beta1 integrin that facilitates cell adhesion. *J Biol Chem* 2011; 286: 24599-607.
89. Zhang M, Maass N, Magit D, Sager R. Transactivation through Ets and Ap1 transcription sites determines the expression of the tumor-suppressing gene maspin. *Cell Growth Differ* 1997; 8: 179-86.
90. Chen L, Gilkes DM, Pan Y, Lane WS, Chen J. ATM and Chk2-dependent phosphorylation of MDMX contribute to p53 activation after DNA damage. *EMBO J* 2005; 24: 3411-22.
91. Zhang M, Volpert O, Shi YH, Bouck N. Maspin is an angiogenesis inhibitor. *Nat Med* 2000; 6: 196-9.
92. Latha K, Zhang W, Cella N, Shi HY, Zhang M. Maspin mediates increased tumor cell apoptosis upon induction of the mitochondrial permeability transition. *Mol Cell Biol* 2005; 25: 1737-48.
93. Zhang W, Shi HY, Zhang M. Maspin overexpression modulates tumor cell apoptosis through the regulation of Bcl-2 family proteins. *BMC Cancer* 2005; 5: 50.
94. Wang H, Fu W, Im JH, et al. Tumor cell alpha3beta1 integrin and vascular laminin-5 mediate pulmonary arrest and metastasis. *J Cell Biol* 2004; 164: 935-41.
95. Nash GF, Turner LF, Scully MF, Kakkar AK. Platelets and cancer. *Lancet Oncol* 2002; 3: 425-30.

96. Khatib AM, Auguste P, Fallavollita L, et al. Characterization of the host proinflammatory response to tumor cells during the initial stages of liver metastasis. *Am J Pathol* 2005; 167: 749-59.
97. Nguyen DX, Bos PD, Massague J. Metastasis: from dissemination to organ-specific colonization. *Nat Rev Cancer* 2009; 9: 274-84.
98. Morgan H, Tumber A, Hill PA. Breast cancer cells induce osteoclast formation by stimulating host IL-11 production and downregulating granulocyte/macrophage colony-stimulating factor. *Int J Cancer* 2004; 109: 653-60.
99. Soriano P, Montgomery C, Geske R, Bradley A. Targeted disruption of the c-src proto-oncogene leads to osteopetrosis in mice. *Cell* 1991; 64: 693-702.
100. Rucci N, Recchia I, Angelucci A, et al. Inhibition of protein kinase c-Src reduces the incidence of breast cancer metastases and increases survival in mice: implications for therapy. *J Pharmacol Exp Ther* 2006; 318: 161-72.
101. Manning BD, Cantley LC. AKT/PKB signaling: navigating downstream. *Cell* 2007; 129: 1261-74.
102. Waning DL, Lehman JA, Batuello CN, Mayo LD. Controlling the Mdm2-Mdmx-p53 Circuit. *Pharmaceuticals (Basel)* 2010; 3: 1576-93.
103. Goldberg Z, Vogt Sionov R, Berger M, et al. Tyrosine phosphorylation of Mdm2 by c-Abl: implications for p53 regulation. *EMBO J* 2002; 21: 3715-27.
104. Schwartz D, Gygi SP. An iterative statistical approach to the identification of protein phosphorylation motifs from large-scale data sets. *Nat Biotechnol* 2005; 23: 1391-8.
105. Cooper JA, Gould KL, Cartwright CA, Hunter T. Tyr527 is phosphorylated in pp60c-src: implications for regulation. *Science* 1986; 231: 1431-4.
106. Mukhopadhyay D, Tsiokas L, Zhou XM, Foster D, Brugge JS, Sukhatme VP. Hypoxic induction of human vascular endothelial growth factor expression through c-Src activation. *Nature* 1995; 375: 577-81.
107. Zou Z, Gao C, Nagaich AK, et al. p53 regulates the expression of the tumor suppressor gene maspin. *J Biol Chem* 2000; 275: 6051-4.
108. Eitel JA, Bijangi-Vishehsaraei K, Saadatzaheh MR, et al. PTEN and p53 are required for hypoxia induced expression of maspin in glioblastoma cells. *Cell Cycle* 2009; 8: 896-901.
109. Takami K, Inui H, Nagayama K, et al. Low Grade Amplification of MDM2 Gene in a Subset of Human Breast Cancers without p53 Alterations. *Breast Cancer* 1994; 1: 95-102.
110. Korkolopoulou P, Christodoulou P, Kouzelis K, et al. MDM2 and p53 expression in gliomas: a multivariate survival analysis including proliferation markers and epidermal growth factor receptor. *Br J Cancer* 1997; 75: 1269-78.
111. Ralhan R, Sandhya A, Meera M, Bohdan W, Nootan SK. Induction of MDM2-P2 transcripts correlates with stabilized wild-type p53 in betel- and tobacco-related human oral cancer. *Am J Pathol* 2000; 157: 587-96.
112. Noon AP, Polanski R, El-Fert AY, et al. Combined p53 and MDM2 biomarker analysis shows a unique pattern of expression associated with poor prognosis in patients with renal cell carcinoma undergoing radical nephrectomy. *BJU Int* 2012.

113. Skomedal H, Kristensen GB, Lie AK, Holm R. Aberrant expression of the cell cycle associated proteins TP53, MDM2, p21, p27, cdk4, cyclin D1, RB, and EGFR in cervical carcinomas. *Gynecol Oncol* 1999; 73: 223-8.
114. Biscardi JS, Ishizawa RC, Silva CM, Parsons SJ. Tyrosine kinase signalling in breast cancer: epidermal growth factor receptor and c-Src interactions in breast cancer. *Breast Cancer Res* 2000; 2: 203-10.
115. Kloth MT, Laughlin KK, Biscardi JS, Boerner JL, Parsons SJ, Silva CM. STAT5b, a Mediator of Synergism between c-Src and the Epidermal Growth Factor Receptor. *J Biol Chem* 2003; 278: 1671-9.
116. Boerner JL, Demory ML, Silva C, Parsons SJ. Phosphorylation of Y845 on the epidermal growth factor receptor mediates binding to the mitochondrial protein cytochrome c oxidase subunit II. *Mol Cell Biol* 2004; 24: 7059-71.
117. Schlaepfer DD, Mitra SK. Multiple connections link FAK to cell motility and invasion. *Curr Opin Genet Dev* 2004; 14: 92-101.
118. Blattner C, Hay T, Meek DW, Lane DP. Hypophosphorylation of Mdm2 augments p53 stability. *Mol Cell Biol* 2002; 22: 6170-82.
119. Okamoto K, Li H, Jensen MR, et al. Cyclin G recruits PP2A to dephosphorylate Mdm2. *Mol Cell* 2002; 9: 761-71.
120. Lindstrom MS, Jin A, Deisenroth C, White Wolf G, Zhang Y. Cancer-associated mutations in the MDM2 zinc finger domain disrupt ribosomal protein interaction and attenuate MDM2-induced p53 degradation. *Mol Cell Biol* 2007; 27: 1056-68.
121. Paliwal P, Radha V, Swarup G. Regulation of p73 by Hck through kinase-dependent and independent mechanisms. *BMC Mol Biol* 2007; 8: 45.
122. Momand J, Zambetti GP, Olson DC, George D, Levine AJ. The mdm-2 oncogene product forms a complex with the p53 protein and inhibits p53-mediated transactivation. *Cell* 1992; 69: 1237-45.
123. Dohmesen C, Koeppl M, Dobbelstein M. Specific inhibition of Mdm2-mediated neddylation by Tip60. *Cell Cycle* 2008; 7: 222-31.
124. Shi HY, Zhang W, Liang R, et al. Blocking tumor growth, invasion, and metastasis by maspin in a syngeneic breast cancer model. *Cancer Res* 2001; 61: 6945-51.
125. Cher ML, Biliran HR, Jr., Bhagat S, et al. Maspin expression inhibits osteolysis, tumor growth, and angiogenesis in a model of prostate cancer bone metastasis. *Proc Natl Acad Sci U S A* 2003; 100: 7847-52.
126. Hojo T, Akiyama Y, Nagasaki K, et al. Association of maspin expression with the malignancy grade and tumor vascularization in breast cancer tissues. *Cancer Lett* 2001; 171: 103-10.
127. Siegel R, Naishadham D, Jemal A. Cancer statistics, 2012. *CA Cancer J Clin* 2012; 62: 10-29.
128. Bertos NR, Park M. Breast cancer - one term, many entities? *J Clin Invest* 2011; 121: 3789-96.
129. Lee YT. Breast carcinoma: pattern of metastasis at autopsy. *J Surg Oncol* 1983; 23: 175-80.
130. Wang SP, Wang WL, Chang YL, et al. p53 controls cancer cell invasion by inducing the MDM2-mediated degradation of Slug. *Nat Cell Biol* 2009; 11: 694-704.
131. Zhang L, Hill RP. Hypoxia enhances metastatic efficiency by up-regulating Mdm2 in KHT cells and increasing resistance to apoptosis. *Cancer Res* 2004; 64: 4180-9.

132. Shi W, Meng Z, Chen Z, et al. RNA interference against MDM2 suppresses tumor growth and metastasis in pancreatic carcinoma SW1990HM cells. *Mol Cell Biochem* 2011; 1208-4
133. Fridman JS, Hernando E, Hemann MT, de Stanchina E, Cordon-Cardo C, Lowe SW. Tumor promotion by Mdm2 splice variants unable to bind p53. *Cancer Res* 2003; 63: 5703-6.
134. Jones SN, Hancock AR, Vogel H, Donehower LA, Bradley A. Overexpression of Mdm2 in mice reveals a p53-independent role for Mdm2 in tumorigenesis. *Proc Natl Acad Sci U S A* 1998; 95: 15608-12.
135. Cailleau R, Young R, Olive M, Reeves WJ, Jr. Breast tumor cell lines from pleural effusions. *J Natl Cancer Inst* 1974; 53: 661-74.
136. Lukashchuk N, Vousden KH. Ubiquitination and degradation of mutant p53. *Mol Cell Biol* 2007; 27: 8284-95.
137. Muller PA, Vousden KH, Norman JC. p53 and its mutants in tumor cell migration and invasion. *J Cell Biol* 2011; 192: 209-18.
138. Frum R, Ramamoorthy M, Mohanraj L, Deb S, Deb SP. MDM2 controls the timely expression of cyclin A to regulate the cell cycle. *Mol Cancer Res* 2009; 7: 1253-67.
139. Polanski R, Warburton HE, Ray-Sinha A, et al. MDM2 promotes cell motility and invasiveness through a RING-finger independent mechanism. *FEBS Lett* 2010; 584: 4695-702.
140. Zhang Y, Shu L, Chen X. Syntaxin 6, a regulator of the protein trafficking machinery and a target of the p53 family, is required for cell adhesion and survival. *J Biol Chem* 2008; 283: 30689-98.
141. Fenouille N, Puissant A, Tichet M, et al. SPARC functions as an anti-stress factor by inactivating p53 through Akt-mediated MDM2 phosphorylation to promote melanoma cell survival. *Oncogene* 2011; 30: 4887-900.
142. Sheridan C, Kishimoto H, Fuchs RK, et al. CD44+/CD24- breast cancer cells exhibit enhanced invasive properties: an early step necessary for metastasis. *Breast Cancer Res* 2006; 8: R59.
143. Zhou S, Gu L, He J, Zhang H, Zhou M. MDM2 regulates vascular endothelial growth factor mRNA stabilization in hypoxia. *Mol Cell Biol* 2011; 31: 4928-37.
144. Minn AJ, Gupta GP, Siegel PM, et al. Genes that mediate breast cancer metastasis to lung. *Nature* 2005; 436: 518-24.
145. Jones SN, Sands AT, Hancock AR, et al. The tumorigenic potential and cell growth characteristics of p53-deficient cells are equivalent in the presence or absence of Mdm2. *Proc Natl Acad Sci U S A* 1996; 93: 14106-11.
146. Sigalas I, Calvert AH, Anderson JJ, Neal DE, Lunec J. Alternatively spliced mdm2 transcripts with loss of p53 binding domain sequences: transforming ability and frequent detection in human cancer. *Nat Med* 1996; 2: 912-7.
147. Li D, Marchenko ND, Schulz R, et al. Functional inactivation of endogenous MDM2 and CHIP by HSP90 causes aberrant stabilization of mutant p53 in human cancer cells. *Mol Cancer Res* 2011; 9: 577-88.
148. Lang GA, Iwakuma T, Suh YA, et al. Gain of function of a p53 hot spot mutation in a mouse model of Li-Fraumeni syndrome. *Cell* 2004; 119: 861-72.

149. Adorno M, Cordenonsi M, Montagner M, et al. A Mutant-p53/Smad complex opposes p63 to empower TGFbeta-induced metastasis. *Cell* 2009; 137: 87-98.
150. Lee YM, Lim JH, Chun YS, et al. Nutlin-3, an Hdm2 antagonist, inhibits tumor adaptation to hypoxia by stimulating the FIH-mediated inactivation of HIF-1alpha. *Carcinogenesis* 2009; 30: 1768-75.
151. Vassilev LT, Vu BT, Graves B, et al. In vivo activation of the p53 pathway by small-molecule antagonists of MDM2. *Science* 2004; 303: 844-8.
152. Lau LM, Nugent JK, Zhao X, Irwin MS. HDM2 antagonist Nutlin-3 disrupts p73-HDM2 binding and enhances p73 function. *Oncogene* 2008; 27: 997-1003.
153. Yang Y, Ludwig RL, Jensen JP, et al. Small molecule inhibitors of HDM2 ubiquitin ligase activity stabilize and activate p53 in cells. *Cancer Cell* 2005; 7: 547-59.
154. Ryu JH, Li SH, Park HS, Park JW, Lee B, Chun YS. Hypoxia-inducible factor alpha subunit stabilization by NEDD8 conjugation is reactive oxygen species-dependent. *J Biol Chem* 2011; 286: 6963-70.

Curriculum Vitae

Christopher N. Batuello

Education

Indiana University, Indianapolis, IN
Ph.D., Biochemistry and Molecular Biology, August 2012

Miami University, Oxford, OH
B.A., Microbiology, May 2005

Research and Professional Experience

Ph.D. Research, Indiana University, Department of Biochemistry and Molecular Biology, Indianapolis, IN. August 2007-August 2012

Concurrent projects to understand the oncogenic functions of Mdm2

- 1) Signaling events involved in regulating Mdm2 E3 ligase activity
- 2) Characterization of Mdm2 as a positive regulator in breast cancer metastasis

Advisor: Lindsey Mayo, Ph.D.

Research Technician, Indiana University, Department of Radiation Oncology, Indianapolis, IN. September 2005-August 2007

- 1) Identification of Mre11 as a target for heat-radiosensitization
- 2) Effects of gender and estrogen on radiation-induced cataractogenesis.

Advisor: Joseph Dynlacht, Ph.D.

Oral Research Presentations

Batuello, C.N., and Mayo, L.D. c-Src phosphorylates and switches Mdm2 ligase activity. Indiana University Cancer Center Floor Meeting, Indianapolis, IN, November 2011.

Batuello C.N., and Mayo, L.D. c-Src is a novel regulator of Mdm2. Indiana University Cancer Center Floor Meeting, Indianapolis, IN, October 2010.

Posters

Batuello, C.N., Lehman, J.A., Waning, D.A., and Mayo, L.D. c-Src phosphorylates and switches Mdm2 ligase activity. Cancer Research Day, Indiana University School of Medicine, Indianapolis, IN, May 2012.

Batuello, C.N., Lehman, J.A., Waning, D.A., and Mayo, L.D. c-Src phosphorylates and switches Mdm2 ligase activity. Biochemistry Day, Indiana University School of Medicine, Indianapolis, IN, April 2012.

Posters (cont.)

Lehman, J.A., Waning, D.A., **Batuello, C.N.**, and Mayo, L.D. A novel interaction of the human tumor suppressor proteins, p73 and PTEN. Cancer Research Day, Indiana University School of Medicine, Indianapolis, IN, May 2010.

Waning, D.L., Lehman, J.A., **Batuello, C.N.**, and Mayo, L.D. c-Abl contributes to Mdm2-Mdmx complex formation protecting p53 levels. American Association for Cancer Research, 101st Annual Meeting, Washington, DC, 2010.

Batuello, C.N., Lehman, J.A., Waning, D.A., and Mayo, L.D. c-Src is a novel regulator of Mdm2. Biochemistry Day, Indiana University School of Medicine, Indianapolis, IN, April 2010.

Waning, D.L., Lehman, J.A., **Batuello, C.N.**, Bijangi-Vishehsaraei K., and Mayo, L.D. c-Abl phosphorylation leads to Mdm2-Mdmx heterodimer formation. Ubiquitin Drug Discovery & Diagnostics 2009. Philadelphia, PA October 2009.

Lehman, J.A., Waning, D.A., Bijangi-Vishehsaraei, K., **Batuello, C.N.**, and Mayo, L.D. A novel auto-ubiquitination of the negative p53 regulator, Hdmx, is regulated by c-Abl. Cancer Biology Chair and Program Directors Retreat (CABTRAC), Clearwater Beach, FL, October 2009.

Henderson, M.A., Valluri, S., Rusek, A., DesRosiers, C., Lopez, J.T., **Batuello, C.N.**, Caperell-Grant, A., Mendonca, M.S., Pearson, C., Powers, E., Bigsby, R.M., and Dynlacht, J.R. Gender-related differences in radiation cataractogenesis. 18th Annual NASA Space Radiation Investigators Workshop. July 2007

Henderson, M.A., Valluri, S., Rusek, A., DesRosiers, C., Lopez, J.T., **Batuello, C.N.**, Caperell-Grant, A., Mendonca, M.S., Pearson, C., Powers, E., Bigsby, R.M., and Dynlacht, J.R. Gender-related differences in radiation cataractogenesis. 13th International Congress of Radiation Research. July 2007

Batuello, C.N., and Dynlacht, J.R. Mre11 as a target for heat radio-sensitization. 8th Annual Midwest DNA Repair Conference, Indianapolis, IN, April 2006.

Honors/Awards

Best Poster Presentation-Honorable Mention, Cancer Research Day, Indiana University School of Medicine, Indianapolis, IN, May, 2012.

Best Poster Presentation-Honorable Mention, Biochemistry Day, Indiana University School of Medicine, Indianapolis, IN, April, 2012.

Training and Teaching Experience

Mentor, Student Research Program in Academic Medicine for first year medical students. Indiana University School of Medicine, Indianapolis, IN. Summer 2011

Mentor, Summer Research Program for high school/undergraduate minority scientists. Indiana University Cancer Center, Indianapolis, IN. Summer 2010

Publications

Batuello, C.N., Lehman, J.A., Waning, D.L., and Mayo, L.D. c-Src phosphorylates and switches Mdm2 ligase activity. *Submitted*

Batuello, C.N., Waning, D.L., Pollok, K.E., and Mayo, L.D. Mdm2 enhances breast cancer metastasis to the lung. *In Preparation*

Lehman, J.A., Waning, D.L., **Batuello, C.N.**, Cipriano, R., Kadakia, M.P., and Mayo, L.D. Induction of apoptotic genes by a p73-phosphatase and tensin homolog (p73-PTEN) protein complex in response to genotoxic stress. *J Biol Chem.* 2011 Oct 21;286(42):36631-40.

Dynlacht, J.R., **Batuello, C.N.**, Lopez, J.T., Kim, K.K., Turchi, J.J. Identification of Mre11 as a target for heat radiosensitization. *Radiat Res.* 2011 Sep;176(3):323-32.

Waning, D.L., Lehman, J.A., **Batuello, C.N.**, and Mayo, L.D. c-Abl phosphorylation of Mdm2 facilitates Mdm2-Mdmx complex formation. *J Biol Chem.* 2011 Jan 7;286 (1):216-22.

Waning, D.L., Lehman, J.A., **Batuello, C.N.**, and Mayo, L.D. Controlling the Mdm2-Mdmx-p53 Circuit. *Pharmaceuticals (Basel).* 2010 May 18;3(5):1576-1593.

Araki, S., Eitel, J.A., **Batuello, C.N.**, Bijangi-Vishehsaraei, K., Xie, X.J., Danielpour, D., Pollok, K.E., Boothman, D.A., and Mayo, L.D. TGF-beta1-induced expression of human Mdm2 correlates with late-stage metastatic breast cancer. *J Clin Invest.* 2010 Jan;12 (1):290-302.

Lehman, J.A., Eitel, J.A., **Batuello, C.N.**, and Mayo, L.D. Therapeutic considerations for Mdm2: not just a one trick pony. *Expert Opin Drug Discov.* 2008 Nov;3(11):1309-1321.

Publications (cont.)

Henderson, M.A., Valluri, S., DesRosiers, C., Lopez, J.T., **Batuello, C.N.**, Caperell-Grant, A., Mendonca, M.S., Powers, E.M., Bigsby, R.M., and Dynlacht, J.R. Effect of gender on radiation-induced cataractogenesis. *Radiat Res.* 2009 Jul;172(1):129-33.

Batuello, C.N., Kelley, M.R., and Dynlacht, J.R. Role of Ape1 and base excision repair in the radioresponse and heat-radiosensitization of HeLa Cells. *Anticancer Res.* 2009 Apr;29(4):1319-25.